The physiological and pathological role of Retinal Degeneration Protein 3 (RD3) in the brain

Der Fakultät für Medizin und

Gesundheitswissenschaftender Carl von Ossietzky

Universität Oldenburg

Doctor rerum naturalium (Dr. rer. nat.)

angenommene Dissertation

von Herrn

Yaoyu Chen

geboren am **28.05.1991** in **China**

Betreuender Gutachter: **Prof. Dr. Karl-Wilhelm Koch**

Zweitgutachter: **Prof. Dr. Mark Steffen Hipp**

Weitere Gutachter: **Prof. Dr. Jörg Albert**

Tag der Disputation: **14.03.2024**

Table of content

Abbreviations

°C	degree Celsius
95% CI	95% confidence interval shown as shadow
ANP	atrial natriuretic peptide
ATRX	alpha thalassemia/mental retardation syndrome X-linked
AUC	area under curve
BBB	blood-brain barrier
BNP	brain natriuretic peptide
BRB	blood-retina barrier
[Ca^{2+}]	calcium concentration
C1orf36	chromosome 1 open reading frame 36
CCD	guanylate cyclase catalytic domain
CDKN2A	cyclin-dependent kinase inhibitor 2A
CDKN2B	cyclin-dependent kinase inhibitor 2B
cGMP	3', 5'-cyclic monophosphate
CNP	c-type natriuretic peptide
CNS	central nervous system
CORD6	cone-rod dystrophies
COS	CV-1 in Origin, carrying SV40
DAPI	4′,6-diamidino-2-phenylindole
DD	dimerization domain
DSS	disease specific survival
E	embryonic
ECD	extracellular protein domain
EGFR	epidermal growth factor receptor
ER	endoplasmic reticulum
FACS	fluorescence-activated cell sorting
GBM	Glioblastoma multiforme
GC-A	guanylate cyclase A
GCAPs	neuronal calcium sensor proteins
GC-B	guanylate cyclase B
GC-E	guanylate cyclase E

GC-F	guanylate cyclase F
GCL	ganglion cell layer
GDP	guanosine diphosphate
GMP	guanosine monophosphate
GSE	Genomic Spatial Event database
GTP	guanosine triphosphate
GUK	guanylate kinase
HEK	human embryonic kidney cells
HR	hazard ratio
IC50	half inhibitory concentration
IDH	isocitrate dehydrogenase
IGN	lateral geniculate nucleus
IPL	inner plexiform layer
JMD	juxta membrane domain
KHD	kinase-like (homology) domain
LCA	leber's congenital amaurosis
LCA 12	leber congenital amaurosis type 12
LGG	low grade glioma
mg	milli gram
mGC	membrane guanylate cyclase
ml	milli liter
mM	millimolar
MTT	3-(4,5-Dimethylthiazol-2-yl)-2,5-Diphenyltetrazolium Bromide
NB	neuroblastoma
NFL	cerve fiber layer
nM	nanomolar
Npr1	mouse natriuretic peptide receptor 1 gene
NPR1	natriuretic peptide receptor 1
Npr2	mouse natriuretic peptide receptor 2 gene
NPR2	natriuretic peptide receptor 2
NPs	natriuretic peptides
ONL	outer nuclear layer
OPL	outer plexiform layer
OS	overall survival event
P	postnatal

PFI	progression free survival
rd3	mouse retinal degeneration protein 3 gene
RD3	retinal degeneration protein 3 protein
RFP	red fluorescent protein
RGC	retinal ganglion cells
ROC	receiver operating characteristic
RPE	retinal pigment epithelial
SC	superior colliculus
SD	standard deviation
sGC	soluble guanylate cyclase
TCGA	The Cancer Genome Atlas Program
TERT	telomerase reverse transcriptase
TP53	tumor protein P53
WHO	world health organization
µg	micro gram
µl	micro liter
µM	micromolar

Single-letter amino acid code

A	alanine	**Ala**		**L**	leucine	**Leu**
R	arginine	**Arg**		**K**	lysine	**Lys**
N	asparagine	**Asn**		**M**	methionine	**Met**
D	aspartic acid	**Asp**		**F**	phenylalanine	**Phe**
C	cysteine	**Cys**		**P**	proline	**Pro**
E	glutamic acid	**Glu**		**S**	serine	**Ser**
Q	glutamine	**Gln**		**T**	threonine	**Thr**
G	glycine	**Gly**		**W**	tryptophan	**Trp**
H	histidine	**His**		**Y**	tyrosine	**Tyr**
I	isoleucine	**Ile**		**V**	valine	**Val**

List of figures and tables

Summary

The retina is an outer part of the brain that represents a neuronal network for perceiving and processing light signals. Despite decade-long research, many cellular and molecular events underlying cell-cell communications and signaling pathways remain elusive. A more recently discovered and described protein is the retinal degeneration protein 3 (RD3) that has a critical role in photoreceptor cells. For example, one of its primary functions involves inhibiting photoreceptor specific membrane guanylate cyclases during trafficking from the inner segment to their final destination in the outer segment. Continuing research revealed that RD3 has also been identified in other tissue types, including epithelial cells, suggesting a broader expression. However, the physiological role of RD3 in non-retinal tissue remains unresolved at present, and specific protein targets outside of retinal tissue have not yet been identified. In **chapter 4.1**, we aimed to determine if membrane-bound guanylate cyclase that are not expressed in photoreceptor cells and are activated by natriuretic peptides, can also be regulated by RD3. We assessed the transcript levels of the *rd3* gene, the genes for natriuretic peptide receptors *Npr1* and *Npr2* (encoding GC-A and GC-B, respectively) throughout development from the embryonic to the postnatal stage at P60. The study included the mouse retina, cerebellum, hippocampus, neocortex, and olfactory bulb, and aimed at investigating their co-expression pattern. Enzyme activity measurements revealed that RD3 inhibits natriuretic peptide receptors GC-A and GC-B, resulting in inhibitory constants of approximately 25 nM. A similar regulatory feature of RD3 seems to be present in astrocytes, where it inhibits endogenous GC-A and GC-B activities.

RD3 dysregulation is involved in the apoptosis of photoreceptor cells, indicating a more direct cellular function in the degeneration of the retina. Recent research has uncovered a new pathophysiological role for RD3 in neuroblastoma, suggesting a potential function beyond the retina. Therefore, in **chapter 4.2**, we investigated if RD3 is associated with neurological diseases like glioma and cellular processes such as apoptosis to comprehend its pathological role. Data mining on public databases and

clinical studies revealed that RD3 is significantly downregulated in glioblastoma relative to non-tumor tissues. Further studies of multi-cohort overall survival and receiver operating characteristic testing indicated that a low RD3 transcript level is a potential biomarker for the prognosis and diagnosis of glioblastoma. In functional tests, we found that RD3 can significantly decrease cell viability, leading to cell cycle arrest at the G2/M phase and triggering cell apoptosis. Conversely, the impact of RD3 wild type was diminished by single point mutations at the exposed protein surface involved in RD3 target interaction.

The results of the thesis indicate a new physiological and pathological role of RD3 in the brain. Specifically, RD3 inhibits GC-A and GC-B in brain astrocytes and may also be relevant to retina disease. Additionally, overexpression of RD3 leads to cell cycle arrest and programmed cell death, indicating that RD3 abnormalities are crucial in both retina and non-retina tissues. Any dysfunction of RD3 may be associated with chronic or rapid apoptosis-related cell degeneration. The loss of RD3 has demonstrated diagnostic and prognostic value in glioblastoma, indicating its critical involvement in tumor progression. These findings suggest that the pathophysiological properties of RD3 in both the retina and brain may serve as a good model for elucidating neuro-ophthalmologic manifestations in neurological diseases.

Zusammenfassung

Die Netzhaut wird auch als Außenposten des Gehirns beschrieben und repräsentiert ein neuronales Netzwerk für die Detektion und Verarbeitung von Lichtsignalen. Trotz Jahrzehnte langer Forschung bleiben viele Prozesse der Zell-Zell-Kommunikation und der Signalverarbeitung auf zellulärer und molekularer Ebene unbekannt. Ein in jüngerer Zeit entdecktes und beschriebenes Protein ist das Retinal Degeneration Protein 3 (RD3), das kritische Funktionen in den Photorezeptorzellen ausübt.

Eine der Hauptfunktionen von RD3 besteht darin, Photorezeptor-spezifische membrangebundene Guanylatcyclasen während des Transports vom inneren Segment zu ihrem endgültigen Ziel im äußeren Segment zu hemmen. Weitere Untersuchungen ergaben, dass RD3 auch in anderen Gewebetypen, einschließlich Epithelzellen, identifiziert wurde, was auf eine breitere Expression hindeutet. Allerdings ist die physiologische Rolle von RD3 in nicht-retinalem Gewebe derzeit noch ungeklärt, und spezifische Zielstrukturen außerhalb des retinalen Gewebes wurden noch nicht identifiziert. In Kapitel 4.1 wollten wir herausfinden, ob membrangebundene Guanylatcyclasen, die nicht in Photorezeptorzellen exprimiert sind und durch natriuretische Peptide aktiviert werden, auch durch RD3 reguliert werden können. Wir untersuchten die Transkriptniveaus des rd3-Gens, und der Gene für die natriuretischen Peptidrezeptoren Npr1 und Npr2 (kodierend für GC-A bzw. GC-B), während der gesamten Entwicklung vom Embryonal- bis zum postnatalen Stadium bei P60 in mehreren Hirngeweben, darunter Maus-Retina, Kleinhirn, Hippocampus, Neocortex und Riechkolben, um ihr Koexpressionsmuster zu ermitteln. Enzymatische Aktivitätsmessungen zeigten, dass RD3 die natriuretischen Peptidrezeptoren GC-A und GC-B mit Inhibitorkonstanten von ca. 25 nM hemmt. Ein ähnliches regulatorisches Profil von RD3 kommt in Astrozyten vor, in denen RD3 endogene GC-A und GC-B inhibiert.

Eine RD3-Dysregulation ist an der Apoptose von Photorezeptorzellen beteiligt, was auf eine direktere zelluläre Funktion bei der Degeneration der Netzhaut hinweist. Jüngste Forschungen haben eine neue pathophysiologische Rolle von RD3 beim

Neuroblastom aufgedeckt, was ebenfalls auf eine potenzielle Funktion jenseits der Netzhaut schließen lässt. Daher haben wir in Kapitel 4.2 untersucht, ob RD3 mit neurologischen Erkrankungen wie Gliomen und zellulären Prozessen wie Apoptose assoziiert ist. Unsere Recherche in öffentlichen Datenbanken und klinischen Studien ergab, dass RD3 im Glioblastom im Vergleich zu Nicht-Tumor-Geweben deutlich herunterreguliert ist. Weitere Studien zum Gesamtüberleben mehrerer Kohorten und zum Testen der *Receiver Operating Characteristics* deuten darauf hin, dass ein niedriger RD3-Transkriptwert ein potenzieller Biomarker für die Prognose und Diagnose von Glioblastomen ist. In Funktionstests haben wir herausgefunden, dass RD3 die Lebensfähigkeit der Zellen erheblich verringern kann, was zum Stillstand des Zellzyklus in der G2/M-Phase führt und Apoptose auslöst. Umgekehrt wurde der Einfluss des RD3-Wildtyps durch einzelne Punktmutationen an der exponierten Proteinoberfläche, die an der Wechselwirkung von RD3 mit Zielstrukturen beteiligt sind, verringert.

Die Ergebnisse der Arbeit weisen auf eine neue physiologische und pathologische Rolle von RD3 im Gehirn hin. insbesondere hemmt RD3 GC-A und GC-B in Astrozyten des Gehirns und könnte auch für Netzhauterkrankungen relevant sein. Darüber hinaus führt eine Überexpression von RD3 zum Stillstand des Zellzyklus und zum programmierten Zelltod, was darauf hindeutet, dass RD3-Anomalien sowohl in Netzhaut- als auch Nicht-Netzhautgewebe von entscheidender Bedeutung sind. Jede Funktionsstörung von RD3 kann mit einer chronischen oder schnellen Apoptose-bedingten Zelldegeneration verbunden sein. Der Verlust von RD3 hat einen diagnostischen und prognostischen Wert für das Fortschreiten des Glioms gezeigt, was auf seine entscheidende Beteiligung am Fortschreiten des Tumors hinweist. Insgesamt legen diese Ergebnisse nahe, dass die pathophysiologischen Eigenschaften von RD3 sowohl in der Netzhaut als auch im Gehirn ein gutes Modell zur Aufklärung neuroophthalmologischer Manifestationen bei neurologischen Erkrankungen sein könnten

1. Introduction

1.1 Brain, Retina, and Neurological Cancer: An Intricate Interplay

The human brain is an organ of immense complexity and significance, posing a daunting challenge in the fields of medical research and healthcare, especially regarding neurological cancers. These malignant conditions greatly affect millions on a global scale, resulting in profound and often catastrophic consequences that drastically reduce their quality of life. Despite the progress made in treating cancers that affect the brain and nervous system, a substantial knowledge gap remains. This gap impedes the development of effective drug therapies that target the disease. Therefore, a more extensive investigation into the intricacies of neurological cellular and molecular mechanisms is required. As a distinctive organ with a direct link to the central nervous system (CNS), retina displays significant parallels with the brain and spinal cord in several aspects such as structure, operation, reaction to damage, and immune processes (London et al., 2013). Hence, it presents an innovative approach to investigating the brain and related pathologies. The purpose of our investigation is to uncover the new functions of a particular retinal protein within the nervous system and determine its response or dysfunction when disease-pertinent mutations are present.

1.1.1 Anatomy and functions: Crosslink of the Brain and Eye.

The brain and eye have an anatomical and functional relationship as integral parts of the CNS that is responsible for the nuanced processing of visual information. During embryonic development, the retina and optic nerve grow from the diencephalon and are intertwined with the developmental pathways of the CNS, which include the meticulously orchestrated process of neurogenesis and differentiation of the brain (Liao et al., 2018; London *et al*., 2013). The retina plays a crucial role in vision and can signal numerous systemic and neurodegenerative conditions. For instance, chronic stress may lead to retinal-glia ischemia and inflammation in the retina, as observed in a study of the chronic stress-related phenotype (Malan et al., 2023). This results in a

complex and interconnected system that can impact a person's visual abilities. Therefore, exploring the intricate interplay between the brain and retina is crucial to advance our understanding and management of neurodegenerative conditions.

The retina consists of several functional layers (see Figure 1 A), including the Nerve Fiber Layer (NFL), Ganglion Cell Layer (GCL), Inner Plexiform Layer (IPL), Outer Plexiform Layer (OPL), and Outer Nuclear Layer (ONL). Each layer creates specific microenvironments required for cell survival, morphology, and function (Hoon et al., 2014). Within these layers, there is a barrier structure in the retina that has a similar function and structure to the CNS, called the blood-retina barrier (BRB). The BRB consists of an inner and outer barrier. The outer BRB is formed at the retinal pigment epithelial (RPE) cell layer, while the inner BRB, like the blood-brain barrier (BBB), is located in the inner retinal microvasculature (Campbell and Humphries, 2013). The brain can be classified into three primary divisions based on function: the cerebrum, the cerebellum, and the brainstem (see Figure 1). The cerebrum, which is the largest part of the brain, serves as the primary center for processing signals. It includes areas responsible for language, judgment, thinking, reasoning, problem-solving, emotions, and learning, as well as playing a role in sensory processing, such as vision, hearing, touch, and other senses (Wood, 1996). The cerebellum, similar to the cerebral cortex, comprises two hemispheres located at the posterior part of the brain and is responsible for coordinating movement and balance (Dale Purves, 2012). Brain stem, consists of the midbrain, pons, and medulla, serving as a vital connector between the cerebrum and the spinal cord (Haines and Mihailoff, 2018). To these regions, it is believed that nearly half of the brain direct or indirect participants the vision signaling process, that make ocular manifestations of brain pathologies research reasonable.

Both the retina and the brain harbor neurons and glial cells, their functionalities and interactions exhibit distinct characteristics tailored to their specific roles in the visual and central nervous systems (see Figure 1 C). As the fundamental units of the brain, retina and nervous system, neurons are specialized for transmitting information

throughout the body. In terms of function, size, and structure, neurons were classified into three different types: sensory, interneuron, and motor. Their unique structure - comprising a cell body, axons, and dendrites - facilitates the rapid transmission of electrical and chemical signals. Neurons communicate through synapses, where neurotransmitters are released to propagate signals to adjacent neurons, thereby forming intricate neural networks that underpin various physiological processes and cognitive functions.

In retina, there are five major types of the neurons, the photoreceptor cells (rods and cones), bipolar cells, ganglion cells, horizontal cells, and amacrine cells, each with a distinctive role in processing visual information before transmitting it to the brain through the optic nerve (see Figure 1 A). Photoreceptor cells initiate the conversion of light into electrical signals in the retina, triggering a cascade of neuronal signals that ultimately reach the retinal ganglion cells (RGCs). The axons of RGCs compose the optic nerve, which projects to both the lateral geniculate nucleus (LGN) in the thalamus and the superior colliculus (SC) in the midbrain. Like all fiber tracts in the central nervous system, the optic nerve is ensheathed by myelin, produced by oligodendrocytes, and is surrounded by all three meningeal layers. From these locations, visual information is transmitted to higher centers of visual processing, enabling us to perceive the world around us (London *et al.*, 2013).
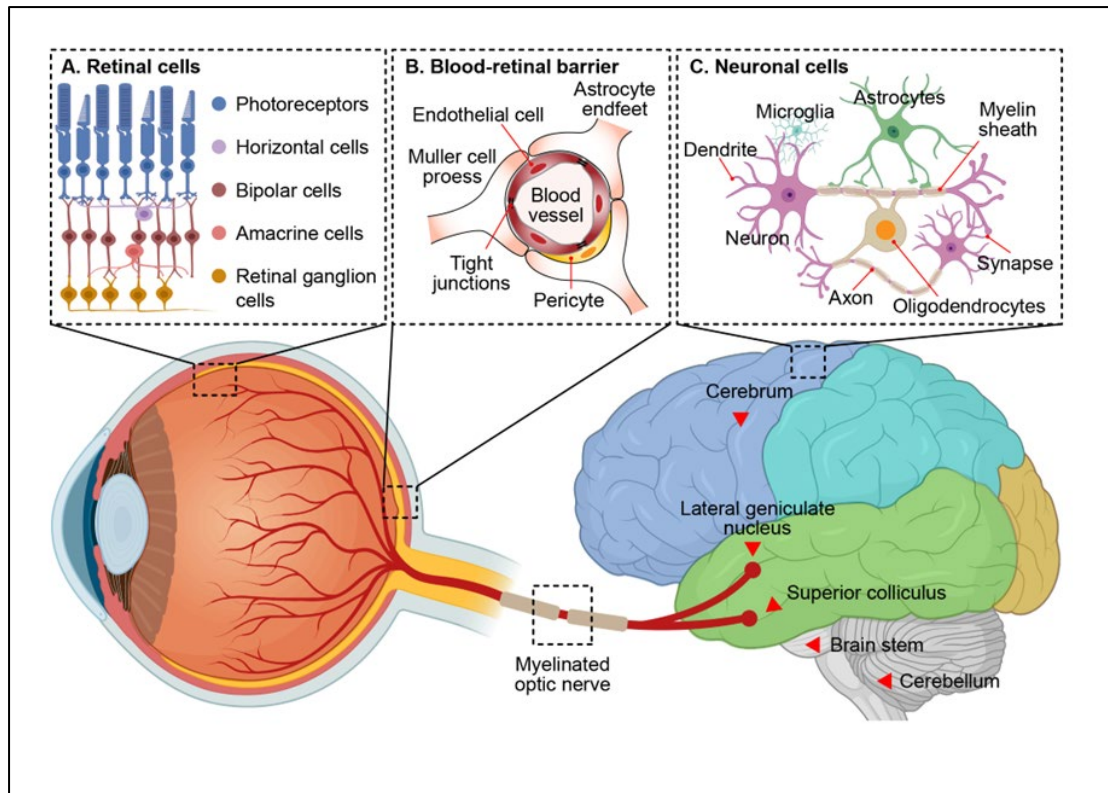
Figure 1: Schematic overview of the connection between the brain and eye, including the anatomical structure and functions. A. The structure and function of the retina and its constituent cells. B. As with the CNS, the eye has a unique immune system involving specialized barriers, the blood-retinal barrier, the retinal analogue of the CNS blood-brain barrier. C. Neuronal cells.

Glial cells are non-neuronal cells widely distributed in the CNS and the peripheral nervous system that provide physical and chemical support to neurons and maintain the microenvironment. Specifically, there are three primary types of glial cells: astrocytes, oligodendrocytes, and microglia (see Figure 1 C). Astrocytes are the predominant type of glial cell that assists the formation of the blood-brain barrier (BBB) and the blood-retina barrier (BRB). It performs several essential functions, including neurotransmitter and blood flow regulation, axon activity synchronization, energy metabolism, and homeostasis (Jäkel and Dimou, 2017; Park and Friston, 2013). Oligodendrocytes are derived from neural stem cells that maintain the structural stability and nutritional support of axons, as well as accelerate the conduction of signals by producing the enveloping myelin sheath. Microglia are tiny glial cells that

function as immune cells in the CNS system. They play an essential role in preserving the brain or retina microenvironment by monitoring pathogens and cellular debris, as well as responding to injury or infection (Kettenmann et al., 2011; Norris and Kipnis, 2019).

Neurodegenerative disorders and neurological cancers were normally caused by the cellular disorder, that subsequently damage the cells within the retinal layers. For example, Parkinson's disease substantively affects dopaminergic cells in distinct retinal layers (Ortuno-Lizaran et al., 2020). Therefore, understanding the intricate functionalities and interactions of neurons and glial cells, as well as the protective mechanisms offered by the BBB and BRB, is crucial in exploring pathological conditions like glioma. It provides a framework for investigating how these barriers may be compromised or leveraged in disease states, and how cellular dynamics within the brain and retina may be altered, thereby offering insights into potential therapeutic targets and strategies.

1.1.2   Neurological Cancers and Retina (with focus on gliomas).

Neurological cancers, including brain and nervous system cancers, arise in the brain, spinal cord, or other regions of the central or peripheral nervous system. They encompass a range of types such as gliomas, meningiomas, schwannomas, pituitary adenomas, central nervous system lymphomas, ependymomas, neuroblastomas, and medulloblastomas. These tumors can be either benign or malignant, with malignant neurological tumors often referred to as brain or nervous system tumors, known for their aggressive and life-threatening nature (Baba AI, 2007). In this thesis, we will focus on gliomas, the most common primary brain tumors in adults, which are thought to arise from neuroglial stem or progenitor cells. Gliomas constitute about 80% of primary malignant tumors in the central nervous system and are linked to low survival rates (Ostrom et al., 2014). The heterogeneity of gliomas poses multiple diagnostic and treatment challenges. Various regions in the same tumor may have different genetic mutations and characteristics. Surgery, radiation therapy, and chemotherapy, which

are the primary treatments, are not curative and the tumors frequently relapse (Barthel et al., 2019; Khasraw et al., 2014; Khasraw and Lassman, 2010). Developing superior diagnostic tools, novel treatments, and a more thorough comprehension of molecular and genetic factors driving glioma progression addresses these limitations.
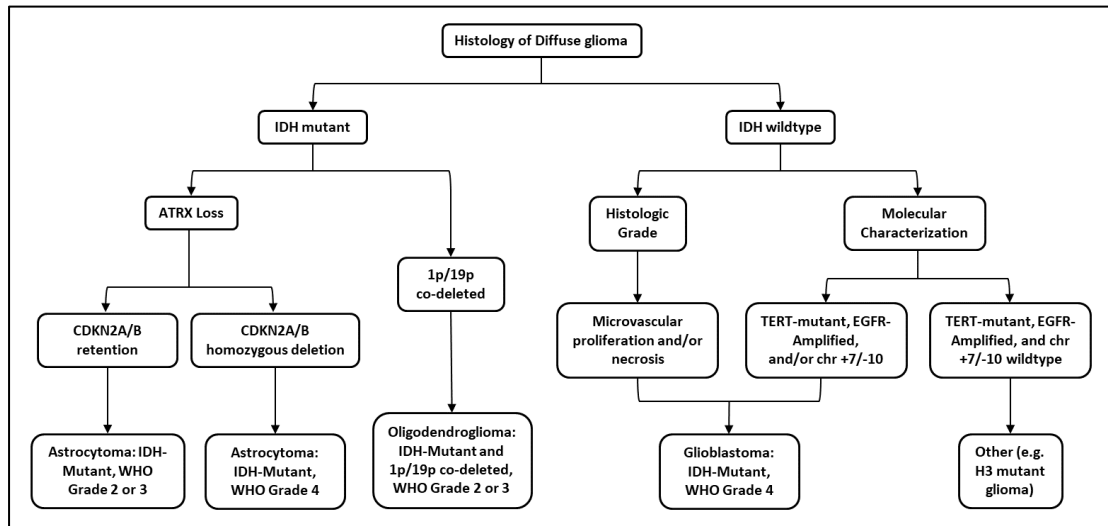
Figure 2: Flowchart illustrating the diagnostic approach for adult diffuse glioma using the most pertinent molecular markers outlined in the World Health Organization (WHO) classification of central nervous system (CNS) tumors (The WHO 2021 5th edition). The isocitrate dehydrogenase (IDH) mutation serves as an initial molecular marker for glioma categorization. The IDH-mutant tumors are subcategorized as alpha thalassemia/mental retardation syndrome X-linked (ATRX) loss astrocytoma or chromosome 1p/19q co-deleted oligodendroglioma. Meanwhile, astrocytoma diagnosis is based on histopathologic grading criterion and cyclin-dependent kinase inhibitor 2A/cyclin-dependent kinase inhibitor 2B (CDKN2A/B) status, with grades 2, 3, or 4 being possible. To rule out glioblastoma, the tumor primarily grouped in IDH wildtype and grade 4, were necessary to have molecular testing of gain of chromosome 7, loss of chromosome 10 (chr +7/-10), epidermal growth factor receptor (EGFR) amplification, and telomerase reverse transcriptase (TERT) promoter, as well as consider microvascular and/or necrosis.

The incorporation of histopathological and genetic attributes in the 2016 WHO CNS Malignancy Classification represents a substantial deviation from previous glioma

classifications (Louis, 2016). Along with the trend, the reports from cIMPACT-NOW (the consortium to inform molecular and practical approaches to CNS tumor taxonomy), proposed numerous molecular biomarkers in diagnosing CNS tumors (Brat et al., 2020; Brat et al., 2018; Ellison et al., 2020; Ellison et al., 2019; Louis et al., 2018a; Louis et al., 2020; Louis et al., 2018b). Drawing on genetic findings, the 2021 WHO classification of CNS malignancies has furnished nomenclature and diagnostic criteria for diffuse gliomas (Louis et al., 2021). In the new disease classification, the IDH status is regarded as a primary molecular diagnosis tool. The IDH-mutant gliomas usually start as low-grade tumors that progress with additional genetic changes, resulting in higher tumor grades. In diffuse astrocytoma, about 90% of cases with IDH mutations exhibit loss-of-function mutations in tumor protein P53 (TP53) and alpha thalassemia/mental retardation syndrome X-linked (ATRX). ATRX mutations are mutually exclusive with 1p/19q codeletion (combined loss of the short arm chromosome 1 and the long arm of chromosome 19), which is a hallmark feature of oligodendrogliomas. Oligodendrogliomas are classified into WHO grade 2 or 3 based on histologic features of anaplasia and are characterized by IDH mutations and 1p/19q codeletion (see Figure 2). Molecular changes affect tumor grading, where the complete loss of both copies of CDKN2A at 9p21 correlates with reduced survival rates in these neoplasms (Bale and Rosenblum, 2022; Gritsch et al., 2022; Jamshidi and Brat, 2022; Louis *et al.*, 2021).

Glioblastoma multiform (GBM) is a prevalent primary malignant brain tumor in adults. It exhibits rapid progression, poor prognosis (with a median overall survival of 16-18 months), and various histologic features such as cellular and nuclear atypia, mitosis, necrosis, and vascular proliferation (Reithmeier et al., 2010). These tumors exhibit significant molecular heterogeneity, with frequent genetic alterations, such as +7/-10 chromosome alterations, changes in receptor tyrosine kinases (frequently involving EGFR amplification), p53 pathway alterations, Phosphatase and tensin homolog (PTEN) mutations or deletions, and abnormal telomere maintenance resulting from TERT promoter mutations (see Figure 2). Moreover, in some cases, the GBM derived

from optic nerve, optic chiasm, or optic tract presented neuro-ophthalmologic manifestations, such as loss of visual acuity or visual field deficits in the ipsilateral eye and loss of color vision (Lin and Huang, 2017; Lincoff et al., 2012; Tan et al., 2020).

Undoubtedly, the 2021 Classification of Central Nervous System Tumors by the World Health Organization (WHO) offers valuable information regarding glioma subtypes and genetic characteristics. This, in turn, has contributed significantly to the development of diagnostic and therapeutic strategies. Nonetheless, the current classification has certain limitations, and clinical therapies for gliomas have yet to demonstrate their efficacy. Therefore, identifying new diagnostic biomarkers and treatment targets for gliomas is imperative for further investigative work. Our focus will be on a retina specific protein to exemplify its possibilities in cancer diagnostics and to explore its prognostic potential.

1.2 Cyclic GMP pathway in brain-retina system.

The second messenger guanosine 3', 5'-cyclic monophosphate (cGMP) signaling system includes the transformation of cGMP to guanosine monophosphate (GMP), which is further transformed to guanosine diphosphate (GDP), guanosine triphosphate (GTP) and guanosine (see Figure 3). cGMP is involved in a variety of physiological processes, including vision, neurotransmission, synaptic plasticity, and regulation of blood flow in the brain (Kuhn, 2016). The synthesis of cGMP is catalyzed by two forms of guanylate cyclase (GCs): a soluble (sGC) and a membrane (mGC) form. The soluble guanylate cyclase (sGC) acts as the primary target of the gaseous messenger molecule nitric oxide (NO). Soluble GCs consist of α and β subunits that form the active protein complex. Several isoforms exist being classified as α1, α2, α2i, β1, and β2 (Derbyshire and Marletta, 2012). The primary sGC isoforms in the brain consist of α1, β1, and α2 (Ibarra et al., 2001). These isoforms are influenced by neurotransmitters, leading to increased levels of cGMP that are crucial for glutamate neurotransmission and synaptic activity (Ghanta et al., 2017). The disruption or dysfunction of the NO-sGC-cGMP pathway is involved in several pathological states, such as

8

neurodegenerative diseases like, Alzheimer's disease, cognitive impairment, and stroke (Correia et al., 2021).
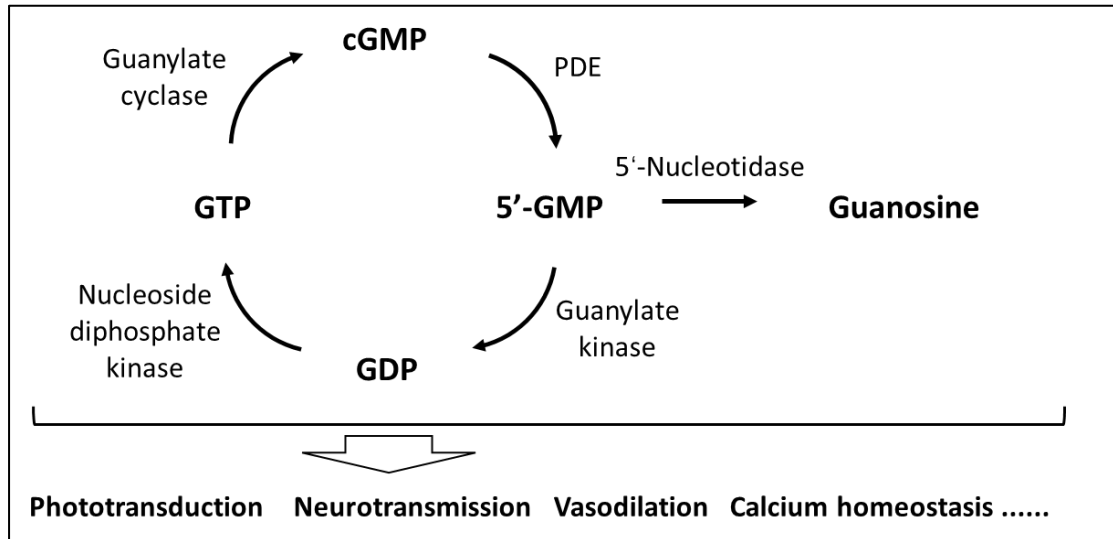
Figure 3: Simplified overview of nucleotide cycle in humans. Phosphodiesterases (PDEs) hydrolyze the second messenger cGMP into 5'-guanosine monophosphate (GMP), which is then degraded by 5'-Nucleotidase or recycled by guanylate kinase (GUK), which catalyzes guanosine diphosphate (GDP) formation. Nucleoside diphosphate kinase assists in the conversion of GDP to guanosine triphosphate (GTP), that later are been used by membrane guanylate cyclase for cGMP synthesis to complete the cycle to regulating various cellular processes.

Membrane bound guanylate cyclases are a family of transmembrane proteins encoded by seven genes in the mammalian genome. Structurally, these proteins possess an extracellular protein domain (ECD), an intracellular kinase-like domain (KHD), a dimerization domain (DD), and a cyclase catalytic domain (CCD) (see Figure 4). GC-A and GC-B serve as receptors for natriuretic peptides like the atrial natriuretic peptide (ANP), brain natriuretic peptide (BNP) and c-type natriuretic peptide (CNP). These hormones, for example, regulate blood pressure and promote skeletal development (Kuhn, 2016). GC-C is binding the ligands guanylin and uroguanylin, leading to the water and ion transport in the gut (Kuhn, 2016). The photoreceptor guanylate cyclases, GC-E and GC-F are expressed in the photoreceptor cell, having a crucial function in

phototransduction and visual recovery (Koch and Dell'Orco, 2015). GC-D and GC-G are sensory receptors expressed in mice that respond to CO2, guanylin and cold temperatures thereby mediating olfaction and thermosensation. However, they are not present in human (Kuhn, 2016). Although there is no direct evidence implicating mGCs like GC-A and GC-B in brain diseases as there is for sGC, recent studies suggest functions in astrocytes and dopaminergic neurons (Chen et al., 2022; Giovannini et al., 2021). Our focus here is on two categories of mGCs: the natriuretic peptide receptors GC-A and GC-B, and the photoreceptor specific GC-E and GC-F operating in phototransduction.
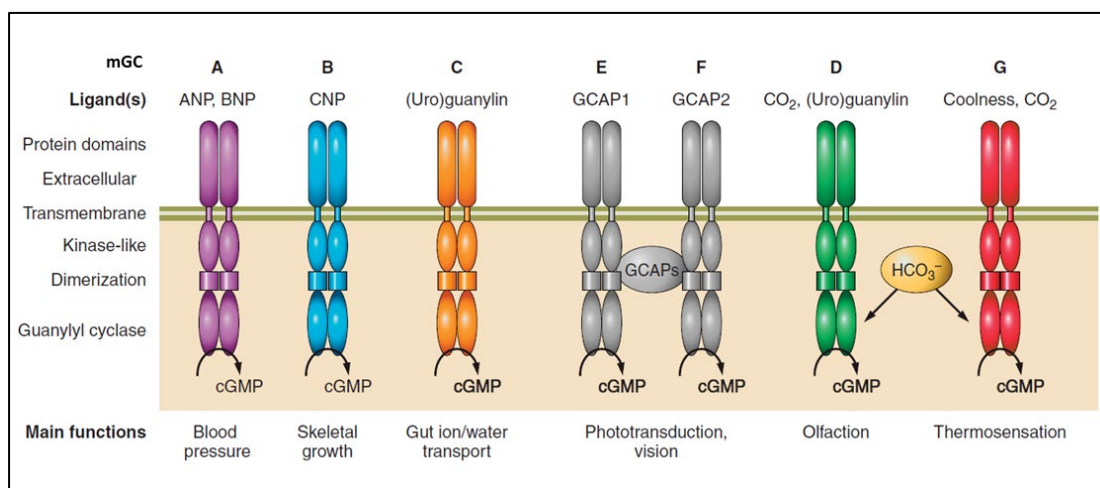
Figure 4: Illustration of the structure and primary functions of membrane-bound guanylate cyclase. GC-A and GC-B serve as the receptors for natriuretic peptides while GC-C functions as the receptor for guanylin and uroguanylin. GC-E and GC-F act as the retinal guanylate cyclase and bind GCAP1 and GCAP2. GC-D and GC-G are operational in rodents and vestigial in humans. (Adapted from Michaela Kuhn, 2016)

1.2.1   The retinal guanylate cyclase.

There are two types of photoreceptor GCs found in the human retina: GC-E and GC-F. These essential enzymes are expressed in rod and cone photoreceptor cells, where they synthesize cGMP, the second messenger in phototransduction (Koch and Dell'Orco, 2015). Photoreceptor GCs are orphan receptors that lack ligands to bind their extracellular domains, but in cooperation with neuronal calcium sensor proteins

(GCAPs), RD3 or bicarbonate, they form complexes that control cGMP synthesis (Peshenko et al., 2011b; Sulmann et al., 2017; Wimberg et al., 2018a).

In vertebrates, the photoreceptor-specific guanylyl cyclases are regulated by guanylyl cyclase activating proteins (GCAPs), which attach to their intracellular sites, allowing a dynamic interaction and interplay of regulatory control (Peshenko *et al.*, 2011b; Sulmann *et al.*, 2017). GCAPs are calcium sensor proteins that respond to changes in cytoplasmic calcium concentration ($[Ca2+]$) with a conformational change thereby switching the target photoreceptor GCs to the active state (see Figure 5) (Dizhoor and Peshenko, 2021; Koch and Dell'Orco, 2015). For instance, the binding of Ca^{2+}-free /Mg^{2+}-bound GCAP1, which shifts the balance to the active state, facilitates the activation of GC-E. Ca^{2+}-bound GCAP1, which maintains the inactive state, inhibits the cyclase.

Point mutations in the GUCY2D and GUCA1A genes coding for GC-E and GCAP1 in humans can cause various forms of retinal degeneration, including cone-rod dystrophies (CORD6) and Leber's congenital amaurosis (LCA). CORD6 is an early-onset progressing degeneration of cone and rod functions due to point mutations in the GC-E with several mutations cluster in dimerization domain, for example in specific positions E837, R838, T839 (Sharon et al., 2018). LCA is a particularly severe type of retinal dysfunction that results in blindness either after birth or during the first year of life. People with LCA type 1 have point mutations in GUCY2D, which can cause GC-E dysfunction in living cone photoreceptor cells, which can be dispersed throughout the entire enzyme (Sharon *et al.*, 2018). The relevant pathological studies of both CORD6 and LCA were caused by the abnormalities of Ca^{2+} sensitivity of the GC-GCAP complex (Duda and Koch, 2002; Koch et al., 2002; Sharon *et al.*, 2018; Zagel et al., 2013). In this scenario, the rods were still functional due to their expression of GC-F, but they deteriorate progressively at later stages of the disease (Sharma et al., 2023). Although no mutations of GC-F were found that correlate with retinal diseases, the knowledge about photoreceptor GCs including GC-F and their regulatory interactions

with GCAPs can potentially shed light on the pathology of LCA opening routes for gene therapy (Jacobson et al., 2022).
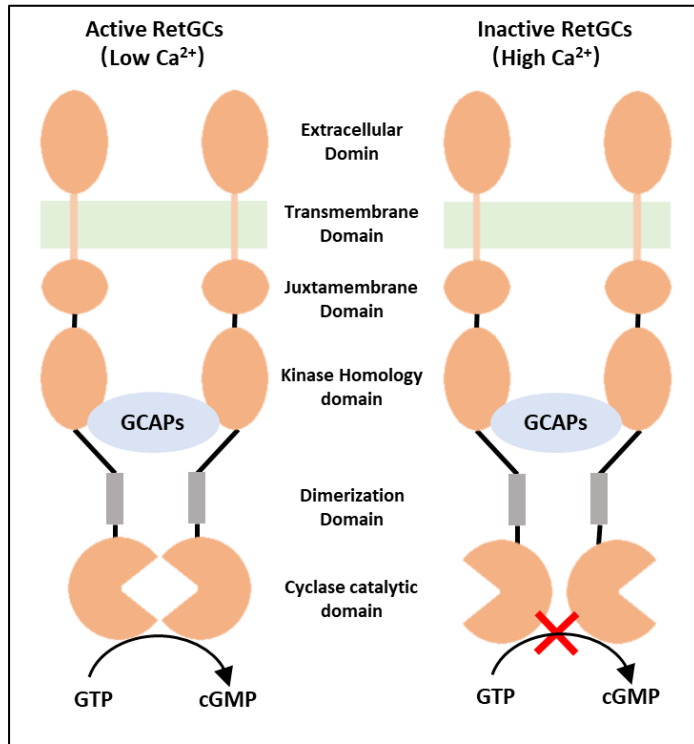
Figure 5: Illustration of photoreceptor GCs regulated by Guanylate Cyclase Activating Proteins (GCAPs). The small Ca^{2+} sensor proteins named GCAPs depend on the concentration of Ca^{2+} when modulating cyclase activity of RetGC. GCAPs undergo a conformational change and lose their bound calcium ions which probably leads to rearrangements in the guanylate cyclase structure and enhances GTP utilization.

1.2.2 The natriuretic peptide coupled guanylate cyclases.

The genes of Natriuretic peptide receptor 1 (*Npr1*) and Natriuretic peptide receptor 2 (*Npr2*) encode the natriuretic peptide-coupled guanylate cyclases GC-A and GC-B, respectively. In contrast to photoreceptor GCs, the extracellular ligand domains of these receptors can bind to natriuretic peptides (ANP, BNP, and CNP), enabling the GCs that switch to an active state (Kuhn, 2016). Both GC-A and GC-B exist as homodimers or homotetramer in their native state (without ligand activation) and can also oligomerize (Iwata et al., 1991; Langenickel et al., 2004; Potter et al., 2009; Shuhaibar et al., 2016). The binding of ligands does not lead to additional

oligomerization of GC-A (Chinkers and Wilson, 1992; Iwata *et al.*, 1991). In terms of receptor binding preferences, GC-A favors ANP>BNP>CNP, whereas GC-B displays a preference for CNP>ANP>BNP (Bennett et al., 1991; Koller et al., 1991; Suga et al., 1992).

Phosphorylation of serine and threonine sites in GC-A and GC-B is essential for hormonal activation, while dephosphorylation leads to inactivation. The ANP and BNP molecules bind to GC-A, inducing the monomer closer together in the juxtamembrane regions in a stoichiometric ratio of 1:2 (Bennett *et al.*, 1991; Koller *et al.*, 1991; Labrecque et al., 2001). Nonetheless, activation of GC-A is regulated via peptides inducing conformational changes in KHD, which relieves the inhibition of GCD. Additionally, in the basal state, the N-terminal portion of KHD is highly phosphorylated containing five serine and two threonine residues (Kuhn, 2016; Potter and Hunter, 1998; Schroter et al., 2010; Yoder et al., 2010). Similar to GC-A, KHD phosphorylation or dephosphorylation is also critical for controlling the state of GC-B, with the difference being that the serine and threonine sites in the juxtamembrane domain are also necessary for CNP-dependent GC-B activation (Shuhaibar *et al.*, 2016; Yoder et al., 2012; Yoder *et al.*, 2010).

The natriuretic peptides (NPs) and their receptors are widely distributed in tissues and cells of vertebrates. Specific gene-knockout in mice produced phenotypes in agreement with important physiological functions (see Table 1). These include vascular hemodynamics, metabolic regulation, immune response, and energy metabolism, renal, cardiac, endocrine, and neural function (Kuhn, 2016; Levin et al., 1998). For instance, ANP and BNP activate GC-A expressed in the cardiovascular system and metabolic organs, thereby regulating blood pressure and metabolism. CNP activates GC-B and the CNP/GC-B signaling system, which is expressed in various organs, but also in cardiovascular cell types (Pandey, 2021). Its proposed primary physiological function is to regulate skeletal growth (Kuhn, 2016).

All three NPs, particularly CNP, are synthesized in the brain and associated with neuronal functions such as neurotransmitter release, synaptic transmission, axonal branching, neuroprotection, and neuroendocrine regulation (Cao and Yang, 2008; Giovannini *et al.*, 2021; Potter *et al.*, 2009). Conversely, plasma ANP and BNP do not pass the blood-brain barrier and can only target the central nervous system outside this boundary (Levin *et al.*, 1998). Both GC-A and GC-B are present in the brain and co-act with neuropeptides to regulate brain development and function. Research studies have explored their involvement in synaptic plasticity in the hippocampus (Barmashenko et al., 2014; Decker et al., 2010), as well as their role in regulating the circadian clock (Olcese et al., 2002). NPs and their receptors have also been detected in the retina (Rollin et al., 2004). They were linked to dopaminergic and cholinergic signaling in amacrine cells (Abdelalim et al., 2008), and modulate GABA-receptor activity in bipolar cells (Yu et al., 2006). Additionally, the natriuretic peptides ANP and BNP provide protective effects against retinal neovascularization, besides their role in neuronal signaling (Spiranec Spes et al., 2020). Although natriuretic peptides (NPs) and their associated guanylate cyclases GC-A and GC-B exhibit multi-potential functions not only in the brain but also in the retina, the underlying mechanisms require further investigation.

Table 1: The cell and tissue distributions and gene-knockout phenotypes of natriuretic peptides and their receptors. (Adapted from Kailash N. Pandey et al., 2011)

Ligand/ Receptor	Cell distribution	Tissue distribution	Gene-knockout phenotype in mice
Nppa (ANP)	Myocytes, Leydig cells, granulosa-lutean cells	Atrium, ventricle, brain, kidney, testis, ovary	High blood pressure, hypertension, cardiac hypertrophy
Nppb (BNP)	Myocytes, ventricular cells	Atrium, ventricle, brain	Ventricular fibrosis, skeletal abnormalities, vascular complications
Nppc (CNP)	Endothelial Cells	Vascular endothelium, aorta, brain, heart, testis	Inhibition of long bone growth, dwarfism, abnormal chondrocyte differentiation
NPRA/GC-A	Renal epithelial and mesangial cells, vascular smooth muscle cells, endothelial cells, Leydig cells, granulosa cells, fibroblasts, Neuroblastoma, LLCPk-1, MDCK cells	Kidney, adrenal glands, brain, heart, liver, lung, olfactory, ovary, pituitary gland, placenta, testis, thymus, vascular beds, liver, ileum, and other tissues	High blood pressure, hypertension, cardiac hypertrophy and fibrosis, inflammation, volume overload, reduced testosterone
NPRB/GC-B	Vascular smooth muscle cells, fibroblasts, chondrocytes	Adrenal glands, brain, cartilage, fibroblast, heart, lung, ovary, pituitary gland, placenta, testis, thymus, vascular beds, and other tissues	Dwarfism, decreased adiposity, female sterility, seizures, vascular complication

1.3 The RD3 protein

The human retinal degeneration protein 3 (RD3) gene is primarily expressed in the retina, with the genomic localization of chromosome 1, open reading frame 36 (C1orf36) and has a 585bp transcript encoding a 195 amino acids protein of estimated molecular mass of 22.7 kDa (Azadi et al., 2010; Lavorgna et al., 2003). It has been demonstrated that RD3 is a highly conserved protein evolutionarily, most vertebrates share more than 80% identity in their amino acids sequence in comparison to human (see Figure 6). Thus the mouse was used as model organism for human RD3 relevant diseases (Molday et al., 2014).

In humans, RD3 is highly abundant in the retina, but also significantly expressed in the lungs and gastrointestinal tissues, whereas the expression rates in other tissues is much lower (Aravindan et al., 2017). The analysis of subcellular localization suggests that RD3 has a significant and strong cell-specific nuclear and cytoplasmic localization in photoreceptor cells (Friedman et al., 2006) and epithelial cells (Aravindan *et al.*, 2017). Further studies on transfected COS-1 cells have demonstrated a simultaneous subnuclear localization of RD3-fusion constructs (Azadi *et al.*, 2010; Friedman *et al.*, 2006), leading to the hypothesis that RD3 is implicated in the formation of subnuclear protein complexes that regulate transcription and splicing. For example, through in vitro and in vivo immunocytochemistry and immunoprecipitation assays, RD3 was found to co-localizes, and directly interacts with GC-E and GC-F in the retina, Friedman et al., (2006) observed a close proximity to leukemia-gene product (PML) bodies in the cell nucleus, but this specific co-localization might have been caused by the large Green-fluorescent protein fusion part that was use in the Friedman et al. study (Azadi *et al.*, 2010).

Current studies supported that the mutations in the RD3 of human patients correlate with the phenotypical characteristics of LCA12 (Cideciyan, 2010; Friedman *et al.*, 2006; Preising et al., 2012). However, the mechanisms underlying the relationship between

RD3 and clinical phenotypes such as thinner ganglion cell and nerve fiber layers in LCA12 patients remain unclear (Preising *et al.*, 2012).
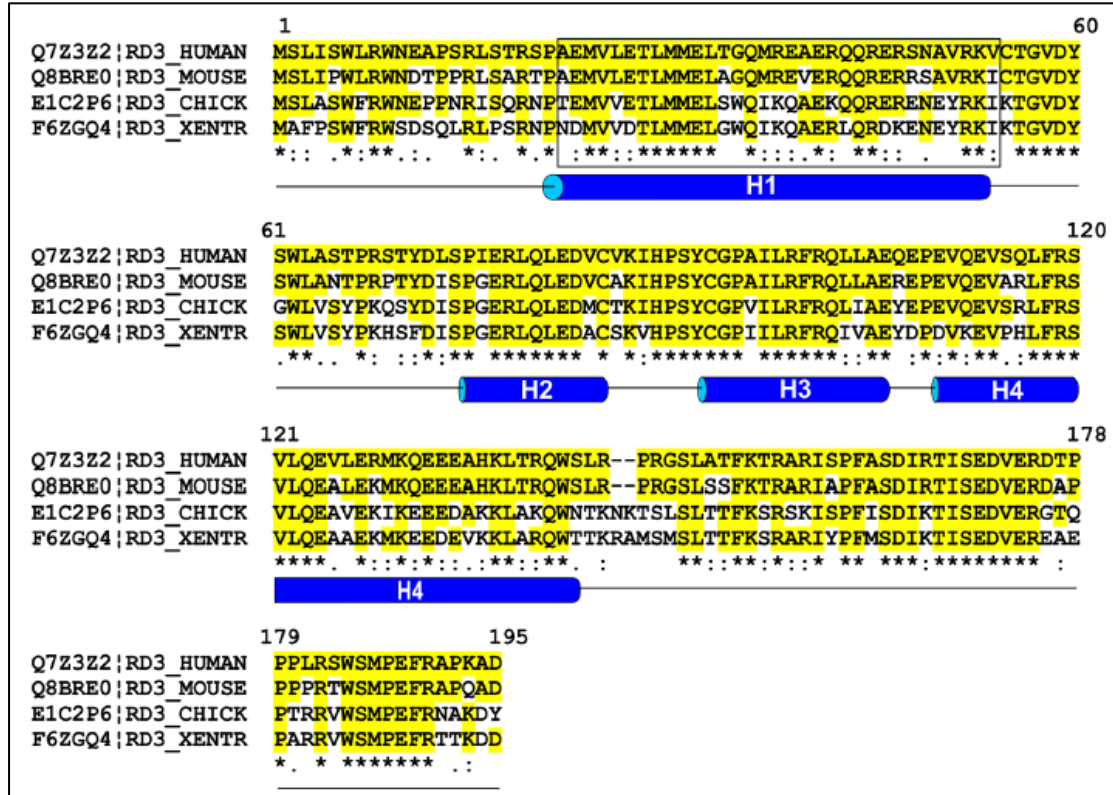
Figure 6: Alignment of amino acid sequences RD3 from different species (human, mouse, chicken, xenopus). The alignment shows four predicted α-helices highlighted in blue. The asterisks (*) indicate identical positions when compared to human RD3, while (:) indicates similar sequence positions. (Adapted from Molday et al., 2014).

1.3.1 The physiological role of RD3

Physiologically, RD3 plays a dominant role in photoreceptor cells and regulates two well characterized processes both involving photoreceptor GC-E and GC-F. RD3 facilitate the trafficking of photoreceptor GCs from inner to outer segments (Azadi *et al.*, 2010; Molday et al., 2013; Zulliger et al., 2015), and inhibits their GCAP-mediated activation at low cytoplasmic [Ca^{2+}] (Peshenko et al., 2011a; Peshenko et al., 2016).These processes are both crucial for the maintenance and function of photoreceptor cells.

In RD3-deficient mice, both GC-E and GC-F were trapped in the endoplasmic reticulum (ER), which led to photoreceptor degradation and rendered photoreceptor GCs undetectable (Azadi *et al.*, 2010; Molday *et al.*, 2013). Subsequent research found out implied that RD3 is involved in the transport of photoreceptor GCs, specifically GC-E, from the ER to the outer segments of photoreceptor cells (see Figure 7) (Azadi *et al.*, 2010; Molday *et al.*, 2013; Zulliger *et al.*, 2015). In these contexts, RD3, GCAP1, and photoreceptor GCs, form a trafficking complex in a vesicle-trafficking pathway associated with Rab5 and Rab11 (Zulliger *et al.*, 2015). Correct trafficking and incorporation of GC-E in photoreceptor outer segments is essential for cell survival and interaction of RD3 with GC-E is a crucial requirement for these processes (Peshenko and Dizhoor, 2020; Peshenko *et al.*, 2016; Plana-Bonamaiso et al., 2020).
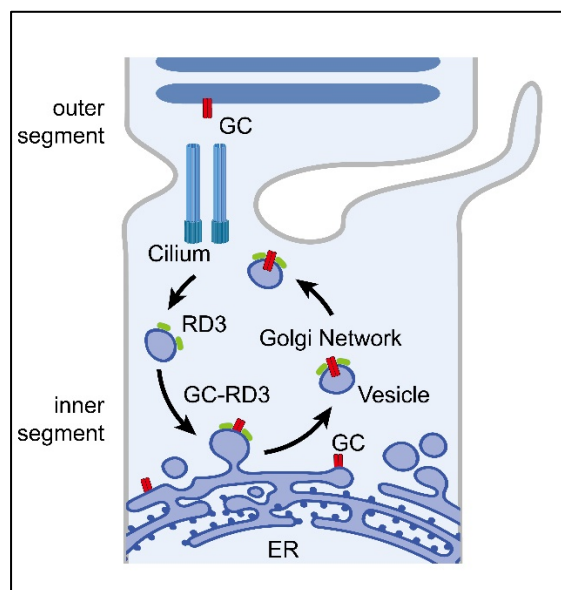
Figure 7: The putative role of RD3 in RetGC trafficking. In the inner segment, the RD3 binds to the photoreceptor GCs produced in the endoplasmic reticulum (ER) and forming up small vesicles containing RD3-GCs complex to inhibit the cyclase activities. These complexes transport with other adaptor proteins and translocate through the Golgi to the base of the connecting cilium to the outer segment. While the RD3 dissociates from GCs, possibly by protein folding or modification, as well as protein-protein interaction like GCAPs. The disassociated RD3 may be covered by vesicles again and sent back to the ER to start another

round of RD3-mediated photoreceptor GCs cellular trafficking.

Studies have shown a correlation between RD3 and two types of prompt photoreceptor degeneration (Peshenko *et al.*, 2011a; Peshenko *et al.*, 2016; Plana-Bonamaiso *et al.*, 2020). In normal state of photoreceptors, RD3 can inhibits the photoreceptor GCs basal activity and prevents photoreceptor GCs activation by GCAPs, to protect the normally proceed of trafficking described (see Figure 7 and 8 A) (Peshenko *et al.*, 2011a; Peshenko *et al.*, 2016). The absence of RD3 in the retina of a RD3 deficient mouse (*rd3⁻/rd3⁻*) directly links to accelerated photoreceptor degeneration and might be due to the uncontrollable synthesis of cGMP of the GCAPs-GCs complex in the inner segment. their might also lead to cell programmed death involving ER stress (see Figure 8 B) (Dizhoor et al., 2019; 2021; Plana-Bonamaiso *et al.*, 2020). In cases of retinal diseases, most of mutations in photoreceptor GCs especially GC-E, exhibit a greater affinity for binding with GCAPs, thereby increasing cGMP production in the photoreceptor, which helps antagonize inhibition from RD3 and plays a dominant role in rapid degeneration (see Figure 8 C). A reasonable pathway to rescue this process is to enhance the content of RD3 in the photoreceptor cell, since the re-gain of RD3 and deletion of GCAP1 suggested to slow down the degeneration in RD3 mouse retina (see Figure 8 D) (Dizhoor *et al.*, 2019; Peshenko et al., 2021). Interestingly, the absence of RD3 in the mouse retina was found to activate cell death, which could be another mechanism causing vision loss (Dizhoor *et al.*, 2019; Plana-Bonamaiso *et al.*, 2020).
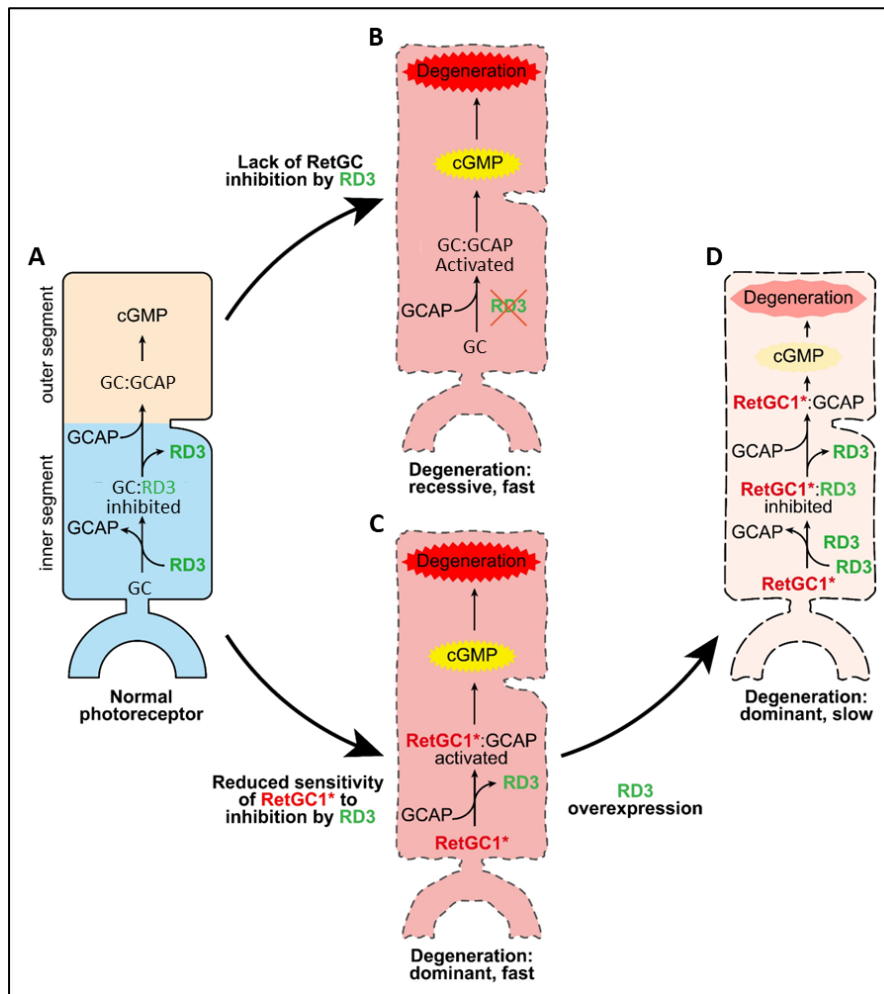
Figure 8: Proposed role of RD3 in mitigating two forms of rapid photoreceptor degeneration. A. In normal photoreceptors, RD3 can deliver GCs from the inner to the outer segment and control guanylate cyclase activation. Once the enzyme reaches the outer segment, GCAPs regulate RetGC by Ca^{2+} feedback. B. In RD3-deficient photoreceptors, GC and cGMP production in the outer segment was reduced, resulting in decreased light responses and potentially slow degeneration. In addition, unprotected GC activation in photoreceptors can cause rapid degeneration. C. In photoreceptors with GUCY2D mutations (RetGC1*) have increased enzyme affinity for GCAP, making RD3 regulation more difficult. This may activate a secondary degeneration pathway similar to that observed in RD3-deficient model. D. The enhanced levels of RD3 via overexpression allow for more efficient competition with GCAPs for RetGC1*, thus counteracting the RD3-based apoptotic pathway. (Adapted from Igor V. Peshenko et al., 2021)

Although studies have highlighted the significance of RD3 in retina diseases, the specific underlying mechanisms are yet to be determined (Ames, 2022; Dizhoor *et al.*,

2021; Dizhoor and Peshenko, 2021; Pandey, 2021; Peshenko *et al.*, 2021; Sharma *et al.*, 2023). Another in vitro study discovered that purified RD3 stimulated an increase in guanylate kinase (GUK) activity, an enzyme involved in the nucleotide cycle, catalyzing the conversion of 5'-GMP to GDP (Wimberg *et al.*, 2018a). Both proteins directly interact and co-localize in photoreceptor inner segments and to a lesser extent in the outer plexiform layer in sections of the mouse retina. However, recent studies involving transgenic mice did not detect a regulatory impact of RD3 on GUK activity (Dizhoor *et al.*, 2021).

Aside from its role in photoreceptor cells, RD3 has been discovered to have a physiological function in neuroblastoma cells. The endogenous expression of RD3 in parental SHSY5Y neuroblastoma cell line is high but low in its aggressive subline metastatic site-derived aggressive cells (MSDACs). Notably, a knockout of RD3 in SHSY5Y results in increased cell migration, invasion, and metastatic potential. Upon RD3 re-expression in MSDACs, aggressive neuroblastoma clones derived from parental SH-SY5Y cells exhibited diminished potential for neuroblastoma progression (Khan et al., 2015).

The physiological role of RD3 in retinal have widely been reviewed (Azadi *et al.*, 2010; Dizhoor *et al.*, 2021; Peshenko and Dizhoor, 2020; Peshenko *et al.*, 2011a; Peshenko *et al.*, 2021; Plana-Bonamaiso *et al.*, 2020; Wimberg *et al.*, 2018a), but the question whether degeneration of photoreceptors caused by the dominant mutations in photoreceptor GCs and GCAP1 can be partially rescued by overexpression of RD3 still needs to be addressed. For the presence of RD3 in non-retinal tissue several questions remain unsolved, for example its expression profile in brain tissue and the identity of its non-retinal targets. A reasonable question in this context is whether GCs activated by natriuretic peptide can also be regulated by RD3. A necessary condition for such a regulation would be the expression of RD3 and GCs in the same tissue.

1.3.2   The pathological role of RD3

Genetic alterations and structural mutations of RD3 may have a significant impact on disease progression. As first mentioned above, RD3 genetic deficiencies and mutations can lead to early-onset photoreceptor degeneration in patients diagnosed with Leber congenital amaurosis type 12 (LCA 12) (Azadi *et al.*, 2010; Friedman *et al.*, 2006; Molday *et al.*, 2013; Perrault et al., 2013; Wimberg *et al.*, 2018a). Furthermore, the loss of RD3 transcript expression correlates with progressive pathogenesis of neuroblastoma patients (Somasundaram et al., 2019).

RD3 is a distinctive protein exhibiting minimal homology to other proteins (Peshenko et al., 2019). It folds into a four-helix bundle structure, characterized by helix α1: P21–V51; α2: P75–K87; α3: P90–Q107; α4: V111–T139, as demonstrated by nuclear magnetic resonance spectroscopy analysis (see Figure 9 A) (Ames, 2022; Peshenko and Dizhoor, 2020; Peshenko et al., 2019). These structural variations can produce either pathogenic or benign effects on the LCA12 vision impairment. The nonsense mutations of RD3 are considered to be pathogenic variants, including R38X, E46X, and Y60X (Perrault *et al.*, 2013; Preising *et al.*, 2012). These mutations trigger the RD3 protein to undergo premature termination, thereby decreasing the gene product and removing the mRNA preceding translation. The R38X and E46X are both located in the helix α1, causing truncation of the RD3 protein that excludes amino acids 38-99 and 46-99 (see Figure 9 B). Notably, the E46 site demonstrates two distinct mutations that affect the codon (Perrault *et al.*, 2013). The Y60X mutation, which settles on the loop connecting helix α1 and α2, was predicted to result in the truncation of about two-thirds of the gene product. This mutation was only shown to be affected in the homozygous state. (Preising *et al.*, 2012). Additional studies were conducted to comprehend RD3 mutations in LCA12, which reveal that the majority of variations in patients are benign (Friedman *et al.*, 2006; Perrault *et al.*, 2013; Peshenko and Dizhoor, 2020). However, these mutations may weaken the RD3 affinity to photoreceptor GCs. Accordingly, Igor V. Peshenko and Alexander M. Dizhoor (2020) concluded from an extensive site-directed mutagenesis study that two clusters of surface-exposed residues are capable of suppressing RD3's ability to inhibit RetGC1. The first cluster

comprises helices α1 and α2, and loop 1/2, with functional residues of Y60, W62, and L63. The second cluster on the helix α3, has been identified as a crucial component of RD3's three-dimensional structure, that provides the interface for binding to the cyclase. Its exposure residues R99, R101, and Q102 (see Figure 9 B, C) (Peshenko and Dizhoor, 2020; Peshenko *et al.*, 2016; Peshenko *et al.*, 2019).

Although several studies have described mutations in RD3 causing LCA12, a severe form of retinal degeneration and cell dysfunction, the sequence changes in the RD3 gene are a very rare cause of LCA (Perrault *et al.*, 2013; Peshenko *et al.*, 2016; Preising *et al.*, 2012). Combining this information with evidence from mouse transgenic phenotypes, it suggests that the lack of RD3 transcript level is the primary cause of LCA12 disease. Furthermore, one of the previous studies reported that loss of RD3 correlates with the development of an aggressive neuroblastoma cancer (Khan et al., 2015). Although these findings seem to contradict an earlier study concluding that inactivation of both RD3 alleles in LCA12 patients does not correlate with extraocular symptoms (Perrault et al., 2013), a more recent study supports the direct involvement of RD3 loss in tumor development and progression (Somasundaram et al., 2019). Additionally, the study discovered that intensive multimodal therapy contributes to the loss of RD3 in surviving cells, resulting in disease progression (Somasundaram et al., 2019). This strongly emphasizes the significance of RD3 transcript alternation in its pathological function. At present however, any causal relationship between the abnormal regulation of RD3 expression and tumor development is unclear.
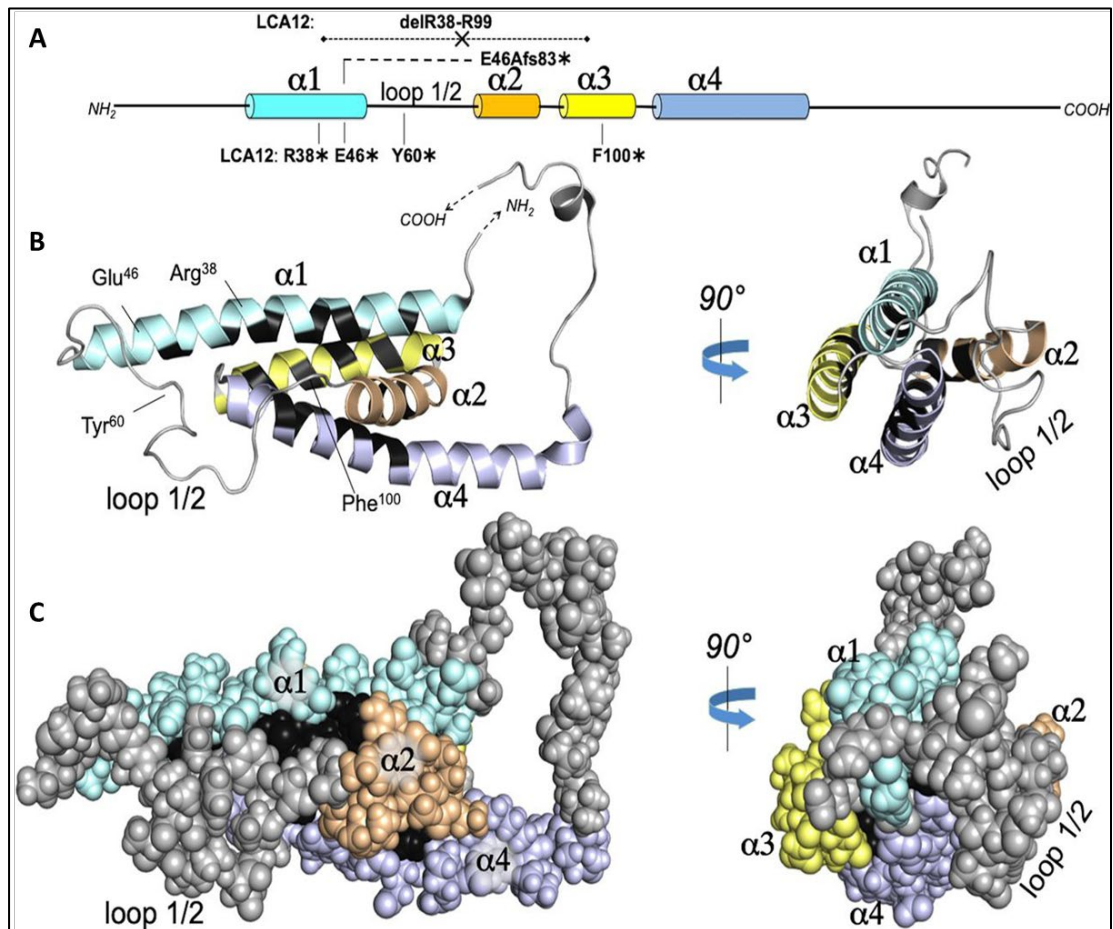
Figure 9: Illustration of RD3 protein structure with LCA12 pathological mutations. (A) RD3 four α-helices (cylinders α1 to α4) from the N terminal to the C terminal protein structure and its bridge unstructured regions (straight line) with the nonsense mutants R38*, E46*, Y60*, and F100* that is correlated to LCA12, as well as a two-base deletion causing a frameshift at residue 46 leading to premature termination downstream (E46Afs83*) (Friedman *et al.*, 2006; Perrault *et al.*, 2013; Preising *et al.*, 2012). (B) Three-dimensional structure of RD3 protein with the marked residues substituted by LCA12 nonsense mutations (Peshenko *et al.*, 2019). (C) Spheres based three-dimensional structure to illustrate the location of buried residues (in black) compared to surface-exposed residues (colored to match corresponding helices in the primary structure diagram) (Asterisk * stand for terminal codon X). (Adapted from Igor V. Peshenko and Alexander M. Dizhoor, 2020)

2. Objectives

The objective of this thesis is to understand the physiological and pathological role of RD3 in the CNS and its involvement in brain diseases. The questions posed and addressed are as follows:

<u>To understand the physiological role of RD3 in the brain, our questions were: what is the expression pattern of RD3 during mouse brain development? Which role might RD3 play in neuronal cells?</u>

The transient or dynamic expression of genes plays a crucial role in regulating diverse biological processes during development, including cell differentiation, tissue formation, and organ development. Previous studies (see introduction) showed a ubiquitous expression of RD3, but expression profiles during brain developmental were not reported. Therefore, brain and retina tissue samples are collected from mice at various developmental stages to analyze shifts in gene expression for *rd3*, *Npr1*, and *Npr2*. Then, we will focus on whether RD3 can regulate the gene products of *Npr1* and *Npr2* coding for GC-A and GC-B, respectively. This approach includes functional guanylate cyclase assays with cultured cells.

<u>Research indicates that RD3 has potential in tumor progression. We aim to investigate whether RD3 also has a potential impact in the cause and development of glioma.</u>

RD3 has demonstrated efficacy in prognostic and diagnostic approaches for progressive neuroblastoma. However, further studies are still missing to illustrate and elucidate the pathological involvement of RD3 in neurological cancers. The study will involve reviewing literature and analyzing large databases, as well as incorporating clinical samples from hospitals. These efforts will provide insight into the molecular characteristics of RD3 in gliomas or other cancers, potentially allowing for an understanding of its association with brain diseases and the manifestation of related phenotypes.

RD3 mutations are found in various diseases that are associated with benign or pathogenic processes. The inquiry we made is whether there is any genotype-phenotype-function correlation of mutations in RD3 and disease processes.

In the comprehensive assessment of RD3 expression in normal human tissues, strong immunoreactivities were observed in epithelial cells, suggesting a functional role for RD3 in these cells. In combination with the novel finding of RD3 in inducing the apoptosis of photoreceptor cells, this study will explore whether RD3 can also induce programmed cell death in human embryonic kidney derived epithelial cells (HEK293T cell) and the underlying mechanisms. Further, we are focus on somatic mutations of RD3 found in diseases of cancers and LCA 12 to understand the impact of point mutations on the three-dimensional structure of RD3, and how they might define a pathological role of RD3 in brain diseases progression.

3. Summary of the results

3.1 The novel physiological functions of RD3 in controlling the nucleotide cycle of the brain through the incorporation of natriuretic peptide guanylate cyclase. Additionally, its expression pattern in neuronal tissues. (Chen *et al.*, 2022).

To examine the potential mechanisms connected with RD3 function, our research targets were the two natriuretic peptide couple guanylate cyclases. These natriuretic peptide associated guanylate cyclases, present throughout the human body, share similar protein functional regions with those in the retina (Kuhn, 2016). In the amino acid blast alignment, the protein sequences of GC-A (P16066), GC-B (P20594), GC-E (Q02846), and GC-F (P51841) exhibited significant homology in the kinase homology domain, dimerization domain, and cyclase catalytic domain (see Figure 10). The presence of these functional intracellular domains is critical for signaling and ligand binding, which suggests that RD3 potentially interacts with GC-A and GC-B to catalyze the synthesis of cGMP.

Figure 10: The sequence alignment of selected human membrane bound guanylate cyclases, GC-A, GC-B, GC-E and GC-F. with its structure domain.

GC-A and GC-B are involved of many physiologically important processes including bone growth in human development (Kuhn, 2016). To further understand the physiological aspects of RD3 and its potential functional partners, we must first identify the tissues in which the gene is predominantly expressed and its developmental dynamics. Thus, we used qRT-PCR to map the genetic patterns of *rd3*, *Npr1*, and *Npr2* in mice tissues at different developmental stages. In agreement with published reports (Azadi *et al.*, 2010; Zulliger *et al.*, 2015), the high expression levels of *rd3* were observed in the mouse retina at P10, P20, and P30, while transcript levels for *Npr2* and *Npr1* were 10 to 100-fold lower (see Figure 11). In comparison to the mouse brain regions, *rd3* relative transcript level is highly abundant in retina, as evidenced by

several orders in normalized to β-actin expression (compare Figure 10 and 11 A). These findings are consistent with previous observations in human, confirmed that the retina being the prominent neuronal tissue of RD3 localization (Aravindan *et al.*, 2017; Chen *et al.*, 2022).
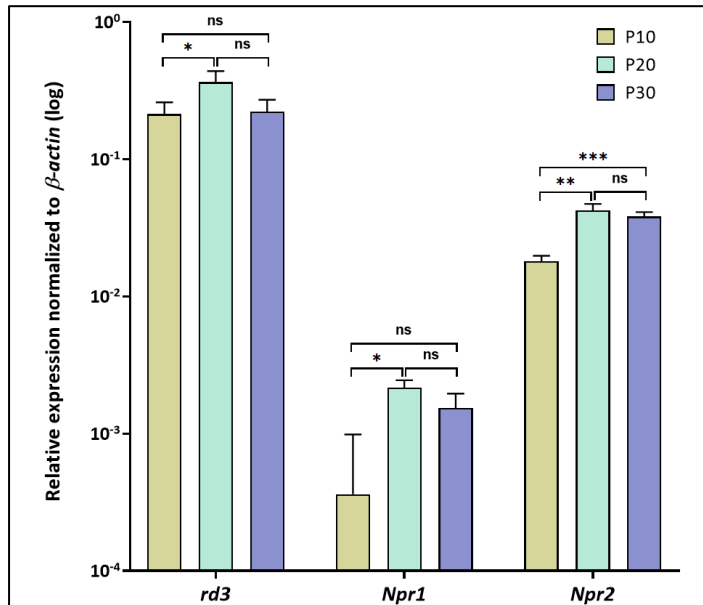
Figure 11: Relative gene expression of *rd3*, *Npr1*, and *Npr2* in mouse retina. The retina tissue at P10, P20 and P30 were collected for quantitative RT-PCR, gene expression profiles were normalized to β–actin expression. Statistical analysis was conducted using one-way ANOVA followed by Bonferroni's multiple comparisons test. The data are presented as mean ± SD.

Mouse cerebellum, hippocampus, neocortex, and olfactory bulb were harvested for qRT-PCR analysis of *rd3*, *Npr1* and *Npr2* from E14 to P60. In this context, *rd3* exhibited a lower transcript level than *Npr1* and *Npr2* (Figure 12 A compared to Figure 12 B, C), and reached the highest steady-state expression level in the olfactory bulb between P20 and P60. In *Npr1*, the highest expression was found in the cerebellum at P60 and in the olfactory bulb from P10 to P60. Furthermore, the gene expression of *Npr1* was more dynamic, showing a steeper progressive increase in expression levels of cerebellum and olfactory bulbs than *Npr2* and *rd3*. In the case of *Npr2*, a stable high expression was observed in all brain regions throughout development, which are generally 10-fold higher than in *rd3*, while reaching normalized expression levels in the

retina that were close to those observed in the cerebellum and olfactory bulb at P60.

Figure 12: The gene expression patterns of *rd3* (A), *Npr1* encoding GC-A (B), and *Npr2* encoding GC-B (C) were analyzed using quantitative RT-PCR in various neuronal tissues as

indicated. The relative expression was normalized to β-actin expression. Statistical analysis was based on one-way ANOVA followed by Bonferroni's multiple comparisons test. The data are presented as mean ± SD and were considered significant for $p \leq 0.05$ ($p \leq 0.05$ = *; $p \leq 0.01$ = **; $p \leq 0.001$ = ***; ns = not significant).

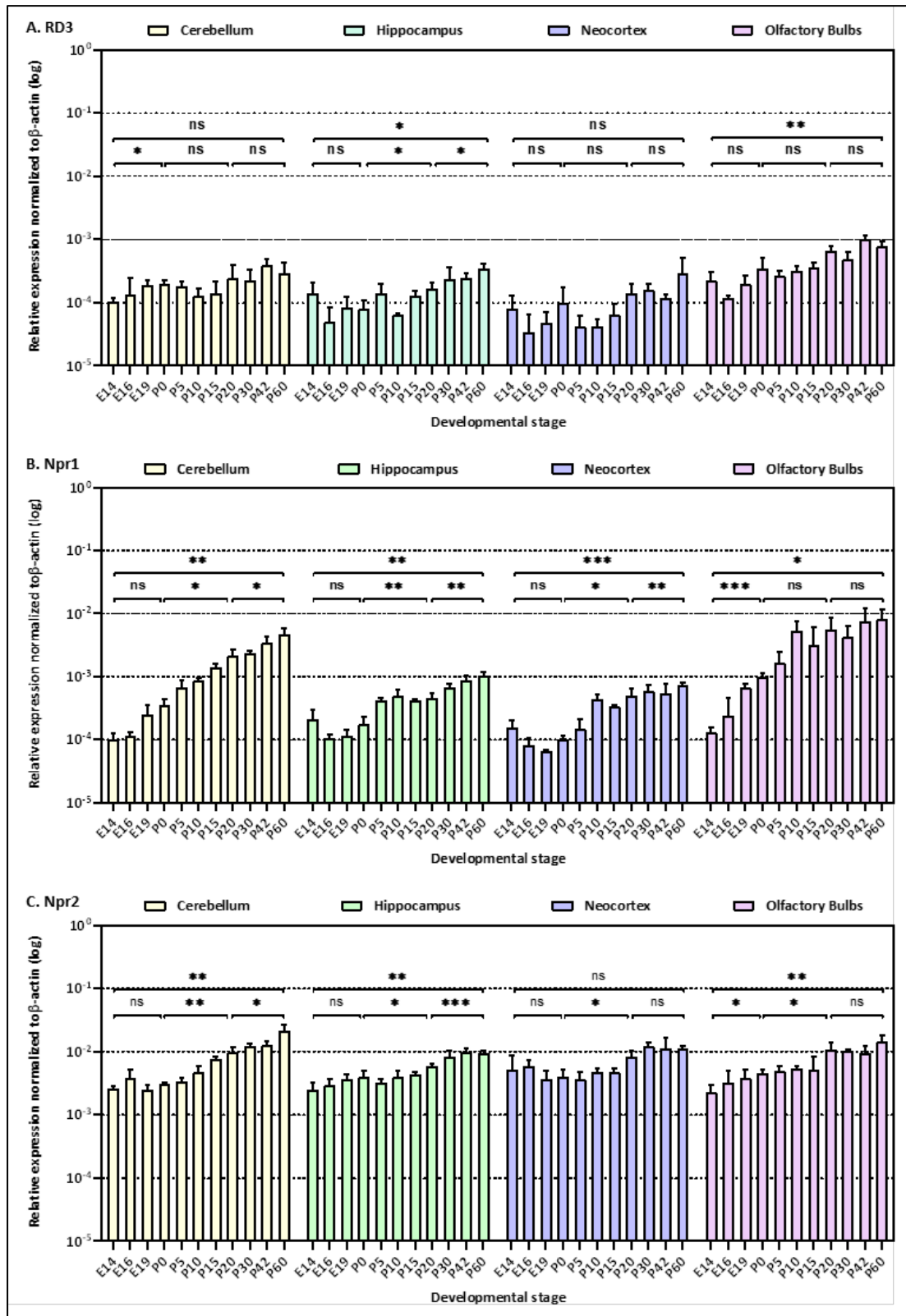As shown in Figure 13, the significant amino acid sequence homology in the cyclase catalase domain between photoreceptor GCs and natriuretic peptide receptor GCs suggests that membrane-bound GCs may possess comparable regulatory features. Despite the lack of a determined binding site, it is suggested that RD3 interacts with regions in the cytoplasmic portion of photoreceptor GC-E (Peshenko *et al.*, 2011b). To investigate the regulatory impact of RD3 on GC-A or GC-B, we utilized reversed-phase chromatography for the cyclase activity assay. Our initial step involved creating HEK 293T cells with transient heterologous GC-A and GC-B expression (see Figure 13). The human GC-A and GC-B inserts were cloned into pcDNA 3.1 backbone and transfected into HEK 293T cells (Chen *et al.*, 2022). The expression of GC proteins was confirmed by immunoblotting with antibodies specific to GCs, which identified a single band at around 120 kDa (see Figure 13 A, B). This finding aligns with the anticipated and documented molecular masses of membrane bound GCs (Kuhn, 2016). Conversely, cells that were not transfected (HEK 293T control) or were transfected with the empty pcDNA3.1 vector did not exhibit GC bands (see Figure 13 A). HA-tagged of GC-A and GC-B were utilized as positive controls in transfections. Polyclonal antibodies targeting GC-A or GC-B identified the HA-tagged GC bands with specificity. Surprisingly, the GC-A variant containing the tag provoked a greater response to the antibody than the untagged variant. To confirm the functional expression of both GCs, a ligand-dependent increase in GC activities was monitored. Increasing concentrations of natriuretic peptides ANP (activates GC-A) or CNP (activates GC-B) were incubated with HEK293T cell membranes containing GC-A or GC-B, and both peptides increased cGMP production approximately 10-fold and reached saturation above 4 µM (see Figures 13 C, D). In order to optimize our assay system, a cyclase activity assay was performed with measurements of GTP-

dependent cGMP synthesis (see Figures 13 E, F) and a time series (see Figures 13 G, H), resulting in a robust assay system suitable for further study.
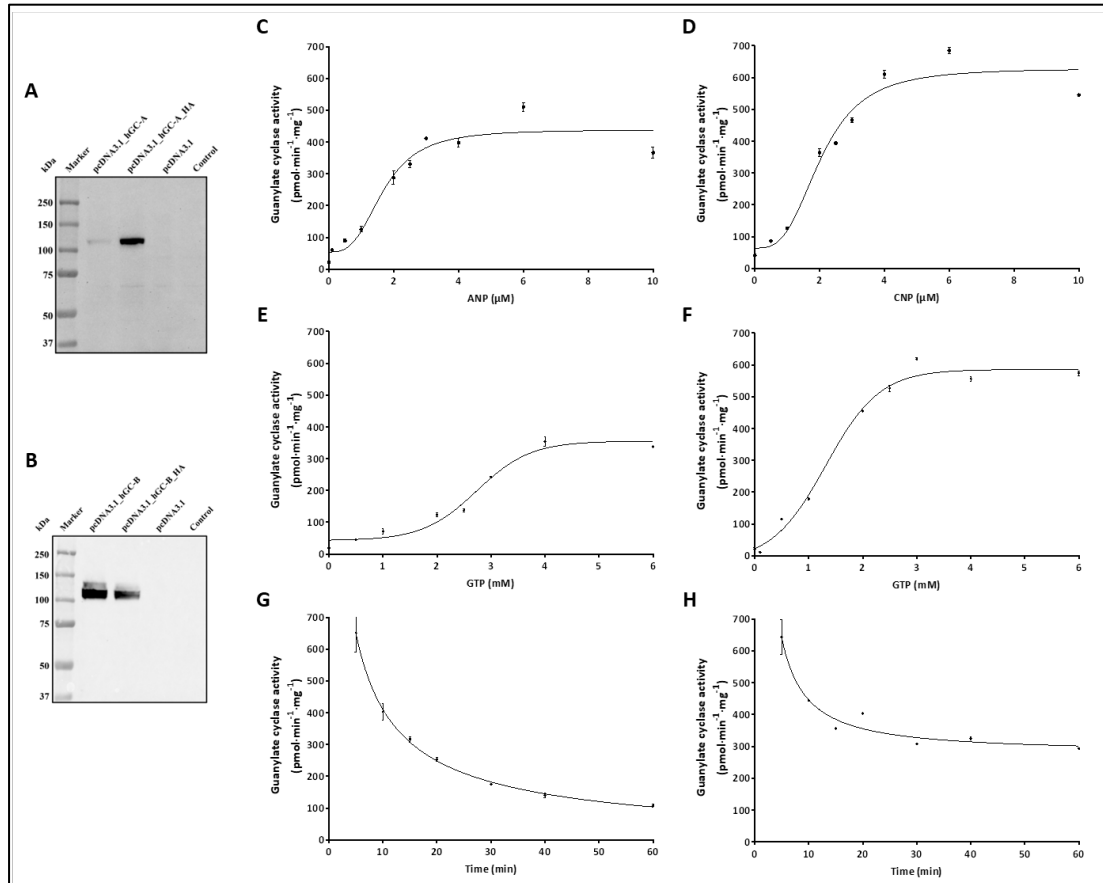
Figure 13: Expression of heterologous human GC-A and GC-B in HEK 293T cells. Cell membranes were collected for immunoblotting and primary antibodies were used to detect (A) GC-A and (B) GCB at a dilution of 1:1000 in both cases. Ligand activities were detected based on GC-activities in the regulation of (C) GC-A by ANP dose and of (D) GC-B by CNP dose. Additionally, GTP concentration was found to affect ligand activities in (E) and (F), while time was found to affect ligand activities in (G) and (H).

To evaluate the effect of RD3 on the cyclase activity of GC-A and GC-B, we utilized purified RD3. We treated membrane proteins from HEK 293T cells expressing recombinant GC-A and GC-B with 2 µM ANP and CNP, respectively, followed by incubation with increasing concentrations of purified RD3. Both GC-A and GC-B significantly decreased cGMP production when mixed with RD3 in a concentration

dependent manner. Replicated and reproducible results showed a half-maximal inhibition with an IC_{50} value (±SD) of 24 ± 13 nM RD3 for GC-A and 29 ± 21 nM RD3 for GC-B (see Figure 14 A, B). However, unlike in GC-E (see Figure 14 C), the RD3 suppression was incomplete at higher concentrations between 0.5 and 1 µM. Rather, the activity of GC-A and GC-B remained constant (see Figure 14 A, B). After eliminating the influence of unstable RD3 protein (Figure 14 C) and GC-E contamination, we confirmed that RD3 actively regulates the activity of GC-A and GC-B in a comparable, albeit not identical, manner to GC-E.
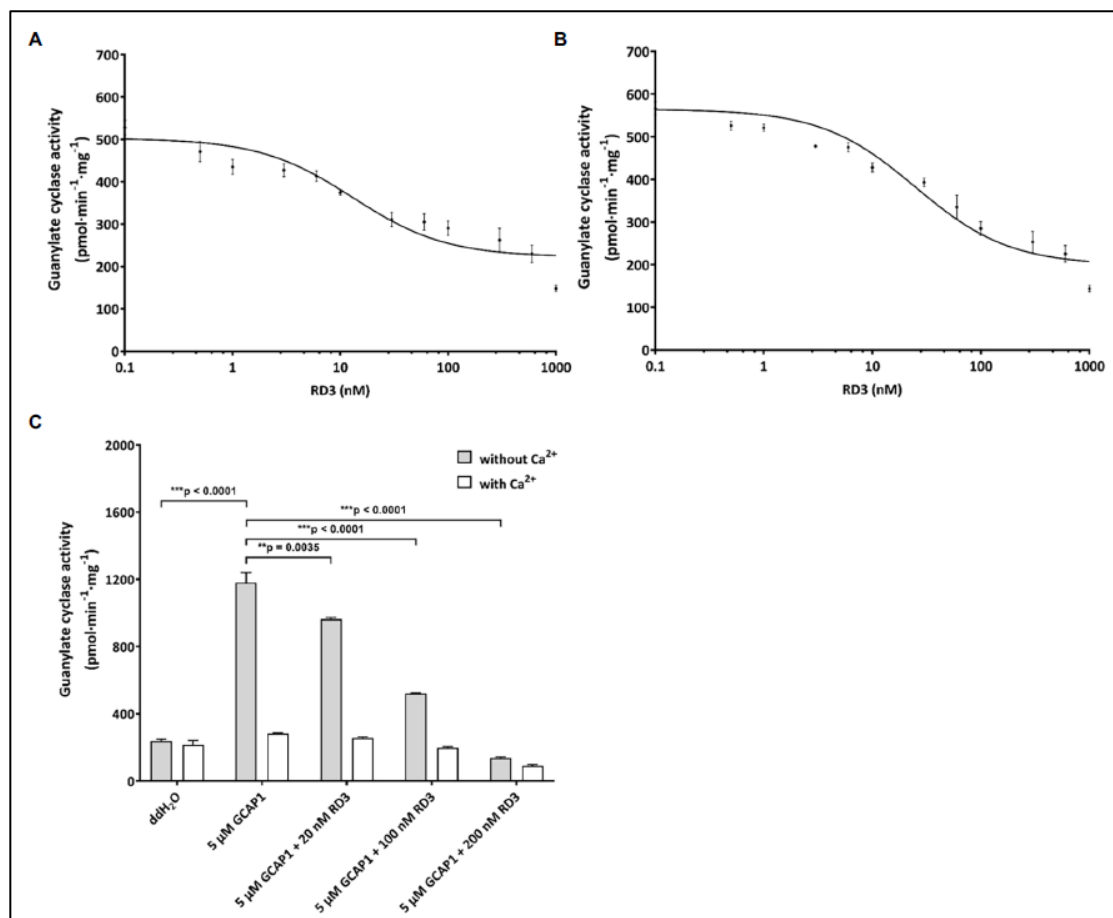
Figure 14: RD3 inhibits selected membrane GCs. Nine sets of reactions were performed to activate the (A) GC-A by 2 µM ANP, and (B) GC-B 2 µM CNP, further inhibition affect was determined by increasing concentrations of RD3. (C) The RD3 protein activity was tested by using GC-E expressed HEK293T cells in activated by 5 µM GCAP1 under the condition of Ca^{2+} absence. The addition of RD3 at concentrations of 20nM, 100nM, and 200nM resulted in a complete decrease in activity between 100 (**p = 4.511 x 10-5) and 200nM (***p = 7.409 x 10-

[6]), N = 3. No cGMP product was observed when double-distilled water (ddH2O) was added to GC-E in HEK293T cell membranes.

We extended our study to primary cultured neurons, astrocytes, and microglia from mice. Our findings revealed that there was a significant expression of *Npr2* in neurons and astrocytes, along with a notably high expression of *rd3* in astrocytes (see Figure 15 A). The prominent transcript levels of *Npr2* and *rd3* in astrocytes motivated us to examine and compare the regulatory characteristics of GC-A and GC-B in primary cultures of astrocytes. Endogenous GC activity levels of approximately 400 pmol x min^{-1} x mg^{-1} of protein were primarily attributed to both GC-A and GC-B, as depicted in Figure 15. These levels were observed under conditions where no exogenous natriuretic peptides were added, using ddH_2O. The addition of natriuretic peptides, specifically ANP and CNP, resulted in a two-fold increase in GC activity. The addition of RD3 at concentrations of 30 or 60 nM prevented the stimulated GC activity induced by ANP or CNP, resulting in only basal levels of GC activity similar to the non-stimulated case (see Figure 15 B). These findings indicated that endogenously expressed GC-A and GC-B in primary astrocyte cell culture were responsive to RD3, further supporting our results with recombinant GC constructs and suggesting a possible physiologically relevant regulation of natriuretic peptide activated GCs by RD3.
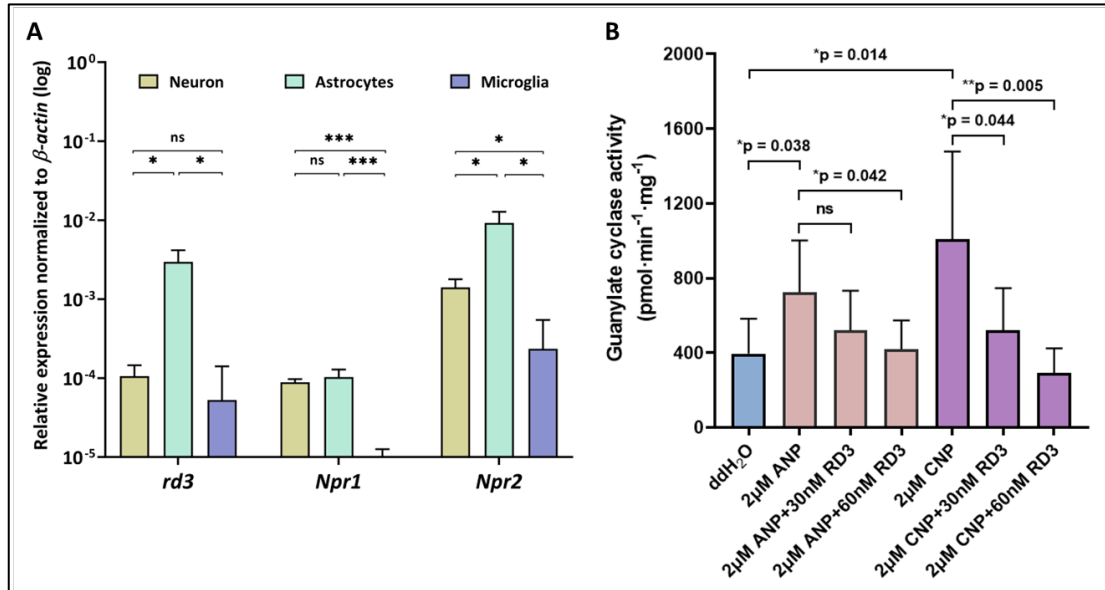
Figure 15: Gene expression profiles and protein cyclase activities in astrocytes. (A) Relative expression of *rd3*, *Npr1* and *Npr2* in neurons, astrocytes, and microglia was normalized to β-actin. Statistical analysis was performed using one-way ANOVA followed by Bonferroni's multiple comparisons test. The data are presented as mean ± SD and were considered significant for $p \leq 0.05$ ($p \leq 0.05$=*; $p \leq 0.01$=**; $p \leq 0.001$=***; ns= not significant). (B) RD3 inhibits GC-A and GC-B in astrocytes.

3.2 A comprehensive analysis for understanding the pathological role of RD3 in glioma.

The above data indicates that RD3 can inhibit cGMP synthesis in mouse astrocytes, the important cells that are crucial for several cellular brain progresses. In this chapter, I will summarize the investigations focusing on the potential pathological role of RD3 in astrocyte-related brain diseases. To date, there is no pathological or etiological indication of RD3 gene expression playing a role in glioma development or disease progression, but current public datasets such as TCGA (https://www.cancer.gov/tcga) provide useful information about hypothetical correlations of RD3 transcript levels and its impact in specific diseases. Accordingly, we first analyzed RD3 transcript levels in the TCGA GBM/LGG, GSE108474, GSE16011, and GSE7696 cohorts in different histological groups and found significant differences between non-tumor and glioblastoma tissue, but not in other gliomas like astrocytoma. When compared to other

glioma types, RD3 expression was generally low in glioblastoma (see Figure 16 A-D). We then performed qRT-PCR for RD3 expression in the glioma tissues from the EV cohort and found a significant downregulation of RD3 expression in GBM compared to non-tumor tissue (see Figure 16 E, expression normalized to TBP and HPRT1).
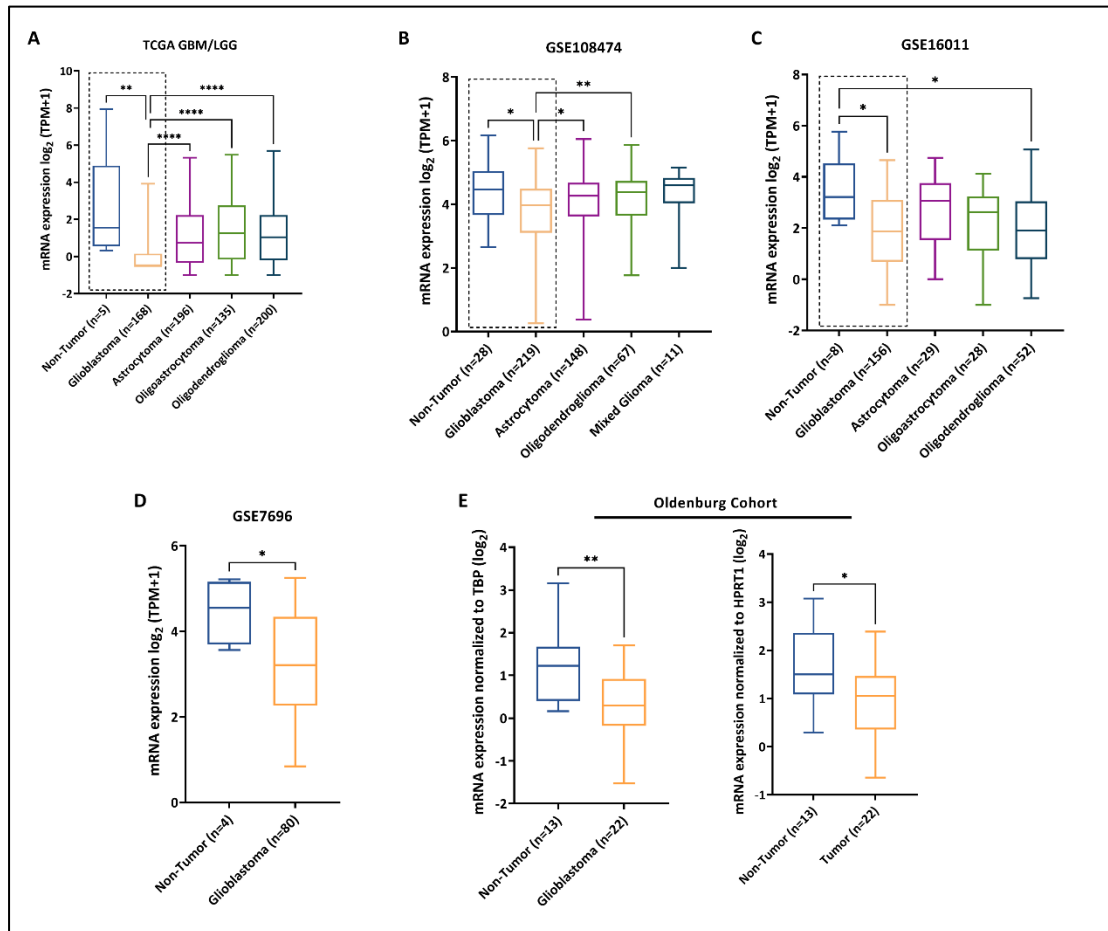
Figure 16: Differential expression of RD3 in glioma. (A) RNA-seq data from TGCA-GBM/LGG. (B) GSE108474, and (C) GSE16011 provide microarray gene expression data. The results indicate that RD3 expression is lower in glioblastoma compared to non-tumor and other gliomas. A further test was based on (D) GSE7696, and qRT-PCR analysis of the glioblastoma tissues from (E) the Oldenburg cohort. The statistical analysis used an unpaired t-test with significance levels were considered significant for $p \leq 0.05$ ($p \leq 0.05$=*; $p \leq 0.01$=**; $p \leq 0.001$=***; ns= not significant).

To examine the correlation between RD3 expression levels and clinical-pathological

characteristics, we divided data from TCGA-GBM/LGG (with 699 individuals) into high-expression and low-expression categories, based on the median expression of RD3 (see Table 2). The clinical features of age, gender, WHO grade, IDH status, primary therapy outcome, histological types, overall survival event (OS), disease specific survival (DSS) and progression free survival (PFI) were considered. OS in cancer research refers to the length of time from a cancer diagnosis or the start of cancer treatment until the patient's death due to any cause. DSS targets survival related to the particular disease under study, excluding deaths from other causes. PFI is used to assess the effectiveness of treatments in controlling the progression of cancer. In terms of the primary therapeutic outcome, the group with high RD3 expression displayed a significant rise in partial and complete response cases. When compared to the low expression group, no discrepancies were observed concerning progressive or stable disease cases. DSS and PFI supported these findings as most of the patients, who died of glioma, with or without treatment, are present in the low RD3 expression level group. Furthermore, the characteristics of RD3 expression revealed that the low RD3 group was classified into the following categories: age over 60 years, glioblastoma, isocitrate dehydrogenase wild type status (IDH wild type), and WHO grade G4. This study suggests a noteworthy reduction of RD3 in GBM, which may function as a biomarker for curative response.

Table 2: Association between RD3 expression and clinicopathological characteristics in the TCGA-GBM/LGG cohort

Characteristics	Low RD3 level	High RD3 level	P value
n	349	350	
Age, n (%)			< 0.001
> 60	108 (15.5%)	35 (5%)	
<= 60	241 (34.5%)	315 (45.1%)	
Gender, n (%)			0.234
Female	141 (20.2%)	157 (22.5%)	
Male	208 (29.8%)	193 (27.6%)	
WHO grade, n (%)			< 0.001
G2	79 (12.4%)	145 (22.8%)	
G3	111 (17.4%)	134 (21%)	
G4	142 (22.3%)	26 (4.1%)	
IDH status, n (%)			< 0.001
WT	185 (26.9%)	61 (8.9%)	
Mut	157 (22.8%)	286 (41.5%)	
Primary therapy outcome, n (%)			0.008
Progressive disease	55 (11.8%)	57 (12.3%)	
Stable disease	59 (12.7%)	89 (19.1%)	
Partial response	16 (3.4%)	49 (10.5%)	
Complete response	48 (10.3%)	92 (19.8%)	
Histological type, n (%)			< 0.001
Astrocytoma	81 (11.6%)	115 (16.5%)	
Oligoastrocytoma	50 (7.2%)	85 (12.2%)	
Oligodendroglioma	76 (10.9%)	124 (17.7%)	
Glioblastoma	142 (20.3%)	26 (3.7%)	
OS event, n (%)			< 0.001
Alive	167 (23.9%)	260 (37.2%)	
Dead	182 (26%)	90 (12.9%)	
DSS event, n (%)			< 0.001
Yes	161 (23.7%)	83 (12.2%)	
No	172 (25.4%)	262 (38.6%)	
PFI event, n (%)			< 0.001
Yes	205 (29.3%)	141 (20.2%)	
No	144 (20.6%)	209 (29.9%)	

From the above data, we found a strong association between the alteration in RD3

mRNA expression and glioblastoma. In order to validate this outcome, we assessed the prognostic significance of RD3 transcript levels in the databases of TCGA GBM/LGG, GSE108474, and GSE16011. Patients were divided into low and high RD3 mRNA expression subgroups according to 50 percentiles of RD3 expression, and overall survival curves with 95% CI (95% confidence interval shown as shadow), HR (hazard ratio), and p-value were generated using Kaplan-Meier Cox regression. Patients with glioma who had a higher expression of RD3 had a significantly better prognosis than those with lower expression according to the results of TCGA GBM/LGG (p<0.001, HR=0.35), GSE16011 (p=0.037, HR=0.76), and GSE106474 (p=0.002, HR=0.72), while the 5 years survival rate to lower RD3 expression is less than 25% (Figure 17 A-C). Additionally, data from healthy donors and GBM patients were selected from a multicohort study to perform a receiver operating characteristic (ROC) test to evaluate the diagnostic value of RD3 in GBM (Figure 17 D-I). If the area under the curve (AUC) is AUC > 0.5, the test effectively determines whether RD3 expression correlates with a higher survival rate in GBM patients compared to healthy donors. The current study's data sets show the following AUC values (in parentheses): TCGA (0.9339), GSE108474 (0.6670), GSE16011 (0.7792), GSE7696 (0.7969), TBP (0.7727), and HPRT1 (0.7168). All ROC curves had an AUC value greater than 0.5, indicating acceptable predictive ability that was significantly better than random chance. There was only one exception with the result of GSE108474, which showed a less obvious discrimination with an AUC value of 0.6670. Consequently, the assessment of the predictive ability suggested that RD3 has a potential as a biomarker for GBM prognosis and diagnosis.
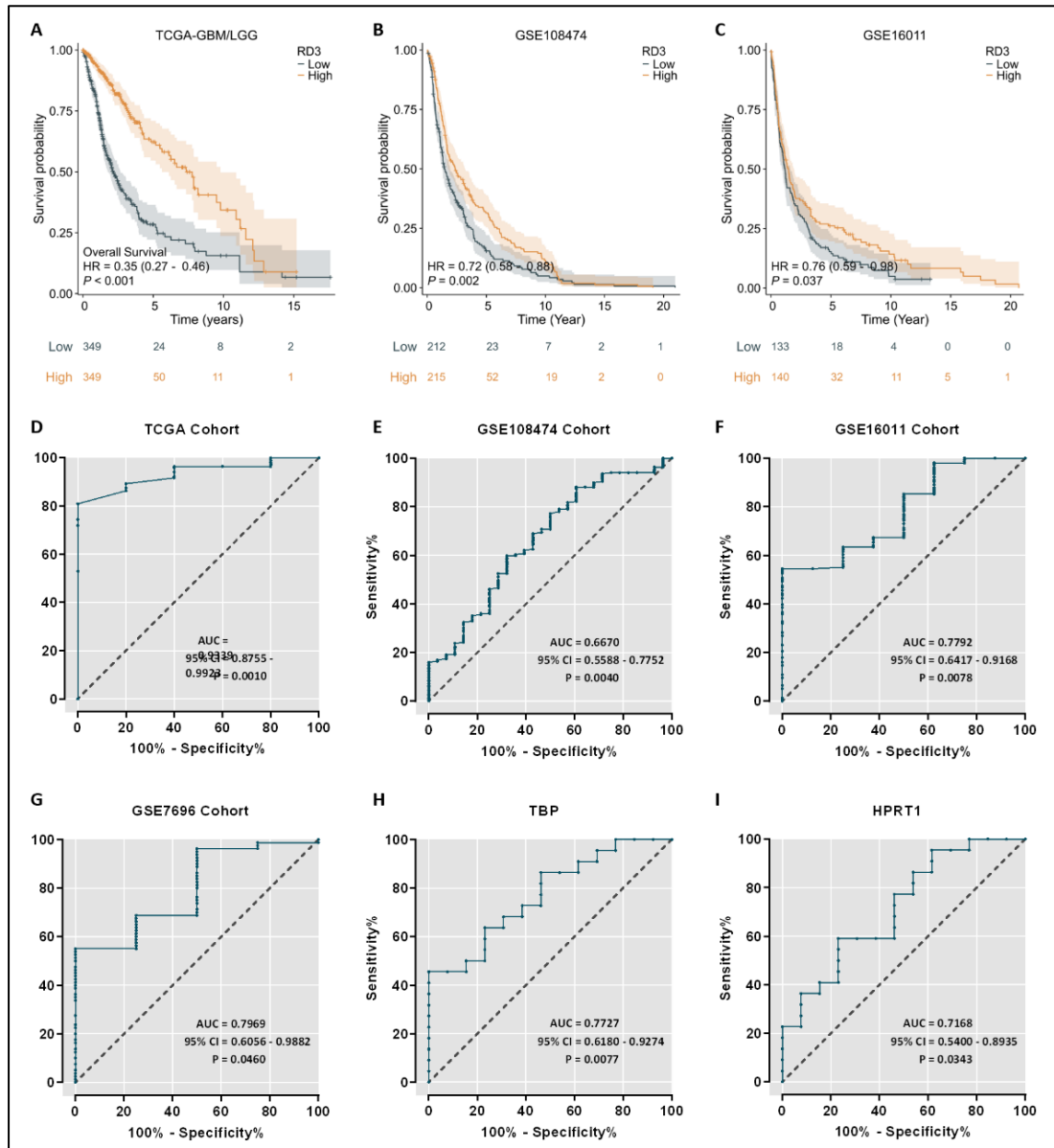
Figure 17: The Kaplan-Meier and receiver operating characteristic (ROC) curve of RD3 in patients with glioma. (A-C). The overall survival probability was assessed based on the RD3 transcript level, (D-I). The diagnostic test of RD3 in Glioblastoma. (HR: Hazard Ratio, AUC: Area Under Curve, 95%CI: 95% Confidence Interval).

3.3 RD3 mutants are associated with cell cycle arrest and apoptosis.

The presented results about RD3 in gliomas and reports in the literature (Somasundaram et al., 2019) correlate dysfunctional expression of RD3 with tumor development. Collectively, these investigations indicate an influence of RD3 on cell viability or even an indirect impact on cell cycle progression. So far, several studies

describe mutations in RD3 that cause LCA12, a severe form of retinal degeneration and cell dysfunction (Peshenko and Dizhoor, 2020; Peshenko et al., 2011b). In order to explore how RD3 expression might interfere with cell viability in non-retinal cells we selected amino acid positions that seem prone to functional impairment. For example, positions that are critical for the development of LCA12 or positions that are found in the RD3-target protein interface. Based on these reasons we designed and obtained RD3 point mutations R38L, R45W, R47H, R68W, P95S, and R119C (Figure 18 A, B). The residues R38 in helix α1 is a recessive mutation linked to LCA12 (Perrault et al., 2013). Positions R45 and R47 were inside the solvent-exposed ends that are connected by series of salt-bridges and belong to a cluster of mutations or polymorphisms found in patients with retinal dysfunctions (Azadi et al., 2010; Zulliger et al., 2015). The same counts for the residue R68. Residue P95 and R119 are also solvent-exposed in helix α3 and helix α4, respectively, and are present in short regions of the binding interface interacting with the target GC-E (Peshenko et al., 2016; Peshenko et al., 2019). We then transfected cells with RD3 and its variants and verified the expression of RD3 in cells by immunoblotting (Figure 18 C).
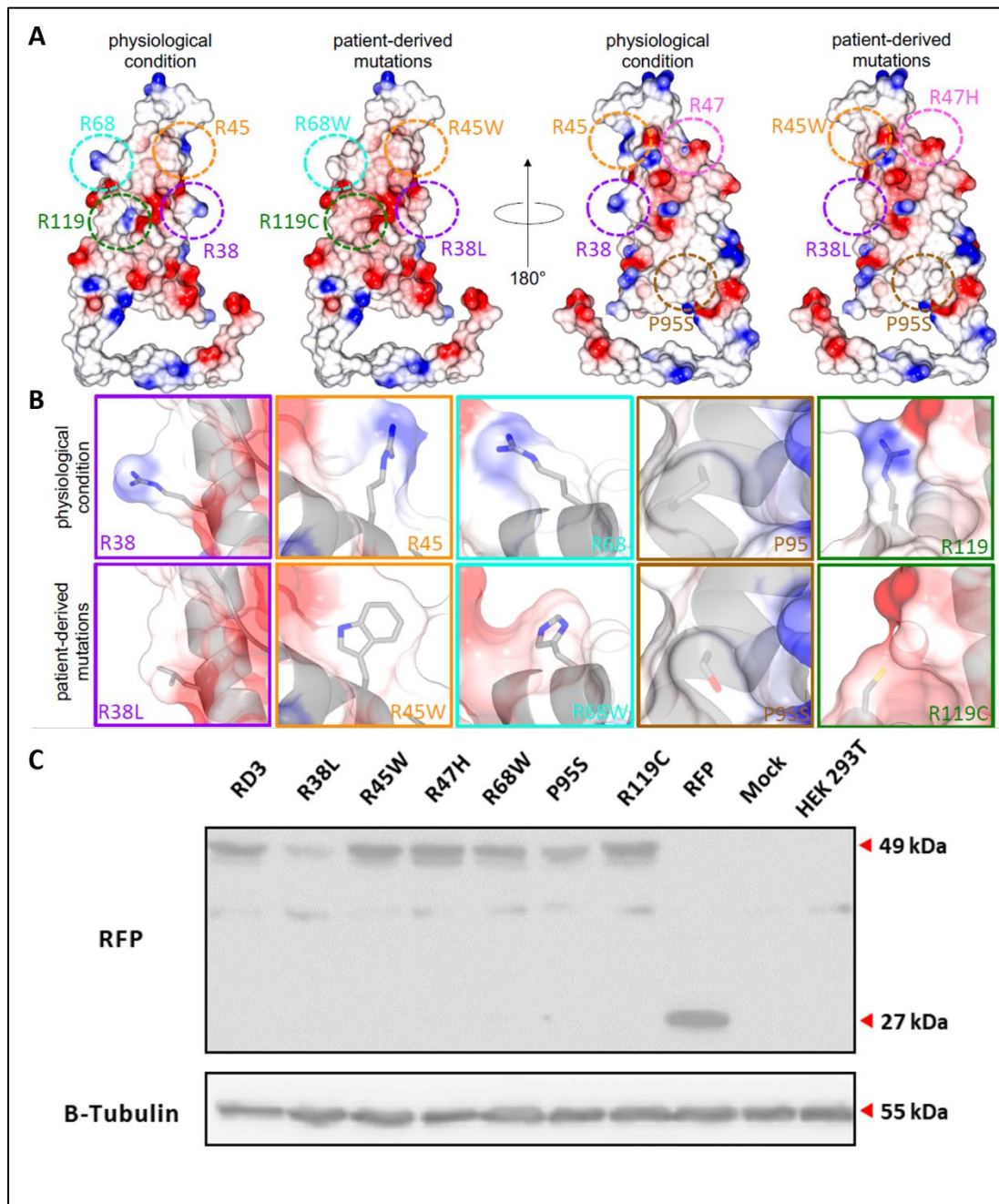
Figure 18: Human RD3 protein structure from PDB entry 6drf. (A) The structure shows electrostatic surface potentials, with residues highlighted by dashed circles that have roles in physiological conditions or were found in patients suffering from diseases. (B) Examine individual residues in native (upper row) and patient-related mutations (lower row) in RD3. native residues and patient-related mutations, which are represented by their side-chain moiety and an overlay of the transparent electrostatic surface potential with secondary structure representation. (C) Western blot test of RD3 and its variants was conducted after transfection in HEK293T cells, and the insertion was detected by the primary mouse anti-RFP antibody

(1:2,000). The band around 27 kDa represents the RFP, and at 49 kDa represents the fusion protein of RD3 and RFP (red fluorescence protein). The β-tubulin was used as housekeeping protein with molecular mass around 55 kDa and detected by its specific mouse derived antibody at dilution of 1:2,000.

Figure 19 shows the subcellular localized of the RD3 and its variants by immunocytochemistry assay in the HEK293T cells after 24 hours of transfection. The results revealed that RD3 and its variants have a similar subcellular localization; they were detected in the cell cytosol and in vesicles. The nuclei of strongly red fluorescence protein (RFP)-positive cells are allocated in the interphase of the M phase. These results indicated that overexpression of RD3 and its variants might be involved and seem to interfere with cellular functions of HEK293T.
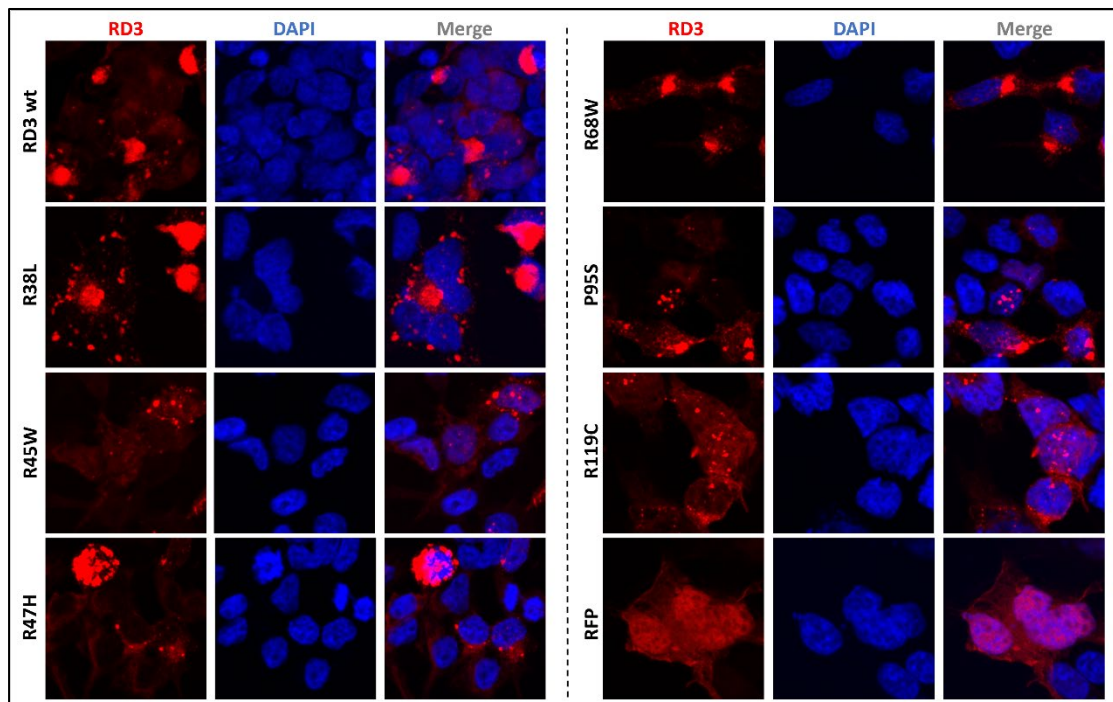
Figure 19: Subcellular localization of RD3 and its variants in the HEK 293T cells. The cells expressing red-fluorescence protein (RFP) were labeled in red, and the cell nuclei were stained with DAPI and shown in blue.

The MTT assay measures cellular metabolic activity as an indicator of cell viability,

proliferation, and cytotoxicity. To analyze the effects of RD3 transient overexpression on HEK293T cells, we employed this assay at 24, 48, and 72 hours post-transfection. Our results demonstrated significantly reduced cell survival (OD_{590} value) in cells transfected with RD3 wild-type plasmids compared to control groups (RFP empty vector, mock, and untreated cells) at all examined time points (Figure 20 A). At 24 hours, there were no significant differences between RD3 mutants and the RD3 wild type in subsequent measurements. However, after 48 hours, only the R38L variant showed a significant improvement in cell viability. Additionally, at 72 hours, no significant differences were observed between R68W and the wild type. Conversely, variants such as R38L, R45W, R47H, P95S, and R119C exhibited more viable cells than the RD3 wild type (Figure 20 B). Compared to the control groups, all variants demonstrated a substantial negative impact on cell viability at 48 and 72 hours. For instance, while the OD_{590} value for control groups ranged from 1 to 2 at 48 hours, it was less than 0.4 for HEK 293 cells transfected with RD3 variants. These findings indicated that overexpression of RD3 and its variants influences the cell viability of HEK293T.
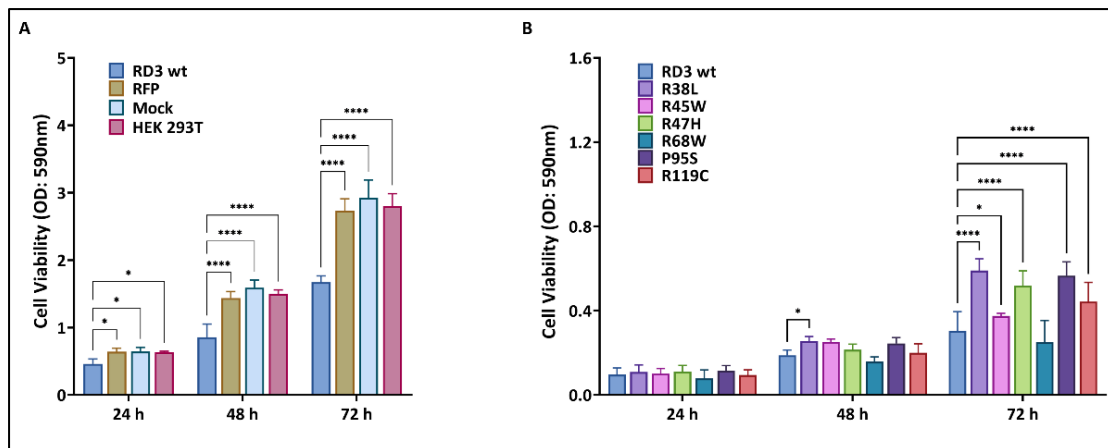
Figure 20. Cell viability analysis of RD3 and its variants. The MTT assay were performed at 24h, 48h, and 72h after transfection. (A) The RD3 wild type was compared to the control group, and (B) the RD3 wild type was compared to the variants. The statistical analysis used a two-way ANOVA (P value: * < 0.05, ** < 0.01, *** < 0.001, **** < 0.0001).

Cell cycle arrest and apoptosis are crucial processes that affect cell growth, therefore we wanted to determine whether transfection of HEK293T cells with RD3 and its pathological variants regulates cell cycle progression and programmed death. To investigate how cell cycle progression would be affected by RD3 and its variant, post-transfected cells were harvested and fixed, nuclear DNA content was measured using DAPI and fluorescence-activated cell sorting (FACS) analysis. Due to the limitation of transient cell transfection efficiency, a cell sorting step based on RFP tag was performed on flow cytometry. Followed with the measurement, the results showed an increase in G2/M phase of RD3, and its variants compared to transfections with an empty RFP vector and a mock transfection (Figure 21 A, B). The summary of distribution of cell cycle phases in five rounds of replicates showed a higher proportion of G2/M phase in the RD3 experimental group and a lower proportion of G0/G1 phase in the control group (Figure 21 C).

Subsequent statistical analysis revealed that in G1 phase cells, only R38L showed a significant decrease, while RD3 wild type, R45W, R47H, R68W, P95S and R119C showed a slightly downregulated trend compared to control (Figure 21 D). In S phase cells, there were no significant differences between experimental and control groups, but a moderate decrease was observed (Figure 21 E). In G2/M phase cells, R38L and R68W show a significant increase, while the others show a global upward trend compared to control RFP and mock. These results showed that RD3 and its variant can disrupt the normal cell cycle of HEK293T cells by arresting these cells in the G2/M phase.
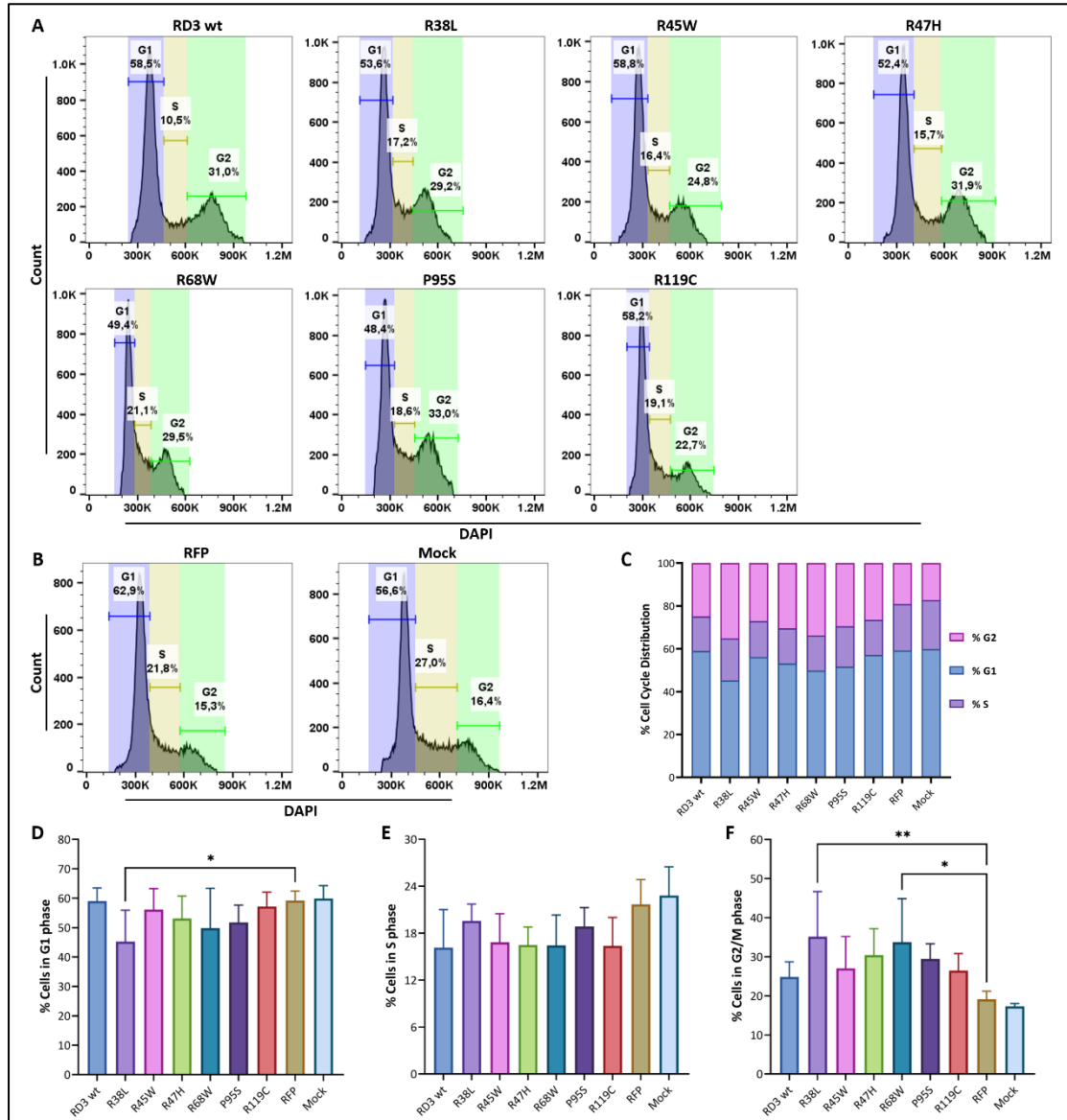
Figure 21. Cell cycle arrest analysis of RD3 and its variants in HEK293T cells. The transfected cells were collected after 24 hours of incubation and stained with DAPI. Flow cytometry was used to detect the distribution of cells across the cell cycle of (A) RD3 and its variants were compared to the (B) empty vector and mock control. (C) The summary of cell cycle distribution was obtained from 5 replicates. The percentage of cells across the cell cycle was analyzed using ANOVA. The results showed a significant difference in the distribution of cells in (D) G1 phase, (E) S phase, and (F) G2/M phase. The statistical analysis used a two-way ANOVA with significance levels of * < 0.05, ** < 0.01, *** < 0.001, and **** < 0.0001.

Disruption of the cell cycle by RD3 could point to an induction of apoptosis by RD3 and

its point mutants. We investigated a possible induction of apoptosis in HEK293T cells, which were carefully collected after transfection and digested with 0.05% trypsin-EDTA. DAPI and Annexin V APC conjugates were used for staining to detect programmed cell death. Using flow cytometry, we first sorted cells by the RFP tag to find positive cell populations of RD3 and its variants. The cells then were selected for measurement, while the unstained cells were used to assist the gate set separating the cell cluster of life (DAPI-, APC-), early apoptosis (DAPI-, APC+), late apoptosis (DAPI+, APC+) and death stages (DAPI+, APC-). Results in Figure 22 A and B showed the cell distribution after apoptosis indicator staining in RD3 and its variants transfected HEK 293T cells after 24 hours. It is clear, in the RFP and Mock group that there are more cells alive than in the cell populations positive with RD3 and its variants. Applying the statistical analysis of the replications, the summary of cell distribution showed that cell populations of RD3, and its variants were mostly present in early apoptosis, with lower number of live cells and similar portion of dead cells in comparison to control groups (Figure 22 C). The following analysis exhibited a significant increase of apoptotic cells in RD3 transfected cells compared to RFP, Mock, and HEK293T control groups (Figure 22 C). While the number of apoptotic cells in R38L, R45W, R47H, P95S and R119C mutants were markedly less than in RD3 wild type, and R68W showed no difference, in accordance with the MTT results (Figure 20).
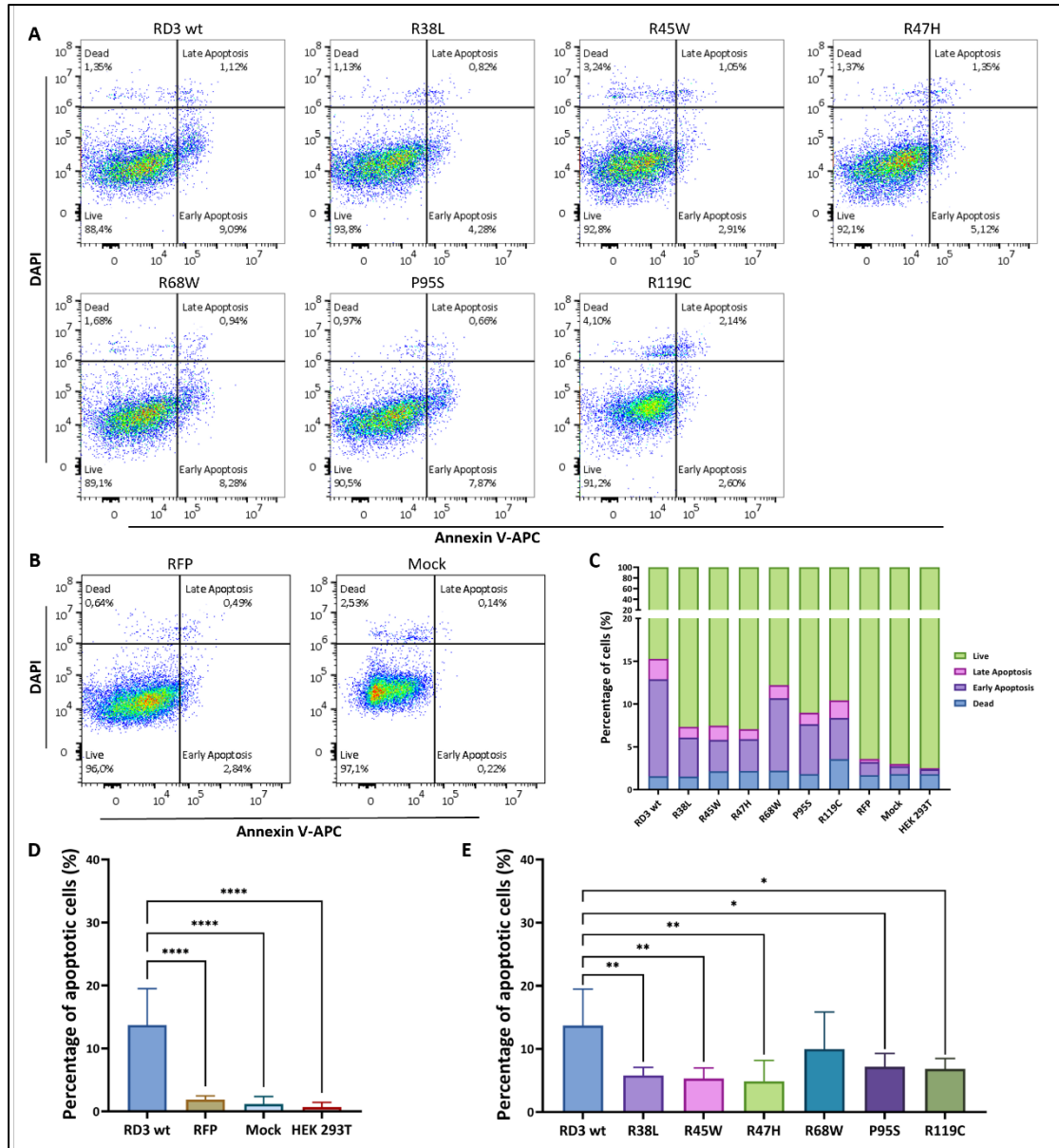
Figure 22: Cell apoptosis analysis of RD3 and its variants. Flow cytometry was used to analyze the programmed cell death of transfected HEK 293T cells. The assay was based on annexin V APC conjugate and DAPI, and results show (A) RD3, and its variants transfected in HEK 293T cell. (B) Vector and Mock control. (C) The summary of apoptotic cells. Apoptotic analysis of cells in (D) RD3 and control group, (E) RD3 and its variants. The statistical analysis used a two-way ANOVA with significance levels of * < 0.05, ** < 0.01, *** < 0.001, and **** < 0. 0001.

4. Publications and manuscript

This dissertation comprises one scientific publication that appeared in peer-reviewed journals (chapters 4.1), and one manuscript that has been submitted for publication (chapter 4.2). Herein, I list these works and outline the individual author contributions for each chapter.

4.1 Retinal degeneration protein 3 controls membrane guanylate cyclase activities in brain tissue

4.2 Retinal degeneration protein 3 mutants are associated with cell cycle arrest and apoptosis

The results in Chapter 4.1 center on the new role of RD3 in regulating the guanylate cyclase activities of natriuretic peptide-coupled guanylate cyclases, GC-A and GC-B, in brain tissue. To the data, we provided gene expression patterns of *rd3*, *Npr1* and *Npr2* in the mouse brain in different developmental stages, as well as in primary neuronal cells. While the guanylate cyclase assay was employed in the research to test the impact of the RD3 in enzyme activities of exogenous and endogenous GC-A and GC-B, respectively. These data displayed a possible physiological role of RD3 in the brain. To extend our knowledge, the results in Chapter 4.2 reveal a novel function of RD3 in activate the cell programming death in the HEK 293T cell, and this function is impact by the somatic mutants, that gives explanation of the interact between RD3 and glioma, indicating a potential pathological role of RD3 in the brain.

Declaration

Hereby I confirm, that Yaoyu Chen contributed to the aforementioned studies as stated below:

Article:

Retinal degeneration protein 3 controls membrane guanylate cyclase activities in brain tissue

Yaoyu Chen, Anja U. Bräuer and Karl-Wilhelm Koch

Published in: Frontiers in Molecular Neuroscience (2022) 15:1076430

Author contributions:

YC, AB, and K-WK designed the study and analyzed the data. YC performed the experiments. K-WK wrote the first draft of the manuscript. YC and AB contributed to the writing of the manuscript. All authors contributed to the article and approved the submitted version.

Manuscript:

Retinal degeneration protein 3 mutants are associated with cell cycle arrest and apoptosis

Yaoyu Chen, Jens Hausmann, Benjamin Zimmermann, Simeon Oscar Arnulfo Helgers, Patrick Dömer, Johannes Woitzik, Ulrike Raap, Natalie Gray, Andreas Büttner, Karl-Wilhelm Koch, and Anja U. Bräuer

Submitted to: Cell Death & Disease

Author contributions:

YC, AUB, and KWK designed the study. YC performed experiments. YC, AUB and KWK analyzed data. JW, BZ, PD, and AB provide human material. NG, UR and SOAH helped with analyzing data. JH created structural analysis. KWK, YC, and AUB contributed to the writing of the manuscript. All authors corrected and approved the final version of the manuscript.

.

_____ (date) _____ (Karl-Wilhelm Koch)

Retinal degeneration protein 3 controls membrane guanylate cyclase activities in brain tissue

Yaoyu Chen[1,2], Anja U. Bräuer[2,3] and Karl-Wilhelm Koch[1,3]*

[1]Division of Biochemistry, Department of Neuroscience, Carl von Ossietzky University, Oldenburg, Germany, [2]Division of Anatomy, Department of Human Medicine, Carl von Ossietzky University, Oldenburg, Germany, [3]Research Center Neurosensory Science, Carl von Ossietzky University, Oldenburg, Germany

The retinal degeneration protein RD3 is involved in regulatory processes of photoreceptor cells. Among its main functions is the inhibition of photoreceptor specific membrane guanylate cyclases during trafficking from the inner segment to their final destination in the outer segment. However, any physiological role of RD3 in non-retinal tissue is unsolved at present and specific protein targets outside of retinal tissue have not been identified so far. The family of membrane bound guanylate cyclases share a high homology of their amino acid sequences in their cytoplasmic domains. Therefore, we reasoned that membrane guanylate cyclases that are activated by natriuretic peptides are also regulated by RD3. We analyzed transcript levels of the *rd3* gene and natriuretic peptide receptor genes *Npr1* and *Npr2* in the mouse retina, cerebellum, hippocampus, neocortex, and the olfactory bulb during development from the embryonic to the postnatal stage at P60. The *rd3* gene showed a lower expression level than *Npr1* and *Npr2* (encoding for GC-A and GC-B, respectively) in all tested brain tissues, but was at least one order of magnitude higher in the retina. RD3 and natriuretic peptide receptor GCs co-express in the retina and brain tissue leading to functional tests. We expressed GC-A and GC-B in HEK293T cells and measured the inhibition of GCs by RD3 after activation by natriuretic peptides yielding inhibitory constants around 25nM. Furthermore, endogenous GCs in astrocytes were inhibited by RD3 to a similar extent. We here show for the first time that RD3 can inhibit two hormone-stimulated GCs, namely GC-A and GC-B indicating a new regulatory feature of these hormone receptors.

KEYWORDS

natriuretic peptide, membrane bound guanylate cyclase, GC-A, GC-B, RD3 protein

Introduction

Membrane bound guanylate cyclases (GC) synthesize the second messenger guanosine 3′,5′-cyclic monophosphate (cGMP) that is involved in a variety of physiological functions including blood pressure, skeletal growth, kidney function, phototransduction, olfaction, and thermosensation (Sharma, 2010; Koch and Dell'Orco, 2015; Kuhn, 2016; Sharma et al.,

51

2016; Pandey, 2021). Extracellular ligands like natriuretic peptides (ANP, BNP, and CNP) bind to natriuretic peptide receptors at their extracellular ligand domains. These natriuretic peptide receptors are GCs switching to the active state, when binding natriuretic peptides. ANP and BNP activate GC-A expressed in the cardiovascular system and metabolic organs being involved in the regulation of blood pressure and metabolism. CNP activates GC-B and the CNP/GC-B signaling system is expressed in various organs, but also in cardiovascular cell types (Pandey, 2021). One of its main suggested physiological roles is to regulate skeletal growth (Kuhn, 2016). Expression of CNP and GC-B in different brain regions also indicate a functional role in neuronal tissue. For example, studies investigated a role in synaptic plasticity in the hippocampus (Decker et al., 2010; Barmashenko et al., 2014) and an involvement in the regulation of the circadian clock (Olcese et al., 2002). Natriuretic peptides and their receptors have also been identified in the retina (Rollín et al., 2004) and were linked to dopaminergic and cholinergic signaling in amacrine cells (Abdelalim et al., 2008), and to the modulation of GABA-receptor activity in bipolar cells (Yu et al., 2006). In addition to neuronal signaling, natriuretic peptides ANP and BNP exert protective effects in retinal neovascularization (Špiranec Spes et al., 2020).

A different activation process is found in membrane GCs expressed in sensory cells. For example, photoreceptor specific GC-E and GC-F form complexes with guanylate cyclase-activating proteins (GCAPs) on their intracellular site (Peshenko et al., 2011; Sulmann et al., 2017). GCAPs are calcium sensor proteins that respond to changes in cytoplasmic calcium concentration ($[Ca^{2+}]$) with a conformational change thereby switching the target GC-E or GC-F to the active state (Koch and Dell'Orco, 2015; Dizhoor and Peshenko, 2021).

Point mutations in the genes *GUCY2D* and *GUCA1A* coding for GC-E and GCAP1 cause forms of retinal degeneration like cone-rod dystrophies. Leber's congenital amaurosis (LCA) is a particularly severe form of retinal dysfunction leading to blindness after birth or in the first year of life. Patients suffering from LCA type 1 have point mutations in *GUCY2D* (Sharon et al., 2018) causing dysfunction of GC-E in alive photoreceptor cells opening routes for gene therapy (Jacobson et al., 2022). Mutations in the retinal degeneration protein 3 (RD3) of human patients correlate with the phenotypical characteristics of LCA12 (Friedman et al., 2006; Cideciyan 2010; Preising et al., 2012). In the physiologically normal state of a photoreceptor cell, RD3 binds to photoreceptor specific GCs and inhibits their GCAP-mediated activation at low cytoplasmic $[Ca^{2+}]$ (Peshenko et al., 2011, 2021). RD3 is further involved in GC-E trafficking from the endoplasmic reticulum to endosomal vesicles (Azadi et al., 2010; Molday et al., 2013; Zulliger et al., 2015). Correct trafficking and incorporation of GC-E in photoreceptor outer segments is essential for cell survival and interaction of RD3 with GC-E is a crucial requirement for these processes (Peshenko et al., 2016; Peshenko and Dizhoor, 2020; Plana-Bonamaisó et al., 2020). Wimberg et al. (2018a) observed in an *in vitro* study that purified RD3 evoked an increase in guanylate kinase (GUK) activity, an enzyme that is involved in the

nucleotide cycle in photoreceptors catalyzing the 5'-GMP to GDP conversion. Both proteins directly interact and co-localize in photoreceptor inner segments and to a lesser extent in the outer plexiform layer in sections of the mouse retina. However, recent studies involving transgenic mice did not detect a regulatory impact of RD3 on GUK activity (Dizhoor et al., 2021).

Recent studies revealed that RD3 is also found in other tissue types such as epithelial cells and seems to be more ubiquitously expressed (Aravindan et al., 2017). Constitutive expression of RD3 was found in different mouse and human tissues including brain, kidney, liver, and spleen (Khan et al., 2015). The same authors further showed that RD3 loss in a mouse model correlates with aggressive neuroblastoma cancer. More recently, Somasundaram et al. (2019) found significant loss of RD3 expression on the transcript and protein level in patient derived tumor cells that survived intensive multi-modal clinical therapy. The authors conclude that transcriptional dysregulation might account for RD3 expression loss associated with advanced disease stage and low survival rate. However, these findings are in disagreement with a previous study showing that inactivation of both *rd3* alleles in LCA12 patients does not correlate with extraocular symptoms (Perrault et al., 2013).

The physiological role of RD3 in non-retinal tissue is unclear at present and basic issues related to its expression profile in brain tissue and the identity of its non-retinal targets are unsolved. A reasonable question in this context is, whether GCs activated by natriuretic peptide can be regulated by RD3. A necessary condition for such a regulation would be the expression of RD3 and GCs in the same tissue. We compared the expression levels of RD3, GC-A and GC-B in mouse retina and further determined their expression profiles in different brain regions during mouse brain development. We further compared gene expression in the retina with those in hippocampal neurons, astrocytes, and microglia. For functional studies, we expressed GC-A and GC-B in HEK293T cells and investigated the activity profiles in the presence and absence of added purified RD3.

Materials and methods

Heterologous expression of membrane GCs in HEK293T cell

HEK293T cells were grown in Dulbecco's Modified Eagle Medium (DMEM; Thermo Fisher Scientific) supplemented with 10% fetal bovine serum (FBS; PAN-Biotech, Aidenbach, Germany), 2 mM L-glutamine (Merck Millipore, Darmstadt, Germany), 100 units/ml Penicillin–Streptomycin (PAN-Biotech) in the incubator set at 5% (v/v) CO_2 and 37°C.

For cell transfection, the cDNA sequence of wildtype human GC-A and human GC-B was inserted into a pcDNA3.1 vector. The cDNA was amplified using the primers listed in the supplementary part (Supplementary Table S1). Cells were seeded for transfection in 100 mm petri dishes with 1.5×10^6 cells per dish. After 24 h, cells

were transfected with the pcDNA3.1 plasmids using the polyethylenimine (PEI) as transfection reagent. Stable cell lines expressing human GC-A or GC-B were created as described previously for GC-E (Wimberg et al., 2018a). The expression of GCs was confirmed *via* western blotting (see below) using commercial antibodies: polyclonal anti-GC-A (cat. Ab14357, Abcam) and polyclonal anti-GC-B (cat. Ab14356, Abcam). For the detection of photoreceptor GC-E we used a polyclonal antibody that was originally made against bovine GC-E, but showed crossreactivity to the human orthologue (Zägel et al., 2013). HA-tagged GC-A and GC-B were used in control experiments applying the pcDNA3.1 vector with HA-tag insertion.

Expression and purification of RD3

The RD3 protein was expressed in *E.coli* and purified following the method as described before Wimberg et al., 2018a. Briefly, *E.coli* BL21+ cells containing the pET-M11-RD3-His6-tag construct was grown overnight in LB-Medium at 37°C after induction by 1 mM isopropyl-thiogalactoside (IPTG). The cell pellets were harvested by centrifugation and suspended in 50 mM Tris/HCl pH 8.0. Cells were lysed by adding 100 mg/ml lysozyme and 5 U/ml DNase and incubation at 30°C for 30 min. The lysate was centrifuged for 1.5 h at $50,000 \times g$ at 4°C after adding 1 mM DTT and 0.1 mM phenylmethyl-sulfonylfluoride (PMSF). The RD3 containing pellet was homogenized in buffer 1 (20 mM phosphate buffer pH 7.4, 8 M urea, 10 mM imidazole, 500 mM NaCl, 5 mM β-mercaptoethanol (β-ME), 1 mM PMSF), and kept overnight at 4°C. The suspension was centrifuged for 1 h at $50,000 \times g$ and 4°C, the supernatant was collected for Ni-NTA column-based purification. After sample loading onto the column, buffer 1 was applied for washing and was then gradually replaced by buffer 2 (20 mM phosphate buffer pH 7.4, 10 mM imidazole, 500 mM NaCl, 5 mM β-ME, 1 mM PMSF, 1 mM histidine, 10% glycerol) to facilitate protein refolding. Buffer 3 (20 mM phosphate buffer pH 7.4, 500 mM imidazole, 20 mM histidine, 500 mM NaCl, 5 mM β-ME, 1 mM PMSF) eluted RD3 containing fractions that were collected in volumes of 1 ml and analyzed *via* sodium dodecyl sulfate polyacrylamide gel electrophoresis (SDS-PAGE). Purified RD3 was tested for biological activity, namely inhibiting GCAP activated human GC-E present in HEK-293T cells that stably expressed GC-E (Wimberg et al., 2018a).

Gel electrophoresis and immunoblotting

HEK-293T cells were harvested and the membrane protein fractions were collected as previously described Wimberg et al., 2018a. The protein fractions were incubated with 5× Laemmli buffer containing 1% (v/v) β-ME at 95°C for 5 min and analyzed by SDS-PAGE having either 12% or 7.5% acrylamide. Immunoblotting was performed using a 0.45 μm nitrocellulose (NC) membrane, and a tank or semi-dry blotting system. RD3 was analyzed by SDS-PAGE on a 12% acrylamide gel and a semi-dry blotting procedure of 200 mA for 30 min. For GC-A and GC-B we used a 7.5% acrylamide gel and the tank blotting procedure (100 V for 70 min at 4°C). Afterwards, the blotted membrane was incubated with blocking solution [either 5% (w/v)] bovine serum albumin (BSA; Carl Roth, Karlsruhe, Germany, or 2.5–5% milk powder (Carl Roth)) in TBST at room temperature (RT) for 1 h. Primary anti-GC antibodies were incubated overnight at 4°C in blocking solution at a dilution of 1:5,000. The blot membranes were washed three-times with TBST at RT. Afterwards, the blot membranes were incubated for 1 h at RT with horseradish peroxidase-conjugated secondary antibodies (GE Healthcare, Boston, MA, United States) at a dilution of 1:10,000 in blocking solution. Membranes were again washed three times at RT with TBST, and immunoreaction was detected with Clarity or Clarity Max ECL substrate (Bio-Rad Laboratories, Hercules, CA, United States) according to the manufacturer's protocol.

Guanylate cyclase activity assay

The guanylate cyclase stimulator human atrial natriuretic factor (1–28; ANP, cat. H-2095) and the human c-type natriuretic peptide (1–53; CNP, cat. H-8420) were purchased from Bachem AG (Switzerland). Ten microliter of HEK-293T membranes expressing GC-A or GC-B were incubated with 2 μM ANP or CNP, or various concentrations RD3 in a final volume of 30 μl for 5 min at RT. The guanylate cyclase reaction was started by adding 20 μl GC buffer (75 mM Mops/KOH pH 7.2, 150 mM KCl, 10 mM NaCl, 2.5 mM DTT, 8.75 mM MgCl₂, 4 mM GTP, 0.75 mM ATP, 0.4 mM Zaprinast). After incubation for 5 min at 30°C, the reaction was stopped by adding 50 μl 0.1 M EDTA and short incubation (5 min) at 95°C. After centrifugation at $13,000 \times g$ for 10 min, the supernatant was harvested and analyzed for cGMP content as previously described (Wimberg et al., 2018a). Assays were pursued in three independent groups, each with 3 replicates ($N = 9$). Test series were performed to find the optimal assay conditions including a concentration dependence of GTP and a time series.

RNA extraction, cDNA synthesis and qRT-PCR

The mRNA from mouse cerebellum, neocortex, hippocampus, and olfactory bulbs of the developmental stages of embryonic days (E) E14, E16, E19, and of postnatal days (P) P0, P5, P10, P15, P20, P30, P42, P60 was collected as described in Gross et al. (2022) and stored at -80°C until use. Briefly, the tissues were dissociated from sacrificed mice, at embryonic stages, one litter of all embryos (7–10 embryos; $N = 21$–30, sex not specified) were pooled. At postnatal stages, tissues from six mice of both sexes were pooled, for all stages with three independent replicates ($n = 3$). The retinas were obtained from the mice at P10, P20, P30 of both sexes with

53

FIGURE 1
Gene expression profiles in mouse retina analyzed by quantitative RT–PCR. Relative transcript levels of *rd3*, *Npr1* and *Npr2* were determined in retina tissue at P10, P20 and P30 and normalized to β–*actin* expression. Analysis of statistics were based on one-way ANOVA followed by Bonferroni's multiple comparisons test. Data are shown as mean±SD. Specific numbers of *p*-values are shown in Supplementary Table S2 (Supplementary material).

3 replicates. Primary hippocampal neurons, astrocytes and microglia cells were obtained as described (Gross et al., 2022). The TRIzol™ reagent (Thermo Fisher Scientific, Waltham, MA, United States) was applied for RNA extraction from homogenized cells and tissues following the protocol from the manufacturer. RNA concentrations were determined by UV/Vis spectroscopy using the BioSpectrometer basic (Eppendorf, Hamburg, Germany). The cDNA was obtained according to the protocol of the high-capacity cDNA reverse transcription kit from Thermo Fisher Scientific.

Quantitative-RT-PCR was performed using the TaqMan™ Fast Universal PCR Master Mix, No AmpErase™ UNG (Thermo Fisher Scientific) on hard-shell 96-Well PCR plates from Bio-Rad Laboratories (Hercules, CA, United States), and TaqMan probes. Reactions were prepared according to the manufacturer's protocols and detected by the CFX96 real-time PCR detection system (Bio-Rad Laboratories) using the following cycling parameters: 95°C for 20 s, 95°C for 1 s and 60°C for 20 s, for 45 cycles. Expression data of three independent preparations with duplicates of each reaction were calculated using the ΔCt method, with normalization to *Gapdh* and *Actb* as housekeeping genes.

Culturing of astrocytes and GC activities in astrocytes

The astrocytes were cultured and collected according to Gross et al. (2022). Membranes containing membrane proteins were harvested after 10–12 days *in vitro* for endogenous guanylate

cyclase activity tests. Guanylate cyclase activities in astrocyte membranes were stimulated by adding ANP or CNP. Inhibitory effects of RD3 were measured adding increasing amounts of purified RD3. The enzyme reaction started by adding 4 mM GTP. After 30 min incubation at 30°C, the reaction stopped by adding 0.1 M EDTA and incubation at 95°C for 5 min. The GC activities were measured using a cGMP ELISA Kit™ from Enzo Life Sciences according to the protocol of the manufacturer, three independent groups with two replicates each ($N = 6$). A cGMP standard curve was created between 0.01 and 500 pmol × mL^{-1} being maximally sensitive between 1 and 100 pmol × mL^{-1}.

Statistical analysis

The qRT-PCR data of developmental stages in retina (Figure 1), in different brain areas (Figure 2) and primary cell cultures (Figure 3A) was processed using a one-way analysis of variance (ANOVA) followed by a Bonferroni's multiple comparisons test. Developmental stages of E14, P0, P20, and P60 were included into gene expression difference analysis of embryonic, birth, adult and elder. Evaluation of cyclase activities regulated by ANP (Figure 4B), CNP, or RD3 (Figures 5A,B) was performed by using the dose response simulation or the inhibition algorithm under nonlinear regression provided by GraphPad Prism 7 (GraphPad Software, San Diego, CA, United States). For the analysis of the functional test of purified RD3 (Figures 3B, 5C) we employed One-Way ANOVA Calculator and Tukey HSD[1].

Results

Expression of natriuretic peptide receptor GCs and RD3 in mouse neuronal tissue

First, we analyzed *rd3*, *Npr1* and *Npr2* transcript levels in the mouse retina at developmental stages P10, P20 and P30 and found high expression levels for *rd3*, but 10-100-fold lower levels for *Npr2* and *Npr1*, respectively (Figure 1). Next, we compared the expression in the retina with those in certain brain regions and observed that *rd3* transcript levels were several orders of magnitude higher in the retina than in brain tissue (compare Figures 1, 2A). For example, the expression of *rd3* in the retina was between 10^{-1} and 10^{0} relative to the β-*actin* expression, but only 10^{-4} to 10^{-3} in the cerebellum, hippocampus, neocortex and the olfactory bulb. These findings confirm the retina being the prominent neuronal tissue of *rd3* localization, but they also showed significant levels of *rd3* transcripts in several brain regions. We tested gene expression pattern of *rd3*, *Npr1* and *Npr2* during development in different mouse brain parts starting from E14 up

---

1 https://www.statskingdom.com/180Anova1way.html
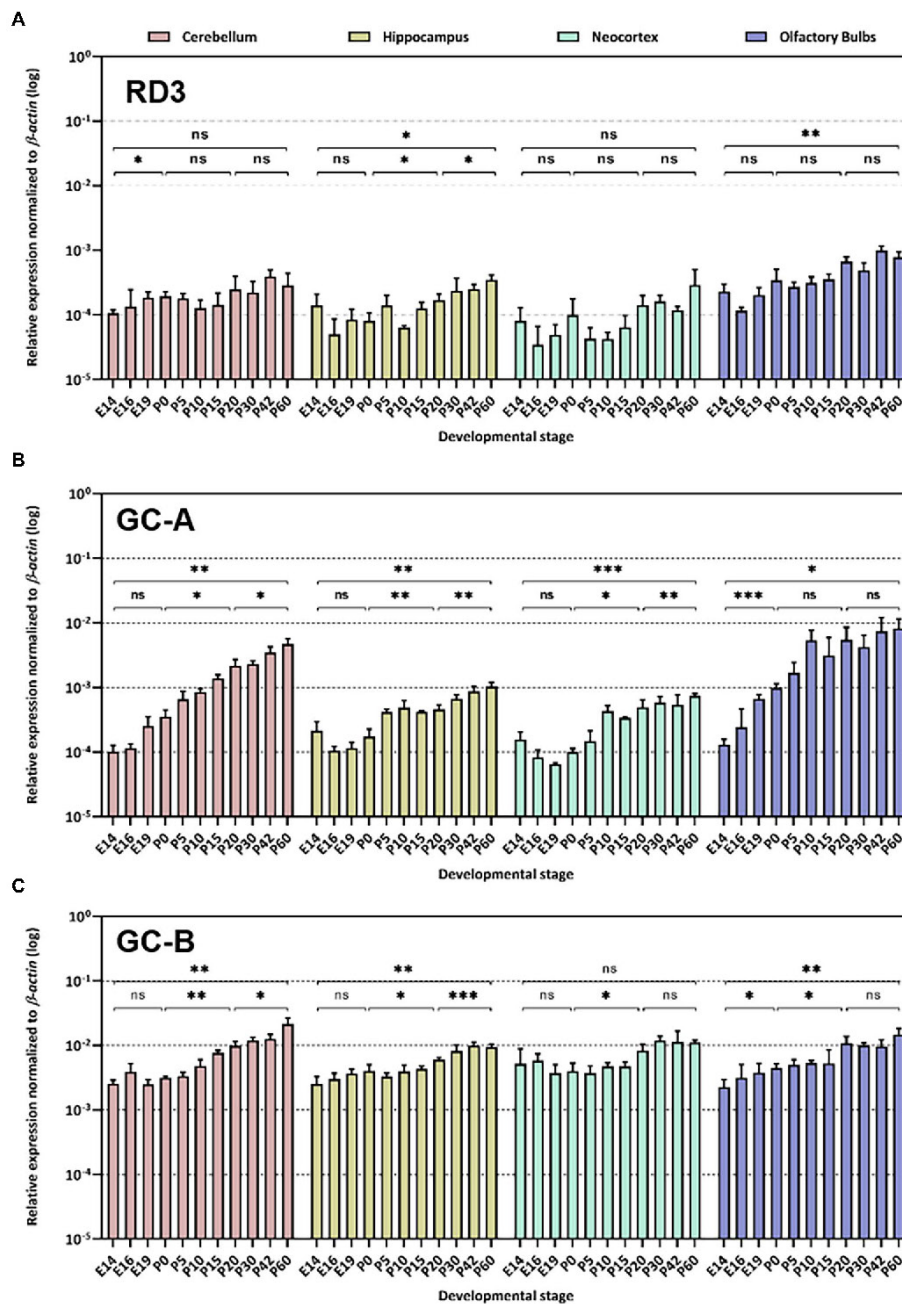
FIGURE 2
Quantitative RT-PCR. Gene expression pattern of *rd3* **(A)**, *Npr1* encoding GC-A **(B)** and *Npr2* encoding GC-B **(C)** was analyzed in different neuronal tissues as indicated. The relative expression was normalized to β−*actin* expression. Analysis of statistics were based on one-way ANOVA followed by Bonferroni's multiple comparisons test. Data are shown as mean±SD and were considered significant for $p \leq 0.05$ ($p \leq 0.05 = *$; $p \leq 0.01 = **$; $p \leq 0.001 = ***$; ns=not significant). Specific numbers of p-values are shown in Supplementary Table S3 (Supplementary material).

to P60 (Figure 2). The analysis performed by qRT-PCR included tissue from cerebellum, hippocampus, neocortex, and olfactory bulb. In general, *rd3* showed a lower expression level than *Npr1* and *Npr2* (Figure 2A compared to Figures 2B,C) and reached the

highest steady-state expression level in the olfactory bulb between P20 and P60. However, the level was at least one order of magnitude lower than that for *Npr2* in all tested brain tissues (Figure 2C), which reached the highest values between P20 and

FIGURE 3
Expression and activity profiles of *rd3, Npr1* and *Npr2* in astrocytes. **(A)** Relative transcript levels of *rd3, Npr1* and *Npr2* in neurons, astrocytes, and microglia. Analysis of statistics were based on one-way ANOVA followed by Bonferroni's multiple comparisons test. Data are shown as mean±SD and were considered significant for $p \leq 0.05$ ($p \leq 0.05$=*; $p \leq 0.01$=**; $p \leq 0.001$=***; ns=not significant). Specific numbers of p-values are shown in Supplementary Table S4 (Supplementary material). **(B)** Inhibition of GC-A and GC-B in astrocytes by RD3.

P60. *Npr1* showed the highest expression at P60 in cerebellum and from P10 onwards in the olfactory bulb. Gene expression of *Npr1* was more dynamic exhibiting a steeper progressive increase in expression levels than *Npr2* and *rd3*. This was particularly visible for patterns observed in cerebellum and olfactory bulb (Figure 2B). Both *Npr* genes types showed lower expression levels in the retina than *rd3*. However, *Npr2* reached normalized expression levels in the retina that were close to those observed in cerebellum and olfactory bulb at P60 (compare Figures 1, 2C).

RD3 can inhibit hormone activated GC-A and GC-B

Coexpression of *rd3* and natriuretic peptide receptor GC genes in brain tissue led to the next question whether RD3 can regulate the enzymatic activities of membrane bound GC-A and GC-B. The high sequence homology of photoreceptor GCs and natriuretic peptide receptor GCs in the cytoplasmic domains (Goraczniak et al., 1994; Lange et al., 1999) could indicate that membrane bound GCs share similar regulatory features. RD3 is supposed to interact with regions in the cytoplasmic part of photoreceptor GC-E (Peshenko et al., 2011), although the exact binding site has not been determined. To test for any influence of RD3 on GC-A or GC-B activity we tested the impact of purified RD3 on GC activities in a cell culture system. Transient expression of GC-A and GC-B in HEK 293T cells was confirmed by immunoblotting using GC specific antibodies that recognized a

single band around 120 kDa (Figure 4A), in agreement with the expectation and the documented molecular masses of membrane bound GCs (Kuhn, 2016). Non-transfected cells (HEK 293T control) or cells transfected with the empty pcDNA3.1 vector showed no GC bands (Figure 4A). HA-tagged variants of GC-A and GC-B were used in positive control transfections. Polyclonal antibodies directed against GC-A or GC-B recognized specifically the HA-tagged GC bands. To our surprise, the tagged variant of GC-A gave a stronger response to the antibody than the non-tagged variant. We have no explanation for this result.

Functional expression of both GCs was tested by monitoring a ligand dependent increase in GC activities. We incubated HEK293T cell membranes containing GC-A or GC-B with increasing concentrations of natriuretic peptides. Both peptides stimulated cGMP production about 10-fold reaching saturation above 4 μM of ANP (activating GC-A) or CNP (activating GC-B; Figures 4B,C). Further controls and test incubations to optimize our assay system included measurements upon GTP dependent cGMP synthesis (Supplementary Figure S1) and a time series resulting in a robust assay system (Materials and Methods) suitable for further studies. Activity tests in the presence and absence of DTT showed no or very negligible differences (Supplementary Figure S1C).

For testing the regulatory impact of RD3 on GC-A or GC-B, we purified RD3 to homogeneity (Supplementary Figure S2) and verified its identity by immunoblotting using two different anti-RD3 antibodies (Supplementary Figure S3). We activated GC-A and GC-B with 2 μM ANP and CNP, respectively, and

56

FIGURE 4
Heterologous expression GC-A and GC-B in HEK 293T cells. **(A)** Immunoblotting of HEK 293 T cell membrane suspension. Primary antibodies were directed against GC-A (left panel) or GC-B (right panel) at a dilution of 1:1000 in both cases. The antibodies detected also the HA-tagged variants. In case of GC-A, the HA-tagged variant was even stronger detected by the polyclonal anti-GC-A antibody. Transfection with the empty vector (pcDNA3.1) or non-transfected HEK293T cells did not react with the antibodies. Ligand dependent increase in GC-activities. **(B)** Regulation of GC-A by ANP and of GC-B **(C)** by CNP.
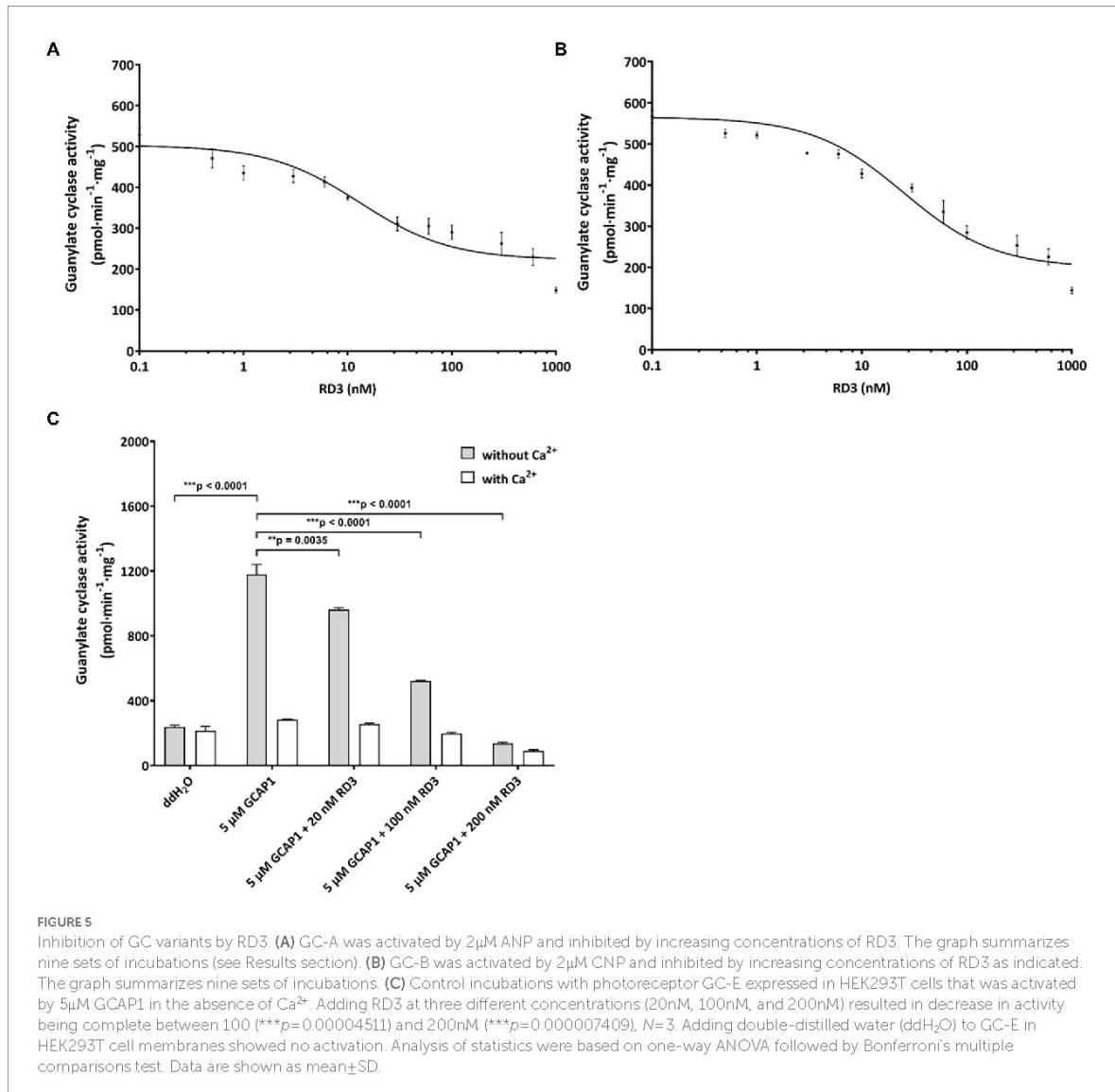
reconstituted the GC containing HEK 293T cell membranes with increasing concentrations of purified RD3. Inhibition of GC-A was significant, and several replicates ($N=9$) showed reproducible results yielding a mean IC_{50} value ($\pm$ SD) of 24 ± 13 nM RD3. A summarizing graph of the experiments is shown in Figure 5A. RD3 had a similar effect upon GC-B activity. The IC_{50} value for half-maximal inhibition was 29 ± 21 nM RD3 ($N=9$) and a summarizing graph is shown in Figure 5B. However, inhibition was not complete for both GCs (Figures 5A,B) as higher concentrations between 0.5 and 1 µM RD3 did not reach a complete inhibition. Instead, the activity of GC-A and GC-B remained at a constant level (Figures 5A,B). We can exclude by immunoblotting any presence of photoreceptor GC-E in HEK293T cell membranes expressing either GC-A or GC-B (Supplementary Figure S4). This inhibitory feature differed significantly from the effect of RD3 upon photoreceptor specific GC-E (Figure 5C; Peshenko et al., 2011; Wimberg et al., 2018b). Since RD3 is a notoriously unstable protein, we controlled the functional activity of purified RD3 in a well-established assay system. HEK293T cell membranes that stably expressed photoreceptor GC-E were activated in the presence of 5 µM GCAP1. Addition of RD3 inhibited GCAP1 stimulated GC-E

activity to a similar extent as reported in the literature (Peshenko et al., 2011; Wimberg et al., 2018b; Figure 5C). This confirmed that RD3 was active and controlled the activity of GC-A and GC-B in a similar, but not identical manner to GC-E.

Regulation of GC-A and GC-B by RD3 in astrocytes

Extending our analysis to cultured neurons, astrocytes, and microglia, revealed highest expression of *Npr2* in neurons and astrocytes, but also quite high expression of *rd3* in astrocytes (Figure 3A). The relative high transcript levels of *Npr2* and *rd3* in astrocytes led us investigate and compare regulatory features of GC-A and GC-B in primary cultures of astrocytes. Endogenous levels of GC activities around $400 \, \text{pmol} \times \text{min}^{-1} \times \text{mg}^{-1}$ resulted mainly from both GC-A and GC-B as seen in Figure 3 under conditions where no exogenous natriuretic peptides were added (ddH$_2$O). Adding natriuretic peptides (ANP and CNP) increased the activities at least twofold. The presence of 30 or 60 nM exogenously added RD3 inhibited the ANP or CNP stimulated GC activity leaving only a basal GC activity level as in the non-stimulated

57

FIGURE 5
Inhibition of GC variants by RD3. **(A)** GC-A was activated by 2μM ANP and inhibited by increasing concentrations of RD3. The graph summarizes nine sets of incubations (see Results section). **(B)** GC-B was activated by 2μM CNP and inhibited by increasing concentrations of RD3 as indicated. The graph summarizes nine sets of incubations. **(C)** Control incubations with photoreceptor GC-E expressed in HEK293T cells that was activated by 5μM GCAP1 in the absence of Ca^{2+}. Adding RD3 at three different concentrations (20nM, 100nM, and 200nM) resulted in decrease in activity being complete between 100 (***$p=0.00004511$) and 200nM (***$p=0.000007409$), $N=3$. Adding double-distilled water (ddH$_2$O) to GC-E in HEK293T cell membranes showed no activation. Analysis of statistics were based on one-way ANOVA followed by Bonferroni's multiple comparisons test. Data are shown as mean±SD.

case (Figure 3B). These results showed that endogenously expressed GC-A and GC-B in primary astrocyte cell culture are sensitive to RD3 confirming our results with recombinant GC constructs and pointing to a potential physiologically relevant regulation of natriuretic peptide activated GCs by RD3.

Discussion

The presence of RD3 in non-retinal tissue seems enigmatic because we lack essential information about its cellular target(s) for defining possible physiological roles. On the other hand, the primary expression site of *rd3* in the mammalian retina (Azadi et al., 2010; Wimberg et al., 2018a; Dizhoor et al., 2019;

Plana-Bonamaisó et al., 2020; Figure 1 in this study) well supports several functional roles of RD3 in the retina. For example, RD3 inhibits the activated form of photoreceptor GC-E and GC-F, it is involved in trafficking processes from photoreceptor inner to outer segments and might regulate the nucleotide cycle in photoreceptor cells. In the present work, we investigated the expression pattern of *rd3* in brain tissue and analyzed the enzymatic features of possible target enzymes. The central finding of our study is that RD3 can inhibit two hormone-stimulated GCs, namely GC-A and GC-B indicating a new regulatory feature of these hormone receptors.

Earlier work identified natriuretic peptides and their receptors GC-A and GC-B (or natriuretic peptide receptors) in mammalian retinae using expression and cloning studies (Fernandez-Durango et al., 1989; Kutty et al., 1992; Duda et al., 1993). Subsequent

studies performed in various vertebrate species showed the expression of natriuretic peptides and/or their receptors in retinal bipolar, retinal Müller cells, amacrine and ganglion cells (Spreca et al., 1999; Blute et al., 2000; Yu et al., 2006; Cao and Yang, 2007; Abdelalim et al., 2008; Xu et al., 2010). Thus, there is evidence for *Npr1* and *Npr2* expression in retina tissue, but it was unclear so far how the expression level relates to protein levels with a critical function in retinal physiology. In the present study, we compared the transcript levels of *rd3* with those of *Npr1* and *Npr2* and found a relatively high expression level of *Npr2* in the retina. The level is about one order of magnitude higher than that of *Npr1*, but about one order of magnitude lower than that of *rd3*.

Natriuretic peptides and their receptors are involved in various physiological processes in the retina. For example, natriuretic peptides are involved in dopaminergic and cholinergic signaling in amacrine cells (Abdelalim et al., 2008), and Yu et al. (2006) reported that they modulate GABA-receptor activity in bipolar cells and strong immunolabeling of GC-A and GC-B in the outer plexiform layer (OPL). RD3 mainly localizes in inner segments of photoreceptor cells, but in addition expresses in the OPL (Azadi et al., 2010; Wimberg et al., 2018a; Dizhoor et al., 2019). Natriuretic peptide signaling *via* GC-A or GC-B leads to an increase in cGMP targeting, for example cyclic nucleotide-gated ion channels or cGMP dependent protein kinase (PKG). The latter had been discussed as part of a signaling pathway mediating the suppression of GABA-receptor current by BNP (Yu et al., 2006). Thus, RD3 could be involved in balancing the cGMP concentration by inhibiting GC-A or GC-B in the OPL, but high resolution immunohistochemistry of GC-A, GC-B and RD3 to support such a physiological role is missing so far.

Recent studies reported expression of RD3 on the transcript and protein level in several organs and tissues including brain (Khan et al., 2015; Aravindan et al., 2017), but the expression levels appear significantly lower than in the retina. We found that expression of *rd3* is more than 100-fold higher in the retina than in different brain parts (compare Figures 1, 2), which was in broad agreement with the report by Aravindan et al. (2017), who reported significant, but modest or low expression in human cerebellum and olfactory bulb in comparison to retinal expression. When we determined the relative expression levels of *rd3*, *Npr1* and *Npr2* during mice development, it became apparent that the expression of *Npr2* is stronger in all analyzed brain parts than those of *rd3* and *Npr1*. Our findings are consistent with reports showing *Npr2* mRNA expressing cell populations in neocortex, hippocampus, and olfactory bulb (Herman et al., 1996). GC-B has a critical role in the bifurcation of axons during development (Schmidt et al., 2018) extending previous observations that the natriuretic peptide systems play roles in regulating neural development (DiCicco-Bloom et al., 2004; Müller et al., 2009). Collectively, these findings support the notion that CNP is a prominent regulatory factor in the nervous system (Kuhn, 2016; Regan et al., 2021).

Therefore, inhibition of GC-A or GC-B by RD3 in brain tissue might be a critical regulatory feature. We observed stimulation of GC activities by ANP and CNP in astrocytes (Figure 3B) that was broadly consistent with a previous investigation that correlates ligand binding to cGMP accumulation by ANP and CNP (Deschepper and Picard, 1994). We here show that RD3 inhibited both GCs in astrocytes demonstrating that RD3 can exert its effects in a primary cell culture. Although this combination of *in situ* and *in vitro* studies provides only circumstantial evidence for RD3 regulating GC-A and GC-B activities, it might already indicate an impact on the development of retinopathies. In astrocytes, the ANP/GC-A/ cGMP signaling counteracts neovascularization in proliferative retinopathies (Burtenshaw and Cahill, 2020; Špiranec Spes et al., 2020). Any inhibitory effect of RD3 would therefore reinforce the development of angiogenic dependent retinopathies indicating how critical the expression level of RD3 is.

Trigger events that up-or downregulate RD3 levels apparently facilitate protein or cell dysfunction. For example, previous work showed that RD3 is downregulated or lost in neuroblastoma cells that remained resistant to multi-modal clinical therapy (Somasundaram et al., 2019). Furthermore, a previous study on the gene expression pattern in the *rd3* mouse, an animal model of congenital blindness with low or no *rd3* expression, reported that more than 1,000 genes are differentially regulated (Cheng and Molday, 2013). An annotation of these genes indicated the involvement of different biochemical pathways including phototransduction, metabolism and a variety of signaling processes. These studies collectively showed that a loss of RD3 is a critical factor in different pathophysiological contexts. It could have an effect on the expression pattern of other proteins in signaling pathways and thereby facilitate tumor development.

In summary, RD3 seems to control the activities of GC-A and GC-B in retinal and non-retinal tissue. These features could be critical for transport processes from the ER to the plasma membrane, but might be involved in different cellular scenarios, where a tight control of intracellular cGMP levels is essential for cell function and survival.

Data availability statement

The original contributions presented in the study are included in the article/Supplementary material, further inquiries can be directed to the corresponding author.

Ethics statement

All protocols were in accordance with the German Animal Protection Law and were approved by the local ethics body of Mecklenburg-Western Pomerania (LALLF) and Lower Saxony (LAVES).

Author contributions

Funding

Acknowledgments

Conflict of interest

The authors declare that the research was conducted in the absence of any commercial or financial relationships that could be construed as a potential conflict of interest.

Publisher's note

All claims expressed in this article are solely those of the authors and do not necessarily represent those of their affiliated organizations, or those of the publisher, the editors and the reviewers. Any product that may be evaluated in this article, or claim that may be made by its manufacturer, is not guaranteed or endorsed by the publisher.

Supplementary material

The Supplementary material for this article can be found online at: https://www.frontiersin.org/articles/10.3389/fnmol.2022.1076430/full#supplementary-material

References

Abdelalim, E. M., Masuda, C., and Tooyama, I. (2008). Expression of natriuretic peptide-activated guanylate cyclases by cholinergic and dopaminergic amacrine cells of the rat retina. *Peptides* 29, 622–628. doi: 10.1016/j.peptides.2007.11.021

Aravindan, S., Somasundaram, D. B., Kam, K. L., Subramanian, K., Yu, Z., Herman, T. S., et al. (2017). Retinal degeneration protein 3 (RD3) in normal human tissues: novel insights. *Sci. Rep.* 7:13154. doi: 10.1038/s41598-017-13337-9

Azadi, S., Molday, L. L., and Molday, R. S. (2010). RD3, the protein associated with Leber congenital amaurosis type 12, is required for guanylate cyclase trafficking in photoreceptor cells. *Proc. Natl. Acad. Sci. U. S. A.* 107, 21158–21163. doi: 10.1073/pnas.1010460107

Barmashenko, G., Buttgereit, J., Herring, N., Bader, M., Ozcelik, C., Manahan-Vaughan, D., et al. (2014). Regulation of hippocampal synaptic plasticity thresholds and changes in exploratory and learning behavior in dominant negative NPR-B mutant rats. *Front. Mol. Neurosci.* 7:95. doi: 10.3389/fnmol.2014.00095

Blute, T. A., Lee, H. K., Huffmaster, T., Haverkamp, S., and Eldred, W. D. (2000). Localization of natriuretic peptides and their activation of particulate guanylate cyclase and nitric oxide synthase in the retina. *J. Comp. Neurol.* 424, 689–700. PMID: 10931490

Burtenshaw, D., and Cahill, P. A. (2020). Natriuretic peptides and the regulation of retinal neovascularization. *Arterioscler. Thromb. Vasc. Biol.* 40, 7–10. doi: 10.1161/ATVBAHA.119.313566

Cao, L. H., and Yang, X. L. (2007). Natriuretic peptide receptor-a is functionally expressed on bullfrog retinal Müller cells. *Brain Res. Bull.* 71, 410–415. doi: 10.1016/j.brainresbull.2006.10.010

Cheng, C. L., and Molday, R. S. (2013). Changes in gene expression associated with retinal degeneration in the rd3 mouse. *Mol. Vis.* 19, 955–969. PMID: 23687432

Cideciyan, A. V. (2010). Leber congenital amaurosis due to RPE65 mutations and its treatment with gene therapy. *Prog. Retin. Eye Res.* 29, 398–427. doi: 10.1016/j.preteyeres

Decker, J. M., Wójtowicz, A. M., Bartsch, J. C., Liotta, A., Braunewell, K. H., Heinemann, U., et al. (2010). C-type natriuretic peptide modulates bidirectional plasticity in hippocampal area CA1 in vitro. *Neuroscience* 169, 8–22. doi: 10.1016/j.neuroscience.2010.04.064

Deschepper, C. F., and Picard, S. (1994). Effects of C-type natriuretic peptide on rat astrocytes: regional differences and characterization of receptors. *J. Neurochem.* 62, 1974–1982. doi: 10.1046/j.1471-4159.1994.62051974.x

DiCicco-Bloom, E., Lelièvre, V., Zhou, X., Rodriguez, W., Tam, J., and Waschek, J. A. (2004). Embryonic expression and multifunctional actions of the natriuretic peptides and receptors in the developing nervous system. *Dev. Biol.* 271, 161–175. doi: 10.1016/j.ydbio.2004.03.028

Dizhoor, A. M., Olshevskaya, E. V., and Peshenko, I. V. (2019). Retinal guanylyl cyclase activation by calcium sensor proteins mediates photoreceptor degeneration in an rd3 mouse model of congenital human blindness. *J. Biol. Chem.* 294, 13729–13739. doi: 10.1074/jbc.RA119.009948

Dizhoor, A. M., Olshevskaya, E. V., and Peshenko, I. V. (2021). Retinal degeneration-3 protein promotes photoreceptor survival by suppressing activation of guanylyl cyclase rather than accelerating GMP recycling. *J. Biol. Chem.* 296:100362. doi: 10.1016/j.jbc.2021.100362

Dizhoor, A. M., and Peshenko, I. V. (2021). Regulation of retinal membrane guanylyl cyclase (RetGC) by negative calcium feedback and RD3 protein. *Pflugers Arch.* 473, 1393–1410. doi: 10.1007/s00424-021-02523-4

Duda, T., Goraczniak, R. M., Sitaramayya, A., and Sharma, R. K. (1993). Cloning and expression of an ATP-regulated human retina C-type natriuretic factor receptor guanylate cyclase. *Biochemistry* 32, 1391–1395. doi: 10.1021/bi00057a001

Fernandez-Durango, R., Sanchez, D., Gutkowska, J., Carrier, F., and Fernandez-Cruz, A. (1989). Identification and characterization of atrial natriuretic factor receptors in the rat retina. *Life Sci.* 44, 1837–1846. doi: 10.1016/0024-3205(89)90301-9

Friedman, J. S., Chang, B., Kannabiran, C., Chakarova, C., Singh, H. P., Jalali, S., et al. (2006). Premature truncation of a novel protein, RD3, exhibiting subnuclear localization is associated with retinal degeneration. *Am. J. Hum. Genet.* 79, 1059–1070. doi: 10.1086/510021

Goraczniak, R. M., Duda, T., Sitaramayya, A., and Sharma, R. K. (1994). Structural and functional characterization of the rod outer segment membrane guanylate cyclase. *Biochem. J.* 302, 455–461. doi: 10.1042/bj3020455

Gross, I., Tschigor, T., Salman, A. L., Yang, F., Luo, J., Vonk, D., et al. (2022). Systematic expression analysis of plasticity-related genes in mouse brain development brings PRG4 into play. *Dev. Dyn.* 251, 714–728. doi: 10.1002/dvdy.428

Herman, J. P., Dolgas, C. M., Rucker, D., and Langub, M. C. (1996). Localization of natriuretic peptide-activated guanylate cyclase mRNAs in the rat brain. *J. Comp. Neurol.* 369, 165–187. doi: 10.1002/(SICI)1096-9861(19960527)369

Jacobson, S. G., Cideciyan, A. V., Ho, A. C., Roman, A. J., Wu, V., Garafalo, A. V., et al. (2022). Night vision restored in days after decades of congenital blindness. *iScience* 25:105274. doi: 10.1016/j.isci.2022.105274

Khan, F. H., Pandian, V., Ramraj, S. K., Aravindan, S., Natarajan, M., Azadi, S., et al. (2015). RD3 loss dictates high-risk aggressive neuroblastoma and poor clinical outcomes. *Oncotarget* 6, 36522–36534. doi: 10.18632/oncotarget.5204

Koch, K.-W., and Dell'Orco, D. (2015). Protein and signaling networks in vertebrate photoreceptor cells. *Front. Mol. Neurosci.* 8:67. doi: 10.3389/fnmol.2015.00067

Kuhn, M. (2016). Molecular physiology of membrane guanylyl cyclase receptors. *Physiol. Rev.* 96, 751–804. doi: 10.1152/physrev.00022.2015

Kutty, R. K., Fletcher, R. T., Chader, G. J., and Krishna, G. (1992). Expression of guanylate cyclase-a mRNA in the rat retina: detection using polymerase chain reaction. *Biochem. Biophys. Res. Commun.* 182, 851–857. doi: 10.1016/0006-291x(92)91810-d

Lange, C., Duda, T., Beyermann, M., Sharma, and R. K., Koch, K. W. (1999). Regions in vertebrate photoreceptor guanylyl cyclase ROS-GC1 involved in Ca(2+)-dependent regulation by guanylyl cyclase-activating protein GCAP-1. *FEBS Lett.* 460, 27–31. doi: 10.1016/s0014-5793(99)01312-5.

Molday, L. L., Djajadi, H., Yan, P., Szczygiel, L., Boye, S. L., Chiodo, V. A., et al. (2013). RD3 gene delivery restores guanylate cyclase localization and rescues photoreceptors in the Rd3 mouse model of Leber congenital amaurosis 12. *Hum. Mol. Genet.* 22, 3894–3905. doi: 10.1093/hmg/ddt244

Müller, D., Hida, B., Guidone, G., Speth, R. C., Michurina, T. V., Enikolopov, G., et al. (2009). Expression of guanylyl cyclase (GC)-a and GC-B during brain development: evidence for a role of GC-B in perinatal neurogenesis. *Endocrinology* 150, 5520–5529. doi: 10.1210/en.2009-0490

Olcese, J., Majora, C., Stephan, A., and Müller, D. (2002). Nocturnal accumulation of cyclic 3′,5′-guanosine monophosphate (cGMP) in the chick pineal organ is dependent on activation of guanylyl cyclase-B. *J. Neuroendocrinol.* 14, 14–18. doi: 10.1046/j.0007-1331.2001.00732.x

Pandey, K. N. (2021). Molecular signaling mechanisms and function of natriuretic peptide receptor-a in the pathophysiology of cardiovascular homeostasis. *Front. Physiol.* 12:693099. doi: 10.3389/fphys.2021.693099

Perrault, I., Estrada-Cuzcano, A., Lopez, I., Kohl, S., Li, S., Testa, F., et al. (2013). Union makes strength: a worldwide collaborative genetic and clinical study to provide a comprehensive survey of RD3 mutations and delineate the associated phenotype. *PLoS One* 8:e51622. doi: 10.1371/journal.pone.0051622

Peshenko, I. V., and Dizhoor, A. M. (2020). Two clusters of surface-exposed amino acid residues enable high-affinity binding of retinal degeneration-3 (RD3) protein to retinal guanylyl cyclase. *J. Biol. Chem.* 295, 10781–10793. doi: 10.1074/jbc.RA120.013789

Peshenko, I. V., Olshevskaya, E. V., and Dizhoor, A. M. (2016). Functional study and mapping sites for interaction with the target enzyme in retinal degeneration 3 (RD3) protein. *J. Biol. Chem.* 291, 19713–19723. doi: 10.1074/jbc.M116.742288

Peshenko, I. V., Olshevskaya, E. V., and Dizhoor, A. M. (2021). Retinal degeneration-3 protein attenuates photoreceptor degeneration in transgenic mice expressing dominant mutation of human retinal guanylyl cyclase. *J. Biol. Chem.* 297:101201. doi: 10.1016/j.jbc.2021.101201

Peshenko, I. V., Olshevskaya, E. V., Savchenko, A. B., Karan, S., Palczewski, K., Baehr, W., et al. (2011). Enzymatic properties and regulation of the native isozymes of retinal membrane guanylyl cyclase (RetGC) from mouse photoreceptors. *Biochemistry* 50, 5590–5600. doi: 10.1021/bi200491b

Plana-Bonamaisó, A., López-Begines, S., Andilla, J., Fidalgo, M. J., Loza-Alvarez, P., Estanyol, J. M., et al. (2020). GCAP neuronal calcium sensor proteins mediate photoreceptor cell death in the rd3 mouse model of LCA12 congenital blindness by involving endoplasmic reticulum stress. *Cell Death Dis.* 11:62. doi: 10.1038/s41419-020-2255-0

Preising, M. N., Hausotter-Will, N., Solbach, M. C., Friedburg, C., Rüschendorf, F., and Lorenz, B. (2012). Mutations in RD3 are associated with an extremely rare and severe form of early onset retinal dystrophy. *Invest. Ophthalmol. Vis. Sci.* 53, 3463–3472. doi: 10.1167/iovs.12-9519

Regan, J. T., Mirczuk, S. M., Scudder, C. J., Stacey, E., Khan, S., Worwood, M., et al. (2021). Sensitivity of the natriuretic peptide/cGMP system to hyperammonaemia in rat C6 glioma cells and GPNT brain endothelial cells. *Cells* 10:398. doi: 10.3390/cells10020398

Rollín, R., Mediero, A., Roldán-Pallarés, M., Fernández-Cruz, A., and Fernández-Durango, R. (2004). Natriuretic peptide system in the human retina. *Mol. Vis.* 10, 15–22. PMID: 14737067

Schmidt, H., Dickey, D. M., Dumoulin, A., Octave, M., Robinson, J. W., Kühn, R., et al. (2018). Regulation of the natriuretic peptide receptor 2 (Npr2) by phosphorylation of juxtamembrane serine and threonine residues is essential for bifurcation of sensory axons. *J. Neurosci.* 38, 9768–9780. doi: 10.1523/JNEUROSCI.0495-18.2018

Sharma, R. K. (2010). Membrane guanylate cyclase is a beautiful signal transduction machine: overview. *Mol. Cell. Biochem.* 334, 3–36. doi: 10.1007/s11010-009-0336-6

Sharma, R. K., Duda, T., and Makino, C. L. (2016). Integrative signaling networks of membrane guanylate cyclases: biochemistry and physiology. *Front. Mol. Neurosci.* 9:83. doi: 10.3389/fnmol.2016.00083

Sharon, D., Wimberg, H., Kinarty, Y., and Koch, K.-W. (2018). Genotype-functional-phenotype correlations in photoreceptor guanylate cyclase (GC-E) encoded by GUCY2D. *Prog. Retin. Eye Res.* 63, 69–91. doi: 10.1016/j.preteyeres.2017.10.003

Somasundaram, D. B., Subramanian, K., Aravindan, S., Yu, Z., Natarajan, M., Herman, T., et al. (2019). De novo regulation of RD3 synthesis in residual neuroblastoma cells after intensive multi-modal clinical therapy harmonizes disease evolution. *Sci. Rep.* 9:11766. doi: 10.1038/s41598-019-48034-2

Špiranec Spes, K., Hupp, S., Werner, F., Koch, F., Völker, K., Krebs, L., et al. (2020). Natriuretic peptides attenuate retinal pathological neovascularization via cyclic guanosine monophosphate signaling in pericytes and astrocytes. *Arterioscler. Thromb. Vasc. Biol.* 40, 159–174. doi: 10.1161/ATVBAHA.119.313400

Spreca, A., Giambanco, I., and Rambotti, M. G. (1999). Ultracytochemical study of guanylate cyclases a and B in light- and dark-adapted retinas. *Histochem. J.* 31, 477–483. doi: 10.1023/a:1003712110751

Sulmann, S., Kussrow, A., Bornhop, D. J., and Koch, K.-W. (2017). Label-free quantification of calcium-sensor targeting to photoreceptor guanylate cyclase and rhodopsin kinase by backscattering interferometry. *Sci. Rep.* 7:45515. doi: 10.1038/srep45515

Wimberg, H., Janssen-Bienhold, U., and Koch, K.-W. (2018a). Control of the nucleotide cycle in photoreceptor cell extracts by retinal degeneration protein 3. *Front. Mol. Neurosci.* 11:52. doi: 10.3389/fnmol.2018.00052

Wimberg, H., Lev, D., Yosovich, K., Namburi, P., Banin, E., Sharon, D., et al. (2018b). Photoreceptor guanylate cyclase (GUCY2D) mutations cause retinal dystrophies by severe malfunction of Ca2+−dependent cyclic GMP synthesis. *Front. Mol. Neurosci.* 11:348. doi: 10.3389/fnmol.2018.00348

Xu, G. Z., Tian, J., Zhong, Y. M., and Yang, X. L. (2010). Natriuretic peptide receptors are expressed in rat retinal ganglion cells. *Brain Res. Bull.* 82, 188–192. doi: 10.1016/j.brainresbull.2010.03.004

Yu, Y. C., Cao, L. H., and Yang, X. L. (2006). Modulation by brain natriuretic peptide of GABA receptors on rat retinal ON-type bipolar cells. *J. Neurosci.* 26, 696–707. doi: 10.1523/JNEUROSCI.3653-05.2006

Zägel, P., Dell'Orco, D., and Koch, K.-W. (2013). The dimerization domain in outer segment guanylate cyclase is a Ca2+−sensitive control switch module. *Biochemistry* 52, 5065–5074. doi: 10.1021/bi400288p

Zulliger, R., Naash, M. I., Rajala, R. V., Molday, R. S., and Azadi, S. (2015). Impaired association of retinal degeneration-3 with guanylate cyclase-1 and guanylate cyclase-activating protein-1 leads to leber congenital amaurosis-1. *J. Biol. Chem.* 290, 3488–3499. doi: 10.1074/jbc.M114.616656

Supplementary Material

Retinal degeneration protein 3 controls membrane guanylate cyclase activities in brain tissue

Yaoyu Chen[1,2], Anja Bräuer[2,3], Karl-Wilhelm Koch[1,3,*]

[1]Division of Biochemistry, Department of Neuroscience, Carl von Ossietzky University, Oldenburg, Germany
[2]Division of Anatomy, Department of Human Medicine, Carl von Ossietzky University, Oldenburg, Germany
[3]Research Center Neurosensory Science, Carl von Ossietzky University Oldenburg, Oldenburg, Germany

*corresponding author: KWK:
Tel.: +49-(0)441-798-3640;
E-mail: karl.w.koch@uni-oldenburg.de

Figure S1

A
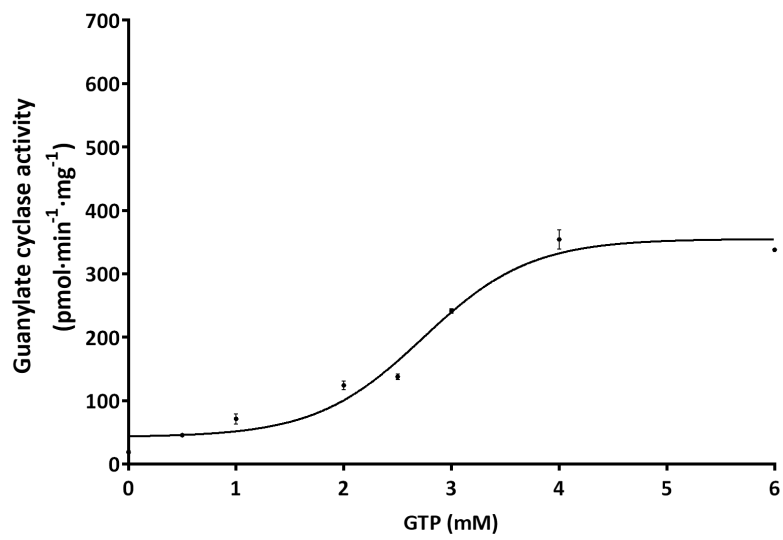
B
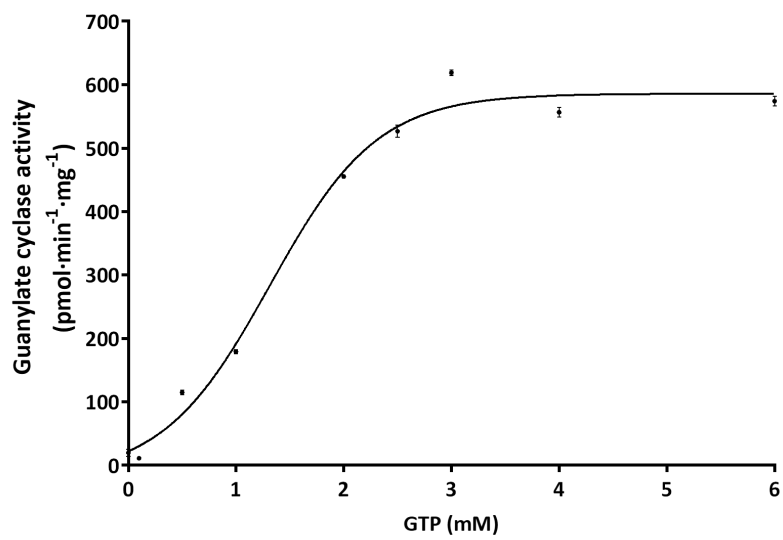
C
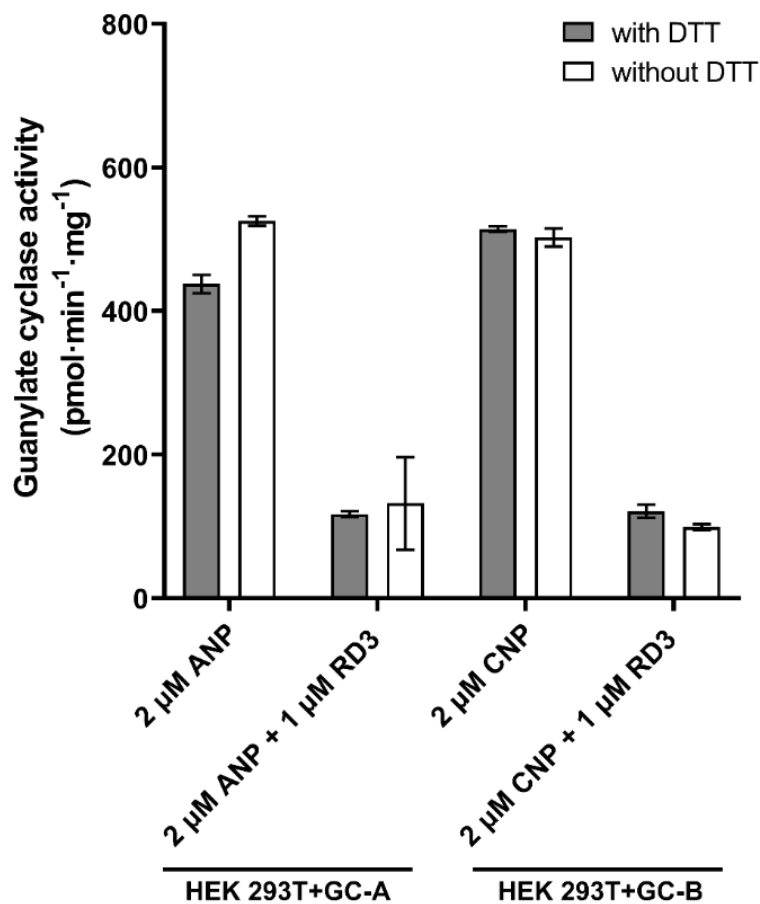
Figure S1. Enzymatic activity of GC-A (A) and GC-B (B) as a function of the substrate GTP concentration. (C) Comparison of GC activities in the presence and absence of DTT. GC-A was activated by 2 µM ANP, GC-B was activated by 2 µM CNP. Addition of 1 µM RD3 decreased GC-activities (N = 3).

Figure S2
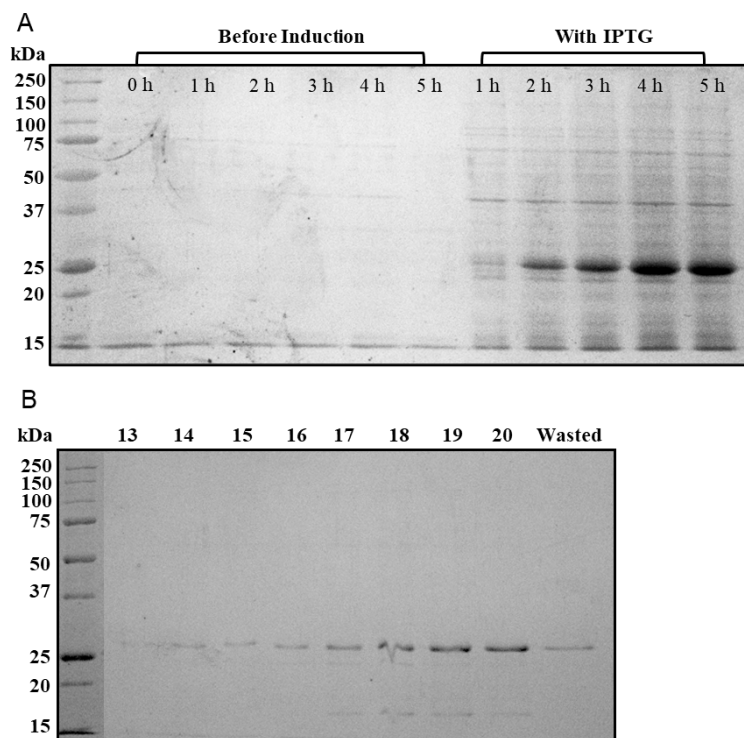
Figure S2. Purification of recombinant RD3 analyzed by SDS PAGE and Coomassie Blue staining. A. RD3 protein expression in *E.coli* before and after the IPTG induction. B. Column chromatography yielding purified RD3 by elution from a Ni-NTA column. Collection of purified samples started at fraction 13.

Figure S3
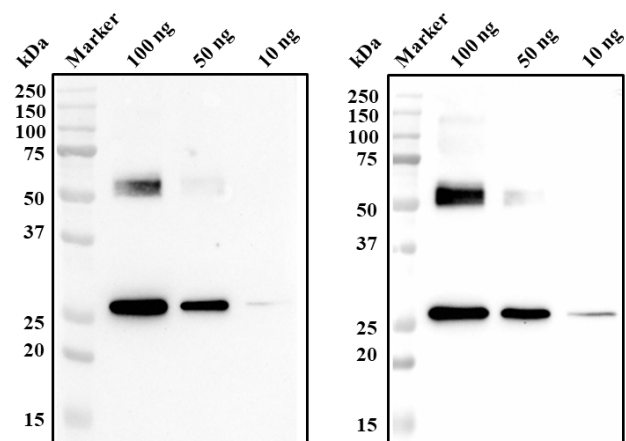
Figure S3. Immunodetection of purified RD3. Immunoblots were incubated with **(A)** mouse anti-RD3 antibody (sc-376516, Abcam) or **(B)** rabbit anti-RD3 antibody (PA598582, Thermo) at protein amounts of 10 ng, 50 ng and 100 ng. Monomers (above 25 kDa) and dimers (above 50 kDa) are visible.

Figure S4
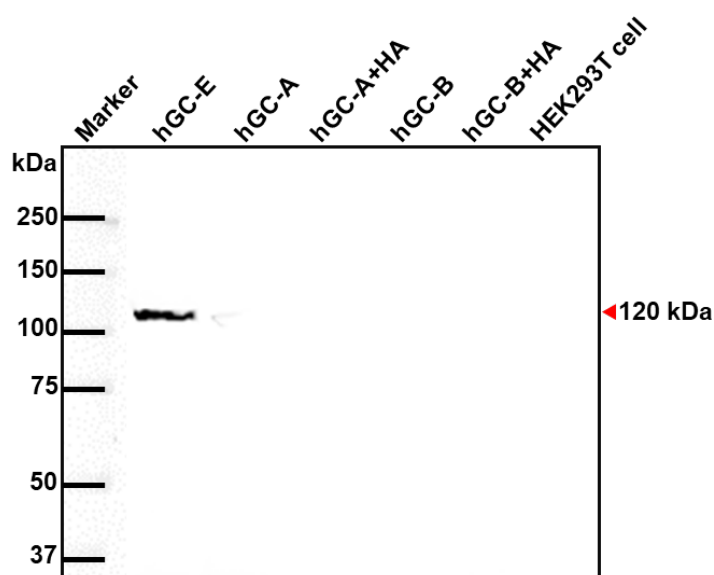
Figure S4. Immunoblotting for testing expression of GC-E. HEK293T cells transfected with human GC-A or GC-B constructs or not transfected (HEK 293 T) were probed a polyclonal anti-GC-E antibody (GC-E #3, see Zägel et al., 2913) at a dilution of 1:1,500. Secondary antibody was a horse-radish peroxidase-coupled goat anti rabbit at a dilution of 1:10,000. Positive control was a sample of HEK293 T cells expressing human GC-E at 120 kDa as indicated. No signal was observed in cells expressing human GC-A or GC-B.

Table S1. Primers for amplification of human GC-A and human GC-B
GC-A: 5'-GCTAGCCCACCATGCCTGGGACCGGC-3'
     3'-GAACGAAGATGGTACTCGTCTCTGTTAATT-5'.
GC-B: 5' -GCTAGCCCACCTGAGTACCTGGCACCGCT-3',
     3'-TGTGACGAAGAGCTTACCTCAT-5'

Table S2. Statistics of relative expression levels of *rd3*, *Npr1* and *Npr2* in the retina as indicated. Significant differences are indicated with asterisks (p ≤ 0.05 = *; p ≤ 0.01 = **; p ≤ 0.001 = ***).

Genes	P10 vs P20		P10 vs P30		P20 vs P30	
rd3	*	0.0422	ns	0.0521	ns	0.8222
Npr1	*	0.0104	ns	0.0538	ns	0.0976
Npr2	**	0.0012	***	0.0006	ns	0.2772

Table S3. Statistics of relative expression levels of RD3, GC-A and GC-B in brain regions as indicated. Significant differences are indicated with asterisks ($p \le 0.05$ = *; $p \le 0.01$ = **; $p \le 0.001$ = ***).

Genes	Group	Cerebellum		Hippocampus		Neocortex		Olfactory bulbs	
rd3	E14 vs P0	*	0.0128	ns	0.2425	ns	0.7289	ns	0.3317
	P0 vs P20	ns	0.5782	*	0.0390	ns	0.5066	ns	0.0508
	P20 vs P60	ns	0.7748	*	0.0136	ns	0.3098	ns	0.4406
	E14 vs P60	ns	0.1129	*	0.0173	ns	0.1724	**	0.0068
Npr1	E14 vs P0	ns	0.0578	ns	0.5123	ns	0.1226	***	0.0009
	P0 vs P20	*	0.0412	**	0.0068	*	0.0107	ns	0.0670
	P20 vs P60	*	0.0189	**	0.0050	**	0.0624	ns	0.3405
	E14 vs P60	**	0.0014	**	0.0014	***	0.0003	*	0.0122
Npr2	E14 vs P0	ns	0.0578	ns	0.1031	ns	0.6380	*	0.0190
	P0 vs P20	**	0.0023	*	0.0365	*	0.0445	*	0.0232
	P20 vs P60	*	0.0198	***	0.0009	ns	0.1072	ns	0.2252
	E14 vs P60	**	0.0030	**	0.0084	ns	0.0552	**	0.0045

Table S4. Statistics of relative expression levels of *rd3*, *Npr1* and *Npr2* in neurons, astrocytes, and microglia. Significant differences are indicated with asterisks ($p \le 0.05$ = *; $p \le 0.01$ = **; $p \le 0.001$ = ***).

Group	*rd3*		*Npr1*		*Npr2*	
Neuron vs Astrocyte	*	0.01426	ns	0.40810	*	0.01968
Astrocyte vs Microglia	*	0.01350	**	0.00309	*	0.01226
Microglia vs Neuron	ns	0.39850	***	0.00015	*	0.01506

Retinal degeneration protein 3 mutants are associated with cell cycle arrest and apoptosis

Yaoyu Chen[1, 2], Jens Hausmann[2], Benjamin Zimmermann[3], Simeon Oscar Arnulfo Helgers[3], Patrick Dömer[3], Johannes Woitzik[3,6], Ulrike Raap[4,6], Natalie Gray[2,4], Andreas Büttner[5], Karl-Wilhelm Koch[1,6]*, and Anja U. Bräuer[2,6]*

[1]Division of Biochemistry, Department of Neuroscience, Carl von Ossietzky University, Oldenburg, Germany

[2]Division of Anatomy, Department of Human Medicine, Carl von Ossietzky University, Oldenburg, Germany

[3] Division of Neurosurgery, Department of Human Medicine, Carl von Ossietzky University Oldenburg, Oldenburg, Germany

[4]Division of Experimental Allergy and Immunodermatology, School of Medicine and Health Sciences, Carl von Ossietzky University Oldenburg, 26129 Oldenburg, Germany

[5]Institute of Forensic Medicine, Rostock University Medical Center, Germany

[6]Research Center Neurosensory Science, Carl von Ossietzky University Oldenburg, Oldenburg, Germany

*equal contributors

Corresponding authors:

Anja U. Bräuer, anja.braeuer@uni-oldenburg.de

Karl-Wilhelm Koch, karl.w.koch@uni-oldenburg.de

Abstract

Retinal degeneration protein 3 (RD3) plays a crucial role in controlling guanylate cyclase activity in photoreceptor rod and cone cells and mediates trafficking processes within photoreceptor cells. Loss of RD3 function correlates with severe forms of retinal dystrophy and the development of aggressive neuroblastoma cancer. In the present study, we analyzed RD3 expression by applying a data mining approach using public databases. In addition, we performed an RD3 transcript analysis on specimens of glioma tissues from patients. We found that RD3 is downregulated in glioblastoma compared to non-tumor tissues. Low expression of RD3 in gliomas was also associated with a poor prognosis of survival rate. Applying a multi-cohort receiver operating characteristic test, we verified significant changes in RD3 expression in glioblastomas indicating a potential use of RD3 in glioblastoma diagnosis. The apparent influence of RD3 on cell viability or on cell cycle progression led us to overexpress RD3 in a cell culture system. Wild type RD3 significantly decreased cell viability, which subsequently led to cell cycle arrest at the G2/M phase and induced cell apoptosis. Conversely, single point mutations in RD3 at the exposed protein surface involved in RD3 target interaction diminished the impact of RD3 wild type showing thereby its specificity. Therefore, expression of wild type RD3 might prevent tumor progression by facilitating cell death of cancer cells or arresting the cell cycle in a developing tumor. Our findings further suggest that RD3 is a potential prognostic factor in glioblastoma.

Key words:

Introduction

Retinal degeneration protein 3 (RD3) is an evolutionarily conserved protein consisting of 195 amino acids and exhibits minimal homology to other proteins (Peshenko *et al.*, 2019). In photoreceptor cells, RD3 serves as crucial regulator of guanosine 3', 5'-cyclic monophosphate (cGMP) synthesis via binding to retinal membrane guanylate cyclases (GC-E and GC-F) thereby inhibiting guanylate cyclase activity. In addition, complex formation of GCs with RD3 facilitates trafficking of GCs from the endoplasmic reticulum (ER) to endosomal vesicles in the retina. The GC-RD3 complex targets to the light-sensitive outer segments of photoreceptors and inhibition of cyclase activity during trafficking prevents production of non-physiological high cGMP levels (Azadi *et al.*, 2010; Molday *et al.*, 2013; Peshenko *et al.*, 2011a; Peshenko *et al.*, 2021; Zulliger *et al.*, 2015). RD3 folds into a three-dimensional structure of a four-helix bundle based on a Nuclear Magnetic Resonance (NMR) spectroscopy study showing the following arrangement: helix α1: P21–V51; α2: P75–K87; α3: P90–Q107; α4: V111–T139. Point mutations in the central helix α3 of RD3 weaken RD3 affinity for GC-E (Ames, 2022; Peshenko and Dizhoor, 2020; Peshenko *et al.*, 2019). Genetic deficiencies and mutations of RD3 cause early-onset photoreceptor degeneration in patients with Leber congenital amaurosis type 12 (LCA 12) (Azadi *et al.*, 2010; Friedman *et al.*, 2006; Molday *et al.*, 2013; Perrault *et al.*, 2013; Wimberg *et al.*, 2018a).

In addition to its high expression in the retina RD3 is expressed in other organs and tissues, including the brain at both the transcriptional and translational level, but expression is significantly lower than in the retina (Aravindan *et al.*, 2017; Chen *et al.*, 2022). A more recent study compared the expression of RD3 in astrocytes and neurons with those in the retina. This study tested, whether RD3 can modulate the activities of non-sensory membrane bound guanylate cyclases GC-A and GC-B that are activated by natriuretic peptides ANP and CNP, respectively (Chen *et al.*, 2022). The active states of recombinant GC-A and GC-B and that of native GCs in astrocytes were inhibited by RD3 (Chen *et al.*, 2022). Collectively, these reports indicate that *RD3* expression and function is not restricted to retinal tissue. Furthermore, one of the

previous studies reported that loss of RD3 correlates with the development of an aggressive neuroblastoma cancer (Khan *et al.*, 2015). Although these findings seem to contradict an earlier study concluding that inactivation of both *RD3* alleles in LCA12 patients does not correlate with extraocular symptoms (Perrault *et al.*, 2013), a more recent study supports the direct involvement of RD3 loss in tumor development and progression (Somasundaram *et al.*, 2019). In addition, the study found that intensive multimodal therapy facilitates RD3 loss in surviving cells, leading to disease progression (Somasundaram *et al.*, 2019). At present however, any causal relationship between the abnormal regulation of RD3 expression and tumor development is unclear. Glioma is a type of tumor that originates in the glial cells of the brain or spine and is classified by the WHO into low-grade glioma (LGG) and glioblastoma (GBM) (Cosnarovici et al., 2021; Goodenberger and Jenkins, 2012). GBM is the most aggressive and common primary brain tumor among gliomas (57.7% of total gliomas). Patients with GBM still have a poor prognosis despite treatment with a combination of maximal surgical resection, radiotherapy, and chemotherapy (Bi et al., 2020). Therefore, to improve the early diagnosis and prognosis of GBM, a better understanding and mapping of the molecular events involved in GBM initiation and progression is important.

In this study, we asked whether expression rates of *RD3* differ between patient cohorts suffering from glioblastoma and healthy volunteers. Strongly connected to this question is a comparison of the overall survival rates of patients and a possible impact of *RD3* expression. Using heterologous expressions of RD3 wildtype and a group of selected RD3 mutants in a common cell culture system, we monitored RD3 dependent cell growth, cell cycle arrest and cell apoptosis. By this approach, we gained more insight into the regulatory features of RD3.

Results

Clinical and molecular characteristics of RD3 in gliomas

To date, there is no pathological or etiological indication of *RD3* gene expression playing a role in glioma development or disease progression, but current public datasets such as TCGA (https://www.cancer.gov/tcga) provide useful information about hypothetical correlations of *RD3* transcript levels and its impact in specific diseases. Accordingly, we first analyzed *RD3* transcript levels in the TCGA GBM/LGG, GSE108474, GSE16011, and GSE7696 cohorts in different histological groups and found significant differences between non-tumor and glioblastoma tissue, but not in other gliomas like astrocytoma. When compared to other glioma types, *RD3* expression was generally low in glioblastoma (Figure 1A-D). We then performed qRT-PCR for *RD3* expression in the glioma tissues from the EV cohort and found a significant downregulation of *RD3* expression in GBM compared to non-tumor tissue (Figure 1E, expression normalized to TBP and HPRT1).

In order to analyze the correlations between the *RD3* expression levels and the clinically pathological characteristics of the patients, the data from TCGA-GBM/LGG (699 individuals) and EV (28 individuals) were subdivided by the median expression of *RD3* and assigned as *high expression* and *low expression* (Supplemental Table S1, S2). For the primary therapy outcome, the *high expression of RD3* group showed a significant increase in partial response and in complete response cases, but no differences in progressive disease and stable disease cases, when compared with the *low expression* group. After Chi-squared test calculation, the clinicopathologic characteristics of *RD3* expression showed a similar trend for the low *RD3* group classified underage over 60, glioblastoma, isocitrate dehydrogenase wild type status (IDH wild type) and WHO grade G4. However, the data was not significant due to less clinical samples (Supplementary Table S2). Based on the above evidence, we suggest that RD3 decreased significantly in GBM pointing to a potential role of RD3 as a biomarker for curative response (Supplemental table S1, S2).

The clinical and prognostic significance of *RD3* expression in gliomas

From our analysis, we infer that the change in *RD3* mRNA expression is strongly associated with glioblastoma, the type of glioma with the lowest probability of survival. To confirm the robustness of this finding, we evaluated the prognostic relevance of *RD3* transcript level in the datasets of TCGA GBM/LGG, GSE108474 and GSE16011. Patients were divided into *low* and *high RD3* mRNA expression subgroups according to 50 percentiles of *RD3* expression, and overall survival curves with 95% CI (95% confidence interval shown as shadow), HR (hazard ratio), and *p-value* were generated using Kaplan-Meier Cox regression. The results showed that in TCGA GBM/LGG (p<0.001, HR=0.35), GSE16011 (p=0.037, HR=0.76) and GSE106474 (p=0.002, HR=0.72), patients suffering from glioma with higher expression of *RD3* had a significantly better prognosis than the subgroup with lower expression, especially the 5-year overall survival ratio in RD3 low group is less than 25% in all cohorts (Figure 2A-C). In addition, to evaluate the diagnostic value of *RD3* in GBM, the data from healthy donors and GBM patients of a multicohort study were selected for a receiver operating characteristic (ROC) test (Figure 2D-I). If the area under the curve gives a parameter AUC > 0.5, the test successfully predicts, whether RD3 expression provides a higher survival rate in GBM patients in comparison to healthy donors. Analysis of the data sets implemented in the current study revealed the following AUC (in brackets) for TCGA (AUC=0.9339), GSE108474 (AUC=0.6670), GSE16011 (AUC=0.7792), GSE7696 (AUC=0. 7969), TBP (AUC=0.7727) and HPRT1 (AUC=0.7168). All ROC curves had an AUC value > 0.5 meaning that the predictive ability was acceptable and significantly better than a random guess. Only the result of GSE108474 with an AUC=0.6670 showed a less obvious discrimination. Accordingly, further ROC analytics of the GBM and LGG from cohorts displayed AUC values of TCGA (AUC=0.7075), GSE108474 (AUC=0.6091) and GSE16011 (AUC=0.5566), indicated an acceptable model to distinguish the GBM from glioma (Supplemental Figure S1). Thus, assessment of the predictive ability indicated that *RD3* may be a potential biomarker for the diagnosis of GBM.

Selected point mutations in RD3

Our data analysis presented above and reports in the literature (Somasundaram *et al.*, 2019) correlate dysfunctional expression of RD3 with tumor development. Collectively, these investigations indicate an influence of *RD3* on cell viability or even an indirect impact on cell cycle progression. So far, several studies describe mutations in RD3 that cause LCA12, a severe form of retinal degeneration and cell dysfunction (Peshenko and Dizhoor, 2020; Peshenko *et al.*, 2011b). In order to explore how *RD3* expression might interfere with cell viability in non-retinal cells we selected amino acid positions that seem prone to functional impairment. For example, positions that are critical for the development of LCA12 or positions that are found in the RD3-target protein interface. Based on these reasons we designed and obtained RD3 point mutations R38L, R45W, R47H, R68W, P95S, and R119C (Figure 3A, B). The residues R38 in helix α1 is a recessive mutation linked to LCA12 (Perrault *et al.*, 2013). Positions R45 and R47 were inside the solvent-exposed ends that are connected by series of salt-bridges and belong to a cluster of mutations or polymorphisms found in patients with retinal dysfunctions (Azadi *et al.*, 2010; Zulliger *et al.*, 2015). The same counts for the residue R68. Residue P95 and R119 are also solvent-exposed in helix α3 and helix α4, respectively, and are present in short regions of the binding interface interacting with the target GC-E (Peshenko *et al.*, 2016; Peshenko *et al.*, 2019).

We transfected cells with RD3 and its variants and verified the expression of RD3 in cells by immunoblotting (Figure 3C). Moreover, we localized RD3 and its variants by immunocytochemistry assay and tested for the involvement in cellular processes. The results revealed that RD3 and its variants have a similar subcellular localization; they were detected in the cell cytosol and in vesicles. After 24 h of transfection, the nuclei of strongly red fluorescence-positive cells are allocated in the interphase of the M phase (Supplemental Figure S2). These results indicated that overexpression of RD3 and its variants might be involved and seem to interfere with cellular functions of HEK293T.

Inhibition of cell viability by RD3 and its variants

The MTT assay measures cellular metabolic activity as an indicator of cell viability, proliferation, and cytotoxicity. To analyze the effects of RD3 transient overexpression on HEK293T cells, we employed this assay at 24, 48, and 72 hours post-transfection. Our results demonstrated significantly reduced cell survival (OD_{590} value) in cells transfected with RD3 wild-type plasmids compared to control groups (RFP empty vector, mock, and untreated cells) at all examined time points (Figure 4A). At 24 hours, there were no significant differences between RD3 mutants and the RD3 wild type in subsequent measurements. However, after 48 hours, only the R38L variant showed a significant improvement in cell viability. Additionally, at 72 hours, no significant differences were observed between R68W and the wild type. Conversely, variants such as R38L, R45W, R47H, P95S, and R119C exhibited more viable cells than the RD3 wild type (Figure 4B). Compared to the control groups, all variants demonstrated a substantial negative impact on cell viability at 48 and 72 hours. For instance, while the OD_{590} value for control groups ranged from 1 to 2 at 48 hours, it was less than 0.4 for HEK 293 cells transfected with RD3 variants. These findings indicated that overexpression of RD3 and its variants influences the cell viability of HEK293T.

The mutation of RD3 is associated with cell cycle arrest at G2/M phase

Cell cycle arrest and apoptosis are crucial processes that affect cell growth, therefore we determined whether transfection of HEK293T cells with RD3 and its variants regulates cell cycle progression and programmed death. To investigate how cell cycle progression would be affected by RD3 and its variant, post-transfected cells were harvested and fixed, nuclear DNA content was measured using DAPI and fluorescence-activated cell sorting (FACS) analysis. Due to the limitation of transient cell transfection efficiency, a cell sorting step based on RFP tag was performed on flow cytometry (Supplemental Figure S3). Overexpression of RD3 and its variants influenced the extent of G2/M phase compared to cells transfected with an empty RFP vector or a mock transfection (Figure 5A-B). The summary of distribution of cell cycle phases in five rounds of replicates showed a higher proportion of G2/M phase in the

RD3 experimental group and a lower proportion of G0/G1 phase in the control group (Figure 5C).

Subsequent statistical analysis revealed that in G1 phase cells, only R38L showed a significant decrease, while RD3 wild type, R45W, R47H, R68W, P95S and R119C showed a slightly downregulated trend compared to control (Figure 5D). In S phase cells, there were no significant differences between experimental and control groups, but a moderate decrease was observed (Figure 5E). In G2/M phase cells, R38L and R68W show a significant increase, while the others exhibited a global upward trend compared to control RFP and mock. These results showed that RD3 and its variant can disrupt the normal cell cycle of HEK293T cells by arresting these cells in the G2/M phase.

The impact of RD3 on cell apoptosis

Disruption of the cell cycle by RD3 could point to an induction of apoptosis by RD3 and its point mutants. We investigated a possible induction of apoptosis in HEK293T cells, which were carefully collected after transfection and digested with 0.05% trypsin-EDTA. DAPI and Annexin V APC conjugates were used for staining to detect programmed cell death. Using flow cytometry, we first sorted cells by the RFP tag to find RD3 and RD3 mutant positive cell populations (Supplemental Figure S4). Positive cells were selected for measurement, while the unstained cells were used to assist the gate set separating the cell cluster of life (DAPI-, APC-), early apoptosis (DAPI-, APC+), late apoptosis (DAPI+, APC+) and death stages (DAPI+, APC-). Results in Figure 6 A and B showed the cell distribution at different stages after staining with an apoptosis indicator. It was obvious that more cells are alive in the RFP and Mock group than in cell populations that are positive with RD3 and its variants. We applied a statistical analysis of replicate transfections yielding a summary of cell distribution, which revealed that a significant percentage of cell populations overexpressing RD3, and its variants were in early stage of apoptosis. These cell populations contain lower numbers of live cells and similar portions of dead cells in comparison to control groups (Figure 6C and D). However,

the numbers of apoptotic cells overexpressing the RD3 mutants R38L, R45W, R47H, P95S and R119C were markedly less than in cells overexpressing RD3 wild type. The mutant R68W was an exception in this row, as it showed no significant difference to RD3 wild type (Figure 6E).

Discussion

The retina specific protein RD3 controls trafficking processes in photoreceptor cells and is critical for the controlled synthesis of the second messenger cGMP. The association of RD3 mutations in patients diagnosed with severe early onset retinal dystrophy (Friedman *et al.*, 2006; Perrault *et al.*, 2013; Preising *et al.*, 2012) brought these 195 amino acids long protein of around 22 kDa also into focus of biomedical research. The *RD3* gene was originally identified in the *rd3* mouse strain exhibiting progressive retinal degeneration(Chang et al., 1993). Mutations in the human *RD3* gene that lead to a loss of function of the RD3 protein correlate with retinal dystrophy type LCA12 (Azadi *et al.*, 2010; Peshenko and Dizhoor, 2020; Preising *et al.*, 2012; Zulliger *et al.*, 2015).

The critical function of RD3 in health and disease seems to extend to non-retinal tissue, since recent investigations in human and mice tissues showed the expression of RD3 in different brain regions and in epithelial cells of various organs (Aravindan *et al.*, 2017; Chen *et al.*, 2022; Khan *et al.*, 2015; Somasundaram *et al.*, 2019). Loss of RD3 expression correlates with the progression of neuroblastoma pathogenesis and a poor survival prognosis (Aravindan *et al.*, 2017; Khan *et al.*, 2015). Interestingly, rare cases of vision impairment were reported as an early indicator of tumor progression in GBM patients (Lin and Huang, 2017; Lincoff *et al.*, 2012; Xie et al., 2015). We extended these previous studies by applying a data mining approach, in which we screened and analyzed multi-cohort data sets with respect to *RD3* expression. In this way, we assessed the prognostic and diagnostic value of *RD3* in glioma, particularly in glioblastoma. Testing the predictive ability of *RD3* expression rates by a ROC test (Figure 2) gave in four out of five patient cohorts AUC values of at least acceptable numbers situated between 0.7 and 0.8 (de Hond et al., 2022). The analysis of the TCGA cohort revealed even an excellent AUC parameter > 0.9 (de Hond *et al.*, 2022). Thus, we suggest that RD3 expression could serve as a diagnostic parameter in glioblastoma development. Furthermore, we found that the lower expression of *RD3* is associated with a poor clinical prognosis for patients with GBM. Our results resemble

previous findings obtained from tissue of neuroblastoma patients, in which the loss of RD3 is associated with tumor invasion, tumorosphere formation, and metastasis (Khan *et al.*, 2015; Somasundaram *et al.*, 2019). Khan et al. (Khan *et al.*, 2015) suggested that RD3 functions as a metastasis suppressor, which would be supported by our findings from GBM samples.

Cancer cells that survive intensive multimodal clinical treatment have lost RD3 (Somasundaram *et al.*, 2019) leading to a worse clinical prognosis. The mechanism of this effect remains unclear, but it demonstrates that the expression RD3 must be set at a critical intracellular level. Furthermore, it is unclear whether loss of RD3 is involved in causing transformation of cells or is an epiphenomenon triggered by processes during tumor development. Previous reports indicated that RD3 is associated with the ER stress induced apoptosis of photoreceptor cell, but any influence aside still remains unknown (Plana-Bonamaiso *et al.*, 2020). In order to investigate a hypothetical role of RD3 in cell cycle progression, we overexpressed RD3 wild type and a set of selected RD3 mutants in HEK293 cells and analyzed cell viability and cell growth. RD3 overexpression had a clear effect on activating the cell death program and arresting the cell cycle in the G2/M phase. This capacity indicates that RD3 might prevent tumor progression by facilitating cell death of neoplastic transformed cells or arresting the cell cycle, however these results seem to contradict to its function in photoreceptor cell. The RD3 mutants had a lower impact on cell cycle arrest and apoptosis than RD3 wild type (Figure 6). We interpret this result to indicate that the effect of RD3 on cell cycle control is specific, because the positions of the point mutations are located at critical positions at the interface region to interact with guanylate cyclases (Friedman *et al.*, 2006), and any disturbance might weaken or diminish the RD3 impact on cell cycle control. Our recent discovery thatthe activity of natriuretic peptide receptor guanylate cyclases is controlled by RD3 in a fashion similar to photoreceptor cyclases (Chen *et al.*, 2022), we assume that RD3 is involved in a signal transduction pathway involving a membrane bound guanylate cyclase. Interestingly, a study indicated that GC-A is associated with the tumor cell cycle, apoptosis and angiogenesis through a VEGF/GC-

A/cGMP cascade (Li et al., 2021). While, the VEGF has been applied as therapeutic target for anti-angiogenesis of GBM (Khasraw *et al.*, 2014). This scenario would provide a link to a signaling pathway involving the second messenger cGMP.

A direct link of the biochemical function of RD3 and cancer might also exist in its ability to regulate the guanylate kinase (GUK) activity (Wimberg *et al.*, 2018a), an enzyme that is involved in catalyzing the 5'-GMP to GDP conversion (Fitzgibbon et al., 1996). GUK is an essential ubiquitous enzyme involved in the nucleotide metabolism of cells and is involved in diverse cellular mechanisms. Due to its crucial housekeeping role the pharmacological targeting of GUK is used in viral and cancer therapies. For example, 5'-GMP analogues serve as potent GUK inhibitors or as antiviral and anticancer prodrugs(Elion, 1989). Furthermore, the loss of GUK is associated to the cellular cancer viability, proliferation, and clonogenic potential, while final activate the programmed cell death (Khan et al., 2019).

Finally, a study investigated the changes in the gene expression profile of the *rd3* mouse and showed that the *RD3* gene is involved in downregulation of gene expression acting in lipid metabolism(Cheng and Molday, 2013). The authors speculate that RD3 plays a central role in the metabolism of phosphatidic acid, because the expression of many enzymes directly involved in lipid metabolism are dysregulated in the retina of the *rd3* mouse. Lysophosphatidic acid is converted to phosphatidic acid, which is a necessary step to produce lipids important for cell membranes and chemical signaling within cells. Lysophosphatidic acid has been described as a factor in cancer progression by stimulating tumor proliferation and cancer cell survival. It further increases invasiveness of various neoplasia's (Mills and Moolenaar, 2003) and contributes to the development of brain malignancies(Kishi et al., 2006).

In summary, we here show that low expression of the RD3 gene is a crucial factor in the development of glioblastoma. Overexpression of RD3 indicated an impact on cell

cycle progression and triggered apoptotic pathways. Our findings extend the established roles of RD3 photoreceptor cells to other cell types in different organs.

Materials and Methods

Data sources and gene differential expression

The mRNA expression profiles and clinical data of LGG and GBM patients originated from The Cancer Genome Atlas (TCGA) and Gene Expression Omnibus (GEO) database. The project ID, TCGA-GBM/LGG, GSE108474, GSE16011 and GSE7696, were pre-analyzed and downloaded from R2 Genomics Analysis and Visualization Platform (https://r2.amc.nl). We set up a filtering step for the cohorts taken into analysis removing duplicated and non-clinical data. After filtering, we obtained 704 individuals (5 non-tumor and 699 tumor) from TCGA-GBM/LGG cohort, 473 individuals (28 non-tumor and 445 tumor) from GSE108474, 273 individuals (8 non-tumor and 265 tumor) from GSE16011, and 84 individuals (4 non-tumor and 80 tumor) from GSE7696. The statistically significance analysis and visualization of gene differential expression was provided by the function of one-way analysis of variance (ANOVA) and unpaired Mann-Whitney test in GraphPad Prism 7 (GraphPad Software, San Diego, CA, United States).

Survival and ROC Curve Analysis

Clinical information of datasets was obtained to investigate the correlation of *RD3* mRNA expression with the prognosis of Glioma survival rate. Duplicated samples and those without clinical data were removed. For the overall survival analysis, we employed specific R packages (*survival, survminer, ggplot2* obtained from https://www.bioconductor.org/). The receiver operating characteristic (ROC) tests were performed using internal algorithms of GraphPad Prism. The area under the ROC curves (AUC) value ranging from 0 to 1 was calculated for assessing and comparing different diagnostic models.

Patients and health donor samples

Donor samples of human brain tissue were taken from 13 individuals of 11 males and 2 females (Supplement Table S3) in the forensic medicine within 130 h after death and stored for further investigation at − 80 ◦C. All procedures were approved by the local Ethics Committee (Rostock University Medical Center; registration ID: A2015− 0143).

None of the donors suffered from a known brain cancer disease. Human glioblastoma specimens were freshly obtained from 28 individual surgeries of 17 males and 11 females (Supplement Table S4) from the Evangelisches Krankenhaus Oldenburg (EV), with informed written patient consent (ethics registration ID: 2018-137). The tissue was snap-frozen in liquid nitrogen and stored at − 80 ∘C.

Clone construction and site-directed mutant

The pTurbo-RFP-N vector (Evrogen, Biocat, GmbH, Germany) was applied for gene expression and vector modification. The human RD3 wild type DNA (Ensembl: ENSP00000505312.1) and its point mutants were generated using the primer listed in Supplemental Table S5 in the Supplement via polymerase chain reaction (PCR). For the clone construction, Nhe I and Xho I digested the vector and PCR product. The Dephos & Ligations Kit (Merck, Darmstadt, Germany) was used for vector dephosphorylation and ligation. For constructing RD3 point mutations the pTurbo-hRD3-RFP clone served as template. Using the Q5® Site-Directed Mutagenesis Kit (New England BioLabs, Ipswich, USA) generated RD3 mutants according to manual protocol provided by the manufacturer. The plasmids with wild type RD3 and its mutants were used for transformation in E. coli cells (XL1 blue, BL21C), with antibiotics (Kanamycin) screening, the positive clones were selected for amplification and further DNA extraction. Insertions were verified by GATC Biotech (Eurofins genomics, Konstanz, Germany).

Cell culture and transfection

HEK293T cells were cultured in Dulbecco's modified Eagle's medium (DMEM; Thermo Fisher Scientific) containing 10% fetal bovine serum (FBS; PAN-Biotech, Aidenbach, Germany), 2 mM L-glutamine (Merck Millipore, Darmstadt, Germany), 100 units/ml penicillin-streptomycin (PAN-Biotech) in an incubator set at 5% (v/v) CO_2 and 37°C. For cell transfection, cells were seeded in 6-well plates at 2 x 10^5 cells per well. The next day, METAFECTENE® liposome-based transfection reagent (Biontex Laboratories GmbH, Germany) was applied for cell transfection in combination with

the established plasmids mentioned above by using the protocol of the manufacturer. After 24 hours, the cell culture medium was changed, and the cells were processed according to the assay in use.

Cell viability assay

The cell viability was determined using the thiazolyl blue tetrazolium bromide (MTT) kit provided by Sigma (product number: M2128). The MTT powder was dissolved in 1 x PBS to a final concentration of 5 mg/ml and then underwent filter sterilization via a 0.22 µm filter. HEK 293T cells were seeded in 96-well plates at a density of 1 x 10^3 cells/well and transfected with the relevant resources described above on the following day. Cell viability was assessed at 24, 48, and 72 hours after transfection. When the time is up, 50 µl of serum-free media and 50 µl of MTT solution was added into each well followed by 3 hours incubation at 37°C. Afterwards, the 150 µl of MTT solvent solution (4 mM HCl, 0.1% NP40 in isopropanol) was used for dissolving any sediment. To accelerate the reaction an orbital shaker was applied. Last, the absorbance at OD=590 nm was monitored using the BioTek Epoch Microplate Spectrophotometer (Agilent Technologies, Santa Clara, USA). Four independent biological groups, each with 2 replicates, were established.

Cell cycle detection

The transfected HEK293T cells were digested with 0.05% trypsin/EDTA at 37° C for 5 minutes. The DMEM medium containing FBS was used to halt the reaction. Next, the cell mixture was collected in a 15 ml Falcon tube and spun at 500 g for 5 minutes at 4 °C. Afterwards, cells were washed twice with 5 ml of cold 1 x PBS, the supernatant was discarded, and the cells were resuspended with 500 µl of fresh, cold PBS. Then cell suspensions were transferred to a new 15 ml Falcon containing 4.5 ml of ice-cold 70% ethanol. The mixture was incubated at 4° C overnight, then centrifuged at 1000 g for 5 minutes and washed with 5 ml of PBS. Cell pellets were resuspended for 10 minutes in 300 µl of DAPI/TritonX-100 solution, which contains 10 µl of 1 mg/ml DAPI and 0.1% (v/v) TritonX-100 in 10 ml of PBS. Five independent replicates were analyzed

for cell cycle using the Cytoflex S flow cytometer (Beckman Coulter, CA, USA) on the cells transfected with red fluorescence protein. The results were analyzed with FlowJo v10.8.1 (BD Life Sciences, Ashland, USA), and the gate settings were displayed on Supplementary Figures S3.

Cell Apoptosis Measurement

The HEK293T cells that had been transfected were detached from the 6-well plates using 0.05% Trypsin-EDTA and then transferred to a 15 ml falcon tube. Following this, the cell mixture was centrifuged at 500 g for 5 minutes and the supernatants were discarded. The cells were washed with cold 1 x PBS and then the cell pellet was resuspended in 300 μl binding buffer (10 mM HEPES, 150 mM NaCl, 2.5 mM $CaCl_2 \cdot 2H_2O$) after the washing step. Cells were counted by aspirating approximately 2.5×10^5 cells for Annexin V-APC Conjugates (Thermo Fisher Scientific, Waltham, MA, USA) and DAPI staining, with a final volume of 50 μl, as recommended by the manufacturer. Cells were incubated at room temperature for 15 minutes, 300 μl of binding buffer was added, briefly vortexed, and loaded onto the Cytoflex S (Beckman Coulter, CA, USA) flow cytometer for measurement. The results were analyzed using FlowJo v10.8.1[30-day free trial] (BD Life Sciences, Ashland, USA) and the gate setting is shown in Supplemental Figure S4.

qRT-PCR

The RNA of human brain tissues from 13 health donors (Supplemental Table S3), and 28 glioma patients (Supplemental Table S4) were homogenized in TRIzol™ reagent (Thermo Fisher Scientific, Waltham, MA, USA) and extracted according to the manufacturer's protocol. After RNA concentration measurement by BioSpectrometer basic (Eppendorf, Hamburg, Germany), the 0.5 μg RNA applied for cDNA synthesis by using high-capacity cDNA reverse transcription kit from Thermo Fisher Scientific. Transcript level of RD3 measurements were based on TaqMan™ Fast Universal PCR Master Mix, No AmpErase™ UNG (Thermo Fisher Scientific, Waltham, MA, USA) on hard-shell 96-Well PCR plates from Bio-Rad Laboratories (Hercules, CA, USA), and

85

TaqMan probes. The human *RD3* probe, and two housekeeping *TBP* and *HPRT1* probes were purchased from Thermo Fisher Scientific (RD3: Hs01650935_m1, TBP: Hs00427620_m1, and HPRT1: Hs01003270_g1).

Western blot

Protein fractions from HEK293T cells were incubated with 5× Laemmli buffer containing 1% (v/v) β-mercapto-ethanol at 95° C for 5 min and analyzed by SDS-PAGE with 12% acrylamide. Immunoblotting was performed using a 0.45 µm nitrocellulose (NC) membrane and semi-dry blotting system. After blotting at 200 mA for 30 min, the membrane was blocked in 5% milk powder (Carl Roth) in TBST at room temperature for 1 h. Primary anti-mouse-RFP antibody (MA5-15257, Thermo Fisher Scientific) were incubated overnight at 4°C in blocking solution at a dilution of 1:2,000. The next day, the membrane was washed with TBST, then incubated with horseradish peroxidase-conjugated secondary antibodies (GE Healthcare, Boston, MA, United States) at a dilution of 1:10,000 in blocking solution. The blot was washed again, and the immunoreaction was detected with Clarity or Clarity Max ECL substrate (Bio-Rad Laboratories, Hercules, CA, United States) according to the manufacturer's protocol.

Immunocytochemistry

The HEK293T cells were washed using 1× PBS and then fixed with ice-cold 4% paraformaldehyde (Merck KGaA, Darmstadt, Germany) and 15% sucrose in 1× PBS for 20 minutes following 24 h of transfection. Afterwards, the fixed cells were washed three times with 1× PBS for 10 min and permeabilized in 0.1% Triton X-100/PBS + 0.1% sodium citrate for 3 min. Cells were washed with 1× PBS for three times again and blocked in buffer containing 10% FCS/1% NGS/PBS for 1 h. For immunostaining, DAPI was applied for staining the nuclei. Coverslips were again washed three times for 10 min with 1× PBS and cells were mounted with Immu Mount Vectashield Hard Set Mounting medium (Vector Laboratories, Burlingame, CA, USA). Imaging of the mounted slides was performed using an Olympus FV3000 confocal microscope.

Statistical analysis

RNA-seq and microarray data from TCGA GBM/LGG, GSE108474 and GSE16011 were analyzed using one-way ANOVA (Figure 1. A-C), while data from GSE7696 and qRT-PCR were analyzed using unpaired Welch's t-test (Figure 1. D-F). The Chi-squared test was used to analyze the association between *RD3* expression (divided by the median mRNA expression of *RD3*) and clinically pathological variables in patients from TCGA GBM/LGG cohort (Supplemental Table S1), while the Fisher's exact test was used for small samples from the EV cohort (Supplemental Table S2), and the statistical analyses by using the R package version of stats [4.2.1]. Kaplan-Meier overall survival curves were generated using Cox regression provided by using the R package with the version of survival [3.3.1] survminer and ggplot2 [3.3.6] packages in R version 4.2.1 (Figure 2A-C). The receiver operating characteristic (ROC) curve (Figure 2D-I) was processed using the algorithm provided by GraphPad Prism 7 (GraphPad Software, San Diego, CA, United States). For multiple comparisons (Figure 4, Figure 5D-F, Figure 6D-E), the two-way ANOVA of GraphPad Prism was used.

Reference

1. Peshenko IV, Yu Q, Lim S, Cudia D, Dizhoor AM, Ames JB. Retinal degeneration 3 (RD3) protein, a retinal guanylyl cyclase regulator, forms a monomeric and elongated four-helix bundle. *J Biol Chem* 2019, **294**(7)**:** 2318-2328.

2. Peshenko IV, Olshevskaya EV, Dizhoor AM. Retinal degeneration-3 protein attenuates photoreceptor degeneration in transgenic mice expressing dominant mutation of human retinal guanylyl cyclase. *J Biol Chem* 2021, **297**(4)**:** 101201.

3. Peshenko IV, Olshevskaya EV, Azadi S, Molday LL, Molday RS, Dizhoor AM. Retinal degeneration 3 (RD3) protein inhibits catalytic activity of retinal membrane guanylyl cyclase (RetGC) and its stimulation by activating proteins. *Biochemistry* 2011, **50**(44)**:** 9511-9519.

4. Azadi S, Molday LL, Molday RS. RD3, the protein associated with Leber congenital amaurosis type 12, is required for guanylate cyclase trafficking in photoreceptor cells. *Proc Natl Acad Sci U S A* 2010, **107**(49)**:** 21158-21163.

5. Molday LL, Djajadi H, Yan P, Szczygiel L, Boye SL, Chiodo VA*, et al.* RD3 gene delivery restores guanylate cyclase localization and rescues photoreceptors in the Rd3 mouse model of Leber congenital amaurosis 12. *Hum Mol Genet* 2013, **22**(19)**:** 3894-3905.

6. Zulliger R, Naash MI, Rajala RV, Molday RS, Azadi S. Impaired association of retinal degeneration-3 with guanylate cyclase-1 and guanylate cyclase-activating protein-1 leads to leber congenital amaurosis-1. *J Biol Chem* 2015, **290**(6)**:** 3488-3499.

7. Peshenko IV, Dizhoor AM. Two clusters of surface-exposed amino acid residues enable high-affinity binding of retinal degeneration-3 (RD3) protein to retinal guanylyl cyclase. *J Biol Chem* 2020, **295**(31)**:** 10781-10793.

8.   Ames JB. Structural basis of retinal membrane guanylate cyclase regulation by GCAP1 and RD3. *Front Mol Neurosci* 2022, **15:** 988142.

9.   Wimberg H, Janssen-Bienhold U, Koch KW. Control of the Nucleotide Cycle in Photoreceptor Cell Extracts by Retinal Degeneration Protein 3. *Front Mol Neurosci* 2018, **11:** 52.

10. Friedman JS, Chang B, Kannabiran C, Chakarova C, Singh HP, Jalali S*, et al.* Premature truncation of a novel protein, RD3, exhibiting subnuclear localization is associated with retinal degeneration. *Am J Hum Genet* 2006, **79**(6)**:** 1059-1070.

11. Perrault I, Estrada-Cuzcano A, Lopez I, Kohl S, Li S, Testa F*, et al.* Union makes strength: a worldwide collaborative genetic and clinical study to provide a comprehensive survey of RD3 mutations and delineate the associated phenotype. *PLoS One* 2013, **8**(1)**:** e51622.

12. Aravindan S, Somasundaram DB, Kam KL, Subramanian K, Yu Z, Herman TS*, et al.* Retinal Degeneration Protein 3 (RD3) in normal human tissues: Novel insights. *Sci Rep* 2017, **7**(1)**:** 13154.

13. Chen Y, Brauer AU, Koch KW. Retinal degeneration protein 3 controls membrane guanylate cyclase activities in brain tissue. *Front Mol Neurosci* 2022, **15:** 1076430.

14. Khan FH, Pandian V, Ramraj SK, Aravindan S, Natarajan M, Azadi S*, et al.* RD3 loss dictates high-risk aggressive neuroblastoma and poor clinical outcomes. *Oncotarget* 2015, **6**(34)**:** 36522-36534.

15. Somasundaram DB, Subramanian K, Aravindan S, Yu Z, Natarajan M, Herman T*, et al.* De novo regulation of RD3 synthesis in residual neuroblastoma cells after

intensive multi-modal clinical therapy harmonizes disease evolution. *Sci Rep* 2019, **9**(1): 11766.

16. Cosnarovici MM, Cosnarovici RV, Piciu D. Updates on the 2016 World Health Organization Classification of Pediatric Tumors of the Central Nervous System - a systematic review. *Med Pharm Rep* 2021, **94**(3): 282-288.

17. Goodenberger ML, Jenkins RB. Genetics of adult glioma. *Cancer Genet* 2012, **205**(12): 613-621.

18. Bi J, Chowdhry S, Wu S, Zhang W, Masui K, Mischel PS. Altered cellular metabolism in gliomas - an emerging landscape of actionable co-dependency targets. *Nat Rev Cancer* 2020, **20**(1): 57-70.

19. Peshenko IV, Olshevskaya EV, Savchenko AB, Karan S, Palczewski K, Baehr W*, et al.* Enzymatic properties and regulation of the native isozymes of retinal membrane guanylyl cyclase (RetGC) from mouse photoreceptors. *Biochemistry* 2011, **50**(25): 5590-5600.

20. Peshenko IV, Olshevskaya EV, Dizhoor AM. Functional Study and Mapping Sites for Interaction with the Target Enzyme in Retinal Degeneration 3 (RD3) Protein. *J Biol Chem* 2016, **291**(37): 19713-19723.

21. Preising MN, Hausotter-Will N, Solbach MC, Friedburg C, Ruschendorf F, Lorenz B. Mutations in RD3 are associated with an extremely rare and severe form of early onset retinal dystrophy. *Invest Ophthalmol Vis Sci* 2012, **53**(7): 3463-3472.

22. Chang B, Heckenlively JR, Hawes NL, Roderick TH. New Mouse Primary Retinal Degeneration (rd-3). *Genomics* 1993, **16**(1): 45-49.

23. Lincoff NS, Chung C, Balos L, Corbo JC, Sharma A. Combing the globe for terrorism. *J Neuroophthalmol* 2012, **32**(1)**:** 82-85.

24. Lin CY, Huang HM. Unilateral malignant optic glioma following glioblastoma multiforme in the young: a case report and literature review. *BMC Ophthalmol* 2017, **17**(1)**:** 21.

25. Xie K, Liu CY, Hasso AN, Crow RW. Visual field changes as an early indicator of glioblastoma multiforme progression: two cases of functional vision changes before MRI detection. *Clin Ophthalmol* 2015, **9:** 1041-1047.

26. de Hond AAH, Steyerberg EW, van Calster B. Interpreting area under the receiver operating characteristic curve. *Lancet Digit Health* 2022, **4**(12)**:** e853-e855.

27. Plana-Bonamaiso A, Lopez-Begines S, Andilla J, Fidalgo MJ, Loza-Alvarez P, Estanyol JM*, et al.* GCAP neuronal calcium sensor proteins mediate photoreceptor cell death in the rd3 mouse model of LCA12 congenital blindness by involving endoplasmic reticulum stress. *Cell Death Dis* 2020, **11**(1)**:** 62.

28. Li Z, Fan H, Cao J, Sun G, Sen W, Lv J*, et al.* Natriuretic peptide receptor a promotes gastric malignancy through angiogenesis process. *Cell Death Dis* 2021, **12**(11)**:** 968.

29. Khasraw M, Ameratunga MS, Grant R, Wheeler H, Pavlakis N. Antiangiogenic therapy for high-grade glioma. *Cochrane Database Syst Rev* 2014(9)**:** CD008218.

30. Fitzgibbon J, Katsanis N, Wells D, Delhanty J, Vallins W, Hunt DM. Human guanylate kinase (GUK1): cDNA sequence, expression and chromosomal localisation. *FEBS Lett* 1996, **385**(3)**:** 185-188.

31. Elion GB. The purine path to chemotherapy. *Science* 1989, **244**(4900)**:** 41-47.

32. Khan N, Shah PP, Ban D, Trigo-Mourino P, Carneiro MG, DeLeeuw L*, et al.* Solution structure and functional investigation of human guanylate kinase reveals allosteric networking and a crucial role for the enzyme in cancer. *J Biol Chem* 2019, **294**(31)**:** 11920-11933.

33. Cheng CL, Molday RS. Changes in gene expression associated with retinal degeneration in the rd3 mouse. *Mol Vis* 2013, **19:** 955-969.

34. Mills GB, Moolenaar WH. The emerging role of lysophosphatidic acid in cancer. *Nat Rev Cancer* 2003, **3**(8)**:** 582-591.

35. Kishi Y, Okudaira S, Tanaka M, Hama K, Shida D, Kitayama J*, et al.* Autotaxin is overexpressed in glioblastoma multiforme and contributes to cell motility of glioblastoma by converting lysophosphatidylcholine to lysophosphatidic acid. *J Biol Chem* 2006, **281**(25)**:** 17492-17500.

Conflict of Interest Statement

The authors declare no conflicts of interest

Author Contribution Statement

YC, AUB, and KWK designed the study. YC performed experiments. YC, AUB and KWK analyzed data. JW, BZ, PD, and AB provided human material. NG and UR helped with analyzing the data of Figure 5 and 6. SOAH helped with analyzing the data of figure 1 and 2. JH created structural analysis. KWK, YC, and AUB contributed to writing of the manuscript. All authors corrected and approved the final version of the manuscript.

Figure 1: Multi-cohort differential expression analysis of RD3 in glioma. The RNA-seq data obtained from (A) TGCA-GBM/LGG, and microarray gene expression data from (B) GSE108474, and (C) GSE16011, with process of one-way ANOVA the results show the lower expressed of RD3 in glioblastoma compared to non-tumor and other gliomas, while validated by (D) GSE7696, and qRT-PCR analysis of the glioblastoma tissues from (E) Oldenburg. The statistical analysis was using unpaired t test. The statistical analyzed results were shown in Supplemental Table S6-S9 (P value: * < 0.05, ** < 0.01, *** < 0.001, **** < 0.0001)
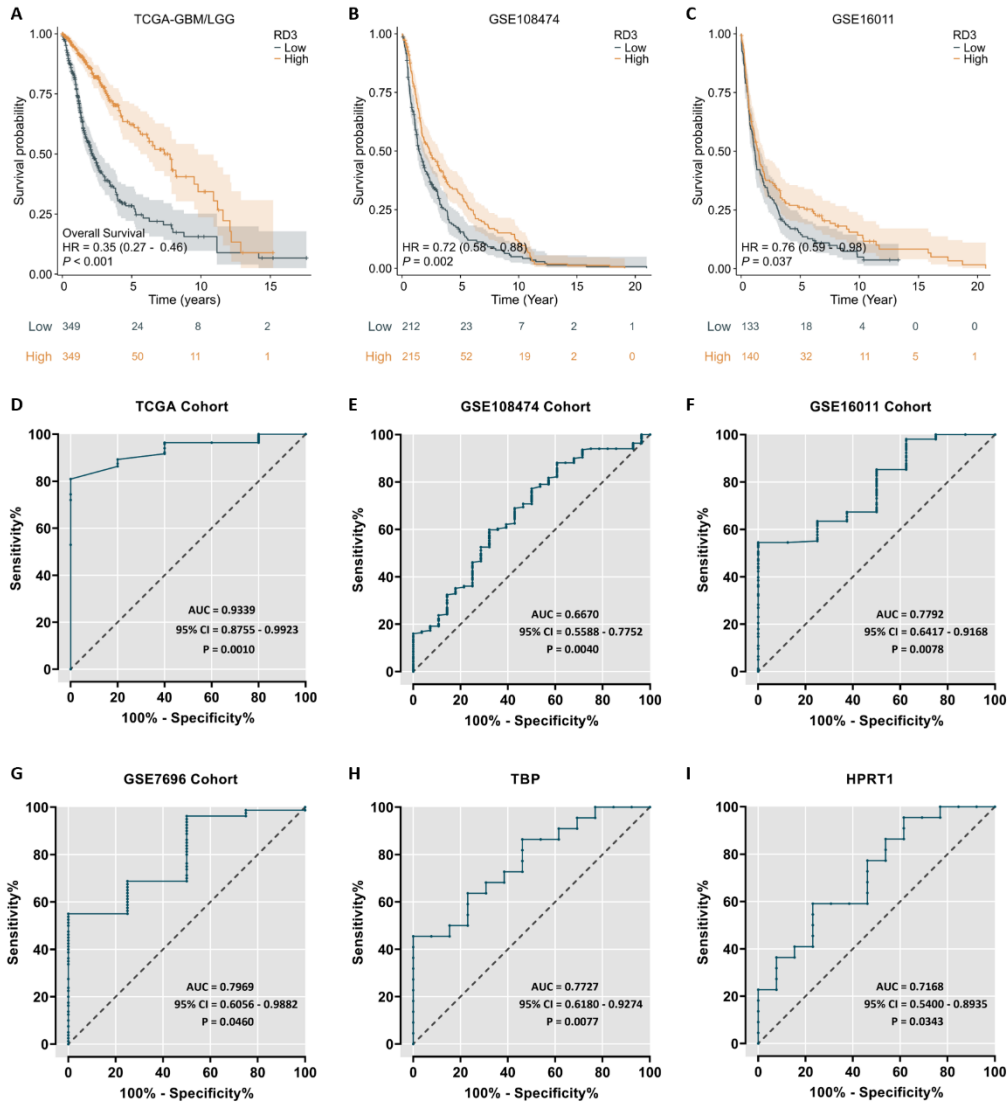
Figure 2: Multi-cohort kaplan-meier and receiver operating characteristic (ROC) curve of RD3 in the patients with glioma. (A-C) Overall survival probability analysis according to RD3 transcript level, (D-I) Diagnostic test of RD3 in Glioblastoma. (HR: Hazard Ratio, AUC: Area Under Curve, 95%CI: 95% Confidence Interval).
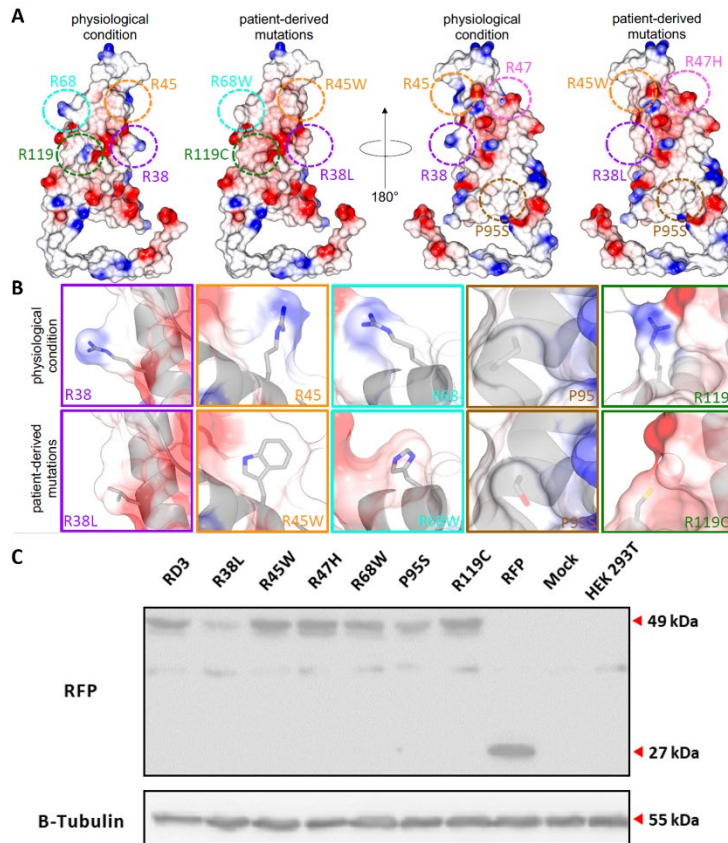
Figure 3: Protein structure of human RD3 based on the PDB entry 6drf. (A) Overview over RD3 structure as electrostatic surface potential representation with highlighted residues by dashed circles in physiological and patient-derived conditions from two different perspectives. (B) Zoom onto individual residues in native (upper row) and patient-derived conditions (lower row) in RD3. Native residues and patient-derived mutations, which are analyzed in this study, are shown by their side-chain moiety and an overlay of the transparent electrostatic surface potential with secondary structure representation. (C) Western blot test of RD3 and its variants in HEK293T cell transfection. The monoclonal RFP antibody (1:2,000) was used to detect the inserted RFP-tag, the band around 27 kDa represent the RFP, and at 49 kDa represent the fusion protein of RD3 and RFP, the mouse β-Tubulin antibody (1: 2,000) was used as housekeeping proteins with molecular weight around 55 kDa., the original full length membrane sees Supplemental Figure S5.
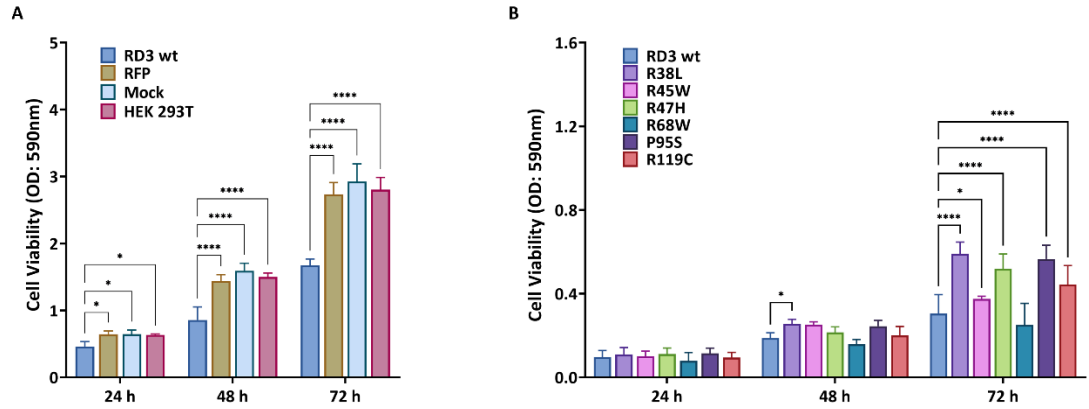
Figure 4: Cell viability analysis by MTT assay at 24 h, 48 h, and 72 h after RD3 and its variants transfection (A) RD3 wild type compared to control group, (B) RD3 wild type compared to variants. The statistical analysis was using two-way ANOVA, and results were shown in Supplemental Table S10, S11 (P value: * < 0.05, ** < 0.01, *** < 0.001, **** < 0.0001).
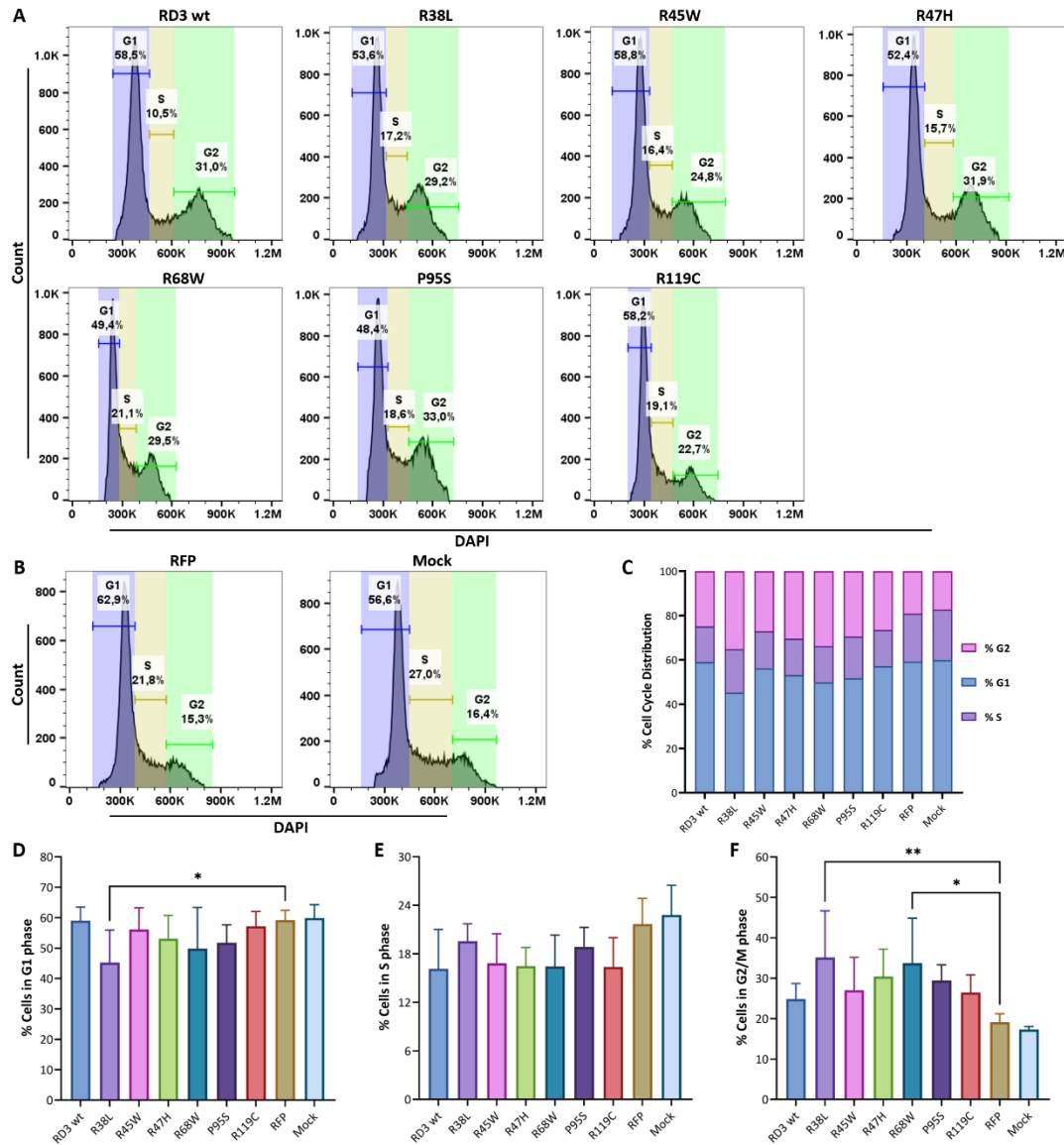
Figure 5: Effects of RD3 and its variants overexpression on cell cycle arrest in transfected HEK293T cell by using DAPI. Flow cytometry was used to detect cell cycle distribution after 24 h (A) The RD3 variants. (B) Empty vector and Mock control. (C) The summary cell cycle distribution of 5 replicates. The ANOVA test was performed to analyze the percentage of cells across cell cycle (D) G1 phase, (E) S phase and (F) G2/M phase. The statistical analysis was using two-way ANOVA, and results were shown in Supplemental Table S12-S14 (P value: * < 0.05, ** < 0.01, *** < 0.001, **** < 0.0001).
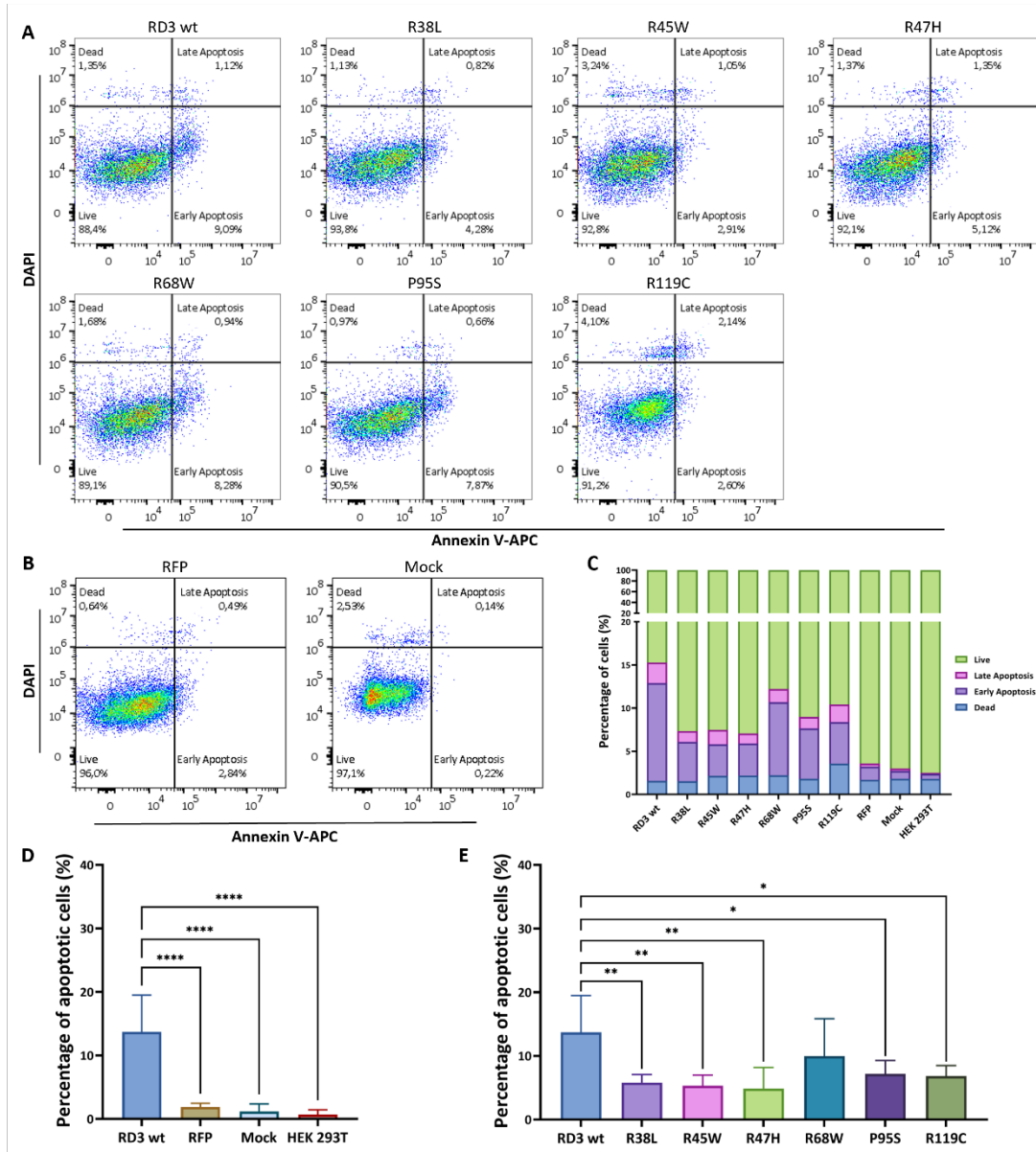
Figure 6: Cell programming death analysis of RD3 and its variants transfected HEK 293T by flow cytometry. The annexin V fuse APC and DAPI were applied for cell apoptosis detection. (A) RD3 and its variants transfected HEK 293T cell. (B) Vector and Mock control. (C) The summary of cell apoptotic analysis 24 h after transfection. Apoptotic analysis of cells in (D) RD3 and control group (E) RD3 and its variants. The statistical analysis was using two-way ANOVA, and results were shown in Supplemental Table S15, S16 (P value: * < 0.05, ** < 0.01, *** < 0.001, **** < 0.0001).

Supplementary Material

Retinal degeneration protein 3 mutants are associated with cell cycle arrest and apoptosis

Yaoyu Chen[1, 2], Jens Hausmann[2], Benjamin Zimmermann[3], Simeon Oscar Arnulfo Helgers[3], Patrick Dömer[3], Johannes Woitzik[3,6], Ulrike Raap[4,6], Natalie Gray[2,4], Andreas Büttner[5], Karl-Wilhelm Koch[1,6]*, and Anja U. Bräuer[2,6]*

[1]Division of Biochemistry, Department of Neuroscience, Carl von Ossietzky University, Oldenburg, Germany

[2]Division of Anatomy, Department of Human Medicine, Carl von Ossietzky University, Oldenburg, Germany

[3] Division of Neurosurgery, Department of Human Medicine, Carl von Ossietzky University Oldenburg, Oldenburg, Germany

[4]Division of Experimental Allergy and Immunodermatology, School of Medicine and Health Sciences, Carl von Ossietzky University Oldenburg, 26129 Oldenburg, Germany

[5]Institute of Forensic Medicine, Rostock University Medical Center, Germany

[6]Research Center Neurosensory Science, Carl von Ossietzky University Oldenburg, Oldenburg, Germany

Supplemental Table S1: Association between RD3 expression and clinicopathologic characteristics in the TCGA cohort

Characteristics	Low expression of RD3	High expression of RD3	P value
n	349	350	
Age, n (%)			< 0.001
> 60	108 (15.5%)	35 (5%)	
<= 60	241 (34.5%)	315 (45.1%)	
Gender, n (%)			0.234
Female	141 (20.2%)	157 (22.5%)	
Male	208 (29.8%)	193 (27.6%)	
WHO grade, n (%)			< 0.001
G2	79 (12.4%)	145 (22.8%)	
G3	111 (17.4%)	134 (21%)	
G4	142 (22.3%)	26 (4.1%)	
IDH status, n (%)			< 0.001
WT	185 (26.9%)	61 (8.9%)	
Mut	157 (22.8%)	286 (41.5%)	
Primary therapy outcome, n (%)			0.008
Progressive disease	55 (11.8%)	57 (12.3%)	
Stable disease	59 (12.7%)	89 (19.1%)	
Partial response	16 (3.4%)	49 (10.5%)	
Complete response	48 (10.3%)	92 (19.8%)	
Histological type, n (%)			< 0.001
Astrocytoma	81 (11.6%)	115 (16.5%)	
Oligoastrocytoma	50 (7.2%)	85 (12.2%)	
Oligodendroglioma	76 (10.9%)	124 (17.7%)	
Glioblastoma	142 (20.3%)	26 (3.7%)	
OS event, n (%)			< 0.001
Alive	167 (23.9%)	260 (37.2%)	
Dead	182 (26%)	90 (12.9%)	
DSS event, n (%)			< 0.001
Yes	161 (23.7%)	83 (12.2%)	
No	172 (25.4%)	262 (38.6%)	
PFI event, n (%)			< 0.001
Yes	205 (29.3%)	141 (20.2%)	
No	144 (20.6%)	209 (29.9%)	

Supplemental Table S2: Association between RD3 expression and clinicopathologic characteristics in the EV Oldenburg cohort.

Characteristics	Low expression of RD3	High Expression of RD3	P value
n	14	14	
Age, n (%)			0.440
<=60	4 (14.3%)	7 (25%)	
>60	10 (35.7%)	7 (25%)	
Gender, n (%)			0.440
Female	7 (25%)	4 (14.3%)	
Male	7 (25%)	10 (35.7%)	
Histology, n (%)			0.297
Glioblastoma	13 (46.4%)	9 (32.1%)	
Pilocytic astrocytoma	0 (0%)	1 (3.6%)	
Oligodendroglioma	0 (0%)	2 (7.1%)	
Anaplastic oligodendroglioma	1 (3.6%)	2 (7.1%)	
IDH status, n (%)			0.165
Wild type	13 (46.4%)	9 (32.1%)	
Mutated	1 (3.6%)	5 (17.9%)	
WHO grade, n (%)			0.165
G1	0 (0.0%)	1 (3.6%)	
G3	1 (3.6%)	4 (14.3%)	
G4	13 (46.4%)	9 (32.1%)	
Deceased, n (%)			1.000
Alive	13 (46.4%)	12 (42.9%)	
Dead	1 (3.6%)	2 (7.1%)	
RD3 (TBP), mean ± sd	-0.15538 ± 0.50575	1.493 ± 0.72084	< 0.001
RD3 (HPRT1), mean ± sd	0.58728 ± 0.6669	1.9985 ± 0.84875	< 0.001

Supplemental Table S3: Summarizing information of RD3 variants and its potential links to diseases

Amino acid change	Potential link to disease form	References and links to databases
p.R38* premature stop codon	Leber congenital amaurosis 12; Ovarian Epithelial Tumor	Perrault et al. (2013) https://www.ncbi.nlm.nih.gov/clinvar/variation/189792/ https://depmap.org/portal/gene/RD3?tab=characterization&characterization=mutation
p.R38L	Papillary renal cell carcinoma;	https://cancer.sanger.ac.uk/cosmic/mutation/overview?id=112398541 https://bit.ly/3QK3tn2
p.R45W	Endometrioid carcinoma; Adenocarcinoma	https://cancer.sanger.ac.uk/cosmic/mutation/overview?id=112398773 https://bit.ly/3QK3tn2
p.R47H	Leber Congenital Amaurosis 12 (variant of uncertain significance) Adenocarcinoma	https://www.ncbi.nlm.nih.gov/clinvar/variation/935765/ https://cancer.sanger.ac.uk/cosmic/mutation/overview?id=112398074 https://depmap.org/portal/gene/RD3?tab=characterization&characterization=mutation https://bit.ly/3QK3tn2
p.R68W	Leber Congenital Amaurosis 12 Endometrioid carcinoma Adenocarcinoma	Friedman et al. (2006) https://www.ncbi.nlm.nih.gov/clinvar/variation/466320/ https://cancer.sanger.ac.uk/cosmic/mutation/overview?id=112397909
p.P95S	Leber Congenital Amaurosis 12 (variant of uncertain significance) Medulloblastoma Small Cell Lung Cancer	https://www.ncbi.nlm.nih.gov/clinvar/variation/838670/ https://depmap.org/portal/gene/RD3?tab=characterization&characterization=mutation https://bit.ly/3QK3tn2
p.R119C	Leber Congenital Amaurosis 12 (variant of uncertain significance) Adenocarcinoma	https://www.ncbi.nlm.nih.gov/clinvar/variation/1045675/ https://cancer.sanger.ac.uk/cosmic/mutation/overview?id=112398638
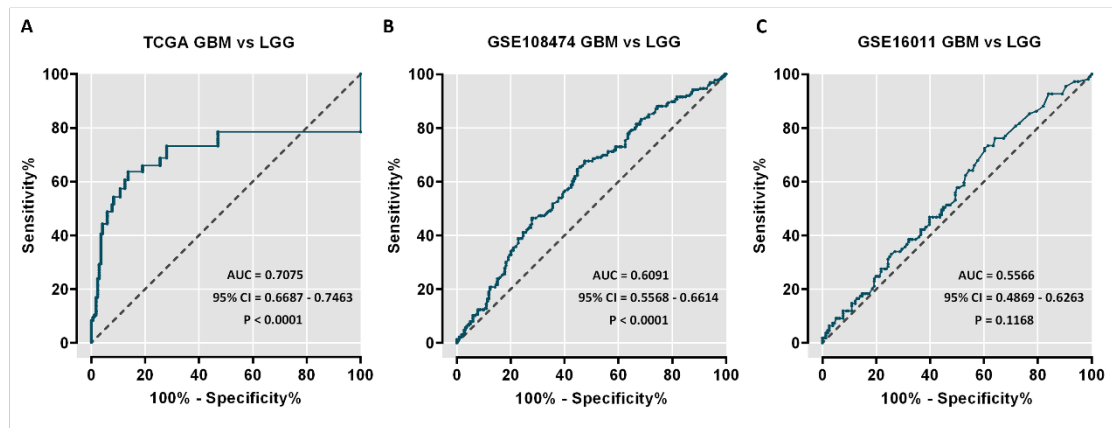
Supplemental Figure S1: Multi-cohort receiver operating characteristic (ROC) curve of RD3 in the patients with glioma. Diagnostic test of RD3 in Glioblastoma (GBM) and Low grade glioma (LGG), A. TCGA cohort, B GSE108474 cohort, and C. GSE16011 cohort (HR: Hazard Ratio, AUC: Area Under Curve, 95%CI: 95% Confidence Interval).
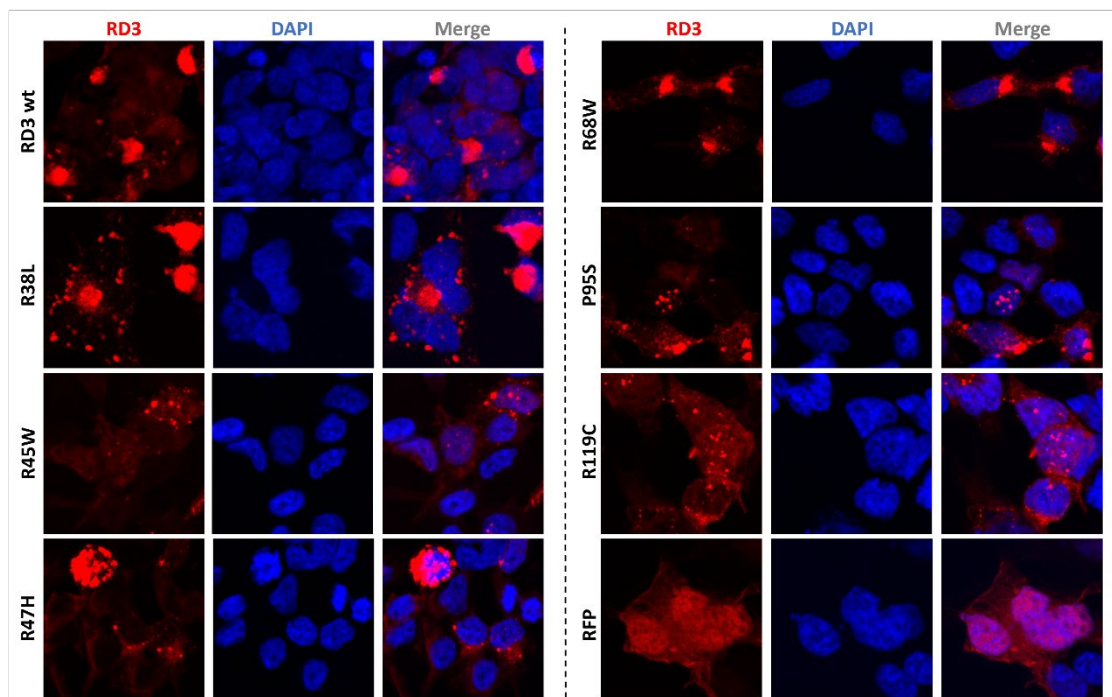
Supplemental Figure S2: Immunocytochemistry of RD3 and its variants in the HEK 293T cells. The cells fused with red-fluorescence protein (RFP) were shown in red, and the DAPI staining for cell nuclei were shown in blue.
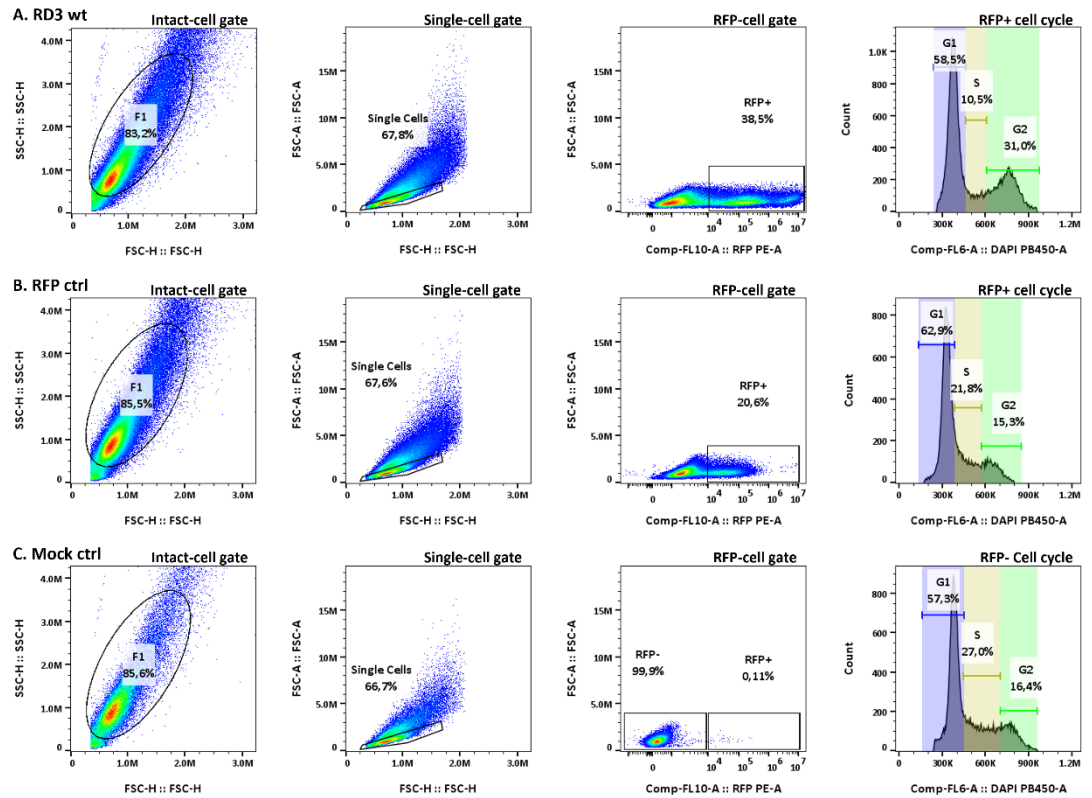
Supplemental Figure S3. Flow cytometry gating strategy for analyzing cell cycle arrest. From left to right, the intact cell gate setting was based on forward scatter (FSC) and side scatter (SSC), then the FSC area was applied to separate the singlet cells. The sorted singlet cells were then distinguished by fused red fluorescent protein (RFP), and in the final, analyzes the cell cycle of gated cells by the DAPI channel. A. RD3 wild type group, B. RFP control group and C. Mock control group.
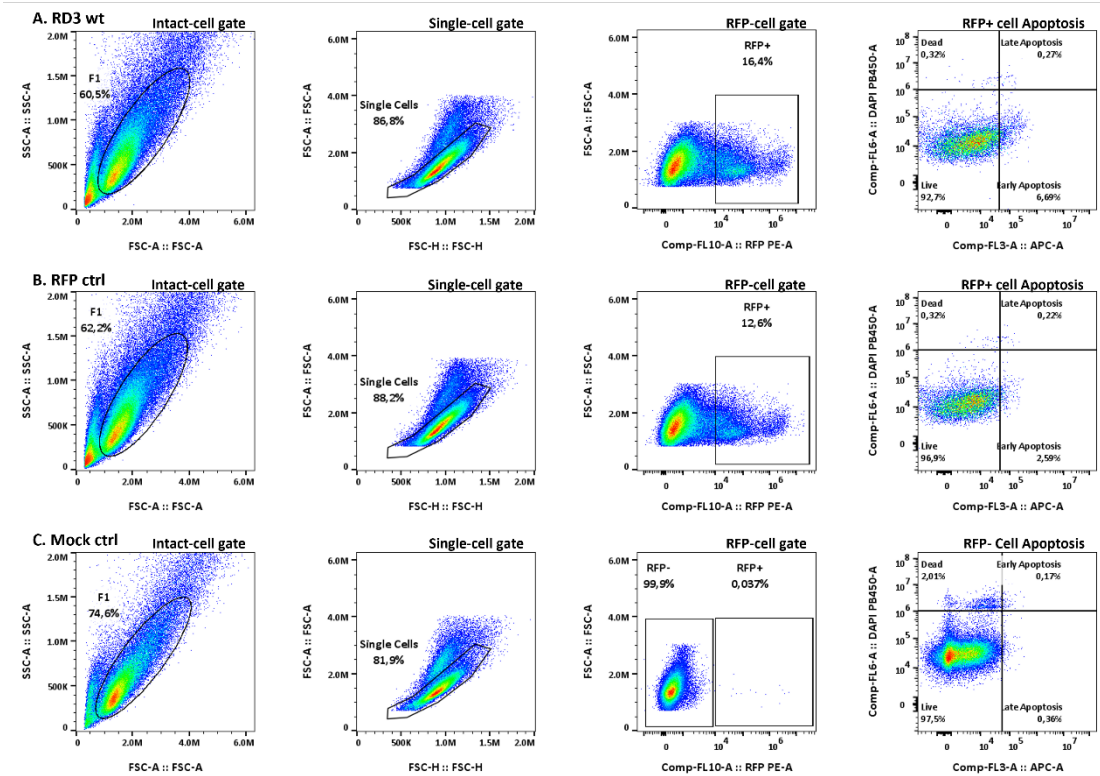
Supplemental Figure S4. Flow cytometry gating strategy for analyzing cell apoptosis.
From left to right, the intact cell gate setting was based on forward scatter (FSC) and side
scatter (SSC), then the FSC area was applied to separate the singlet cells. The sorted singlet
cells were then distinguished by fused red fluorescent protein (RFP), and in the final, analyzed
for cell apoptosis of gated cells by the DAPI and Annexin APC conjugate channel. A. RD3 wild
type group, B. RFP control group and C. Mock control group.
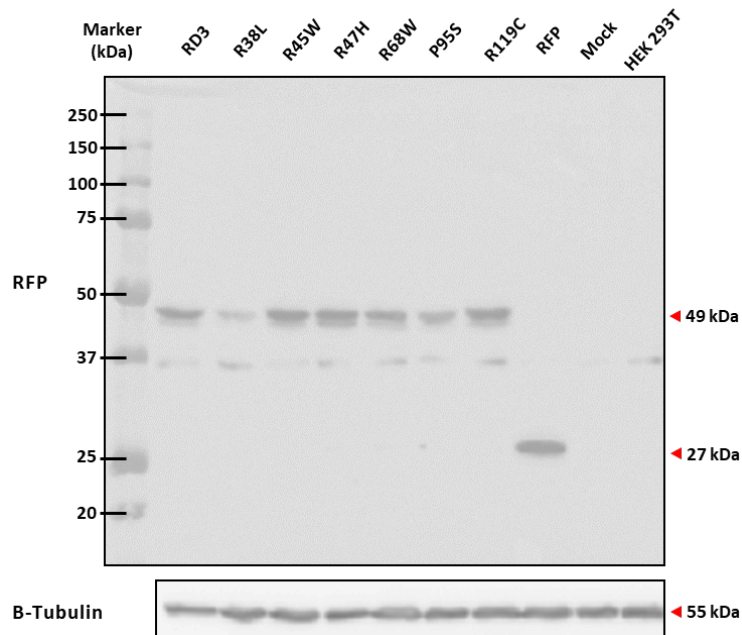
Supplemental Figure S5. The original full length western blots of proteins from RD3 and its variants transfected HEK 293T cells. The blotted membrane containing protein from RD3, and its variants were incubated with mouse anti-RFP antibody (1: 2,000 dilution). Later, the membrane was cut at 50 kDa and incubated with mouse β-Tubulin antibody (1: 2,000).

Supplemental Table S4. Datasheet of donors from HRO.

Sample ID	Age	Sex	Cause of Death	RD3 expression (TBP)	RD3 expression (HPRT1)
G110/20	76	m	Hemorrhagic shock (femoral arterial punction)	0.162	0.290
G099/20	66	m	Hemorrhagic shock (dialysis catheter)	0.273	0.661
K108/20	31	w	Diabetic ketoacidosic	3.155	3.074
P085/20	85	w	Pancreatitis	0.782	1.230
G111/20	60	m	Hemorrhagic shock (ulcus duodeni)	2.069	2.510
G158/20	70	m	Acute cardiac arrest (severe coronary sclerosis)	1.771	2.463
G076/20	64	m	Alcohol intoxication (3,02 ‰)	0.533	0.943
K073/20	30	m	Hepatorenal syndrome	0.234	1.250
G093/20	52	m	Strangulation	1.226	1.496
G140/20	36	m	Alcohol intoxication (5,28 ‰)	1.574	1.928
G171/20	61	m	Myocardial infarction	0.741	1.219
G162/20	39	m	Liver failure (cirrhosis)	1.526	2.263
K042/21	81	m	Pneumonia	1.314	1.756

Supplemental Table S5. Datasheet of patients with glioma.

Patient ID	Date of Birth	Age	Gender	Histology	IDH status	WHO grade	Deceased	RD3 expression (TBP)	RD3 expression (HPRT1)
PLL0001	1967-06-16	56	Female	Glioblastoma	Wild type	G4	-	0.000121514	0.273532467
PLL0003	1952-01-18	71	Male	Glioblastoma	Wild type	G4	-	0.414038962	1.021326163
PLL0004	2010-10-22	13	Male	pilocytic astrocytoma	Mutated	G1	-	1.676857285	1.83770884
PLL0005	1991-12-10	32	Male	Oligodendroglioma	Mutated	G3	-	2.318921114	2.962755753
PLL0006	1941-11-20	82	Male	Glioblastoma	Wild type	G4	-	-0.07575606	0.491625801
PLL0007	1950-12-29	73	Female	Glioblastoma	Wild type	G4	-	1.135832893	1.338361546
PLL0008	1938-05-07	85	Male	Glioblastoma	Wild type	G4	-	-0.422678699	0.379277425
PLL0009	1969-01-31	54	Male	anaplastic oligodendroglioma	Mutated	G3	-	2.593019176	3.45101704
PLL0010	1966-12-18	57	Male	Glioblastoma	Wild type	G4	-	0.322263922	1.189515941
PLL0011	1946-10-21	77	Male	Glioblastoma	Wild type	G4	-	1.70757136	2.389420774
PLL0012	1967-06-21	56	Female	Oligodendroglioma	Mutated	G3	-	2.709053708	3.329727189
PLL0013	1962-10-18	61	Female	Glioblastoma	Wild type	G4	-	0.078755492	0.982558706
PLL0015	1987-10-11	36	Female	Glioblastoma	Wild type	G4	-	0.267973662	1.323833855
PLL0016	1962-07-14	61	Female	Glioblastoma	Wild type	G4	-	0.075852956	0.530646145
PLL0017	1963-03-26	60	Male	anaplastic oligodendroglioma	Mutated	G3	-	0.171466326	1.191752396
PLL0018	1942-05-09	81	Male	Glioblastoma	Wild type	G4	-	0.523681542	0.865275563
PLL0019	1949-06-21	74	Female	Glioblastoma	Wild type	G4	-	0.909896049	1.568563208
PLL0020	1972-09-26	51	Male	anaplastic oligodendroglioma	Mutated	G3	-	2.040021834	2.836942702
PLL0021	1945-10-11	78	Female	Glioblastoma	Wild type	G4	-	-0.187959721	1.678969486
PLL0022	1947-10-10	76	Male	Glioblastoma	Wild type	G4	-	0.936144238	1.432412556
PLL0023	1967-02-08	54	Female	Glioblastoma	Wild type	G4	2021-09-10	0.77913568	1.265887333
PLL0024	1944-02-07	78	Male	Glioblastoma	Wild type	G4	2022-11-10	-0.368715542	-0.026764186
PLL0025	1958-03-03	65	Female	Glioblastoma	Wild type	G4	-	-1.526093074	-0.644940736
PLL0026	1951-09-02	72	Male	Glioblastoma	Wild type	G4	-	0.620816054	1.083331967
PLL0027	1971-04-21	51	Male	Glioblastoma	Wild type	G4	2022-07-01	1.566992212	1.812312075
PLL0028	1941-08-16	82	Male	Glioblastoma	Wild type	G4	-	-0.177099468	0.020631965
PLL0029	1944-05-08	79	Female	Glioblastoma	Wild type	G4	-	-0.747446262	-0.19000944
PLL0030	1950-05-03	73	Male	Glioblastoma	Wild type	G4	-	1.384148022	1.80552174

Supplemental Table S6. Sequence of the primers used.

Mutant	Primer Forward (5'-3')	Primer Reverse (3'-5')
RD3 wt	GTCAGATCCGCTAGCcaccATGTCTCTCATCT CATGGCTTC	AAGCTTGAGCTCGAGGTCGGCTTTG GGCGCCC
R38L	GGGGCAGATGctaGAGGCTGAGA	GTCAGCTCCATCATAAGCGTC
R45W	GAGGCAGCAGtggGAGCGCAGCA	TCAGCCTCTCGCATCTGCCCC
R47H	GCAGCGGGAGcatAGCAATGCGG	TGCCTCTCAGCCTCTCGC
R68W	CAGCACACCCtggTCCACCTATG	GCCAGCCAGCTGTAGTCC
P95S	CTATTGTGGGtcgGCTATCCTCAG	GATGGGTGGATCTTAACG
R119C	CCAGCTCTTCtgtTCGGTGCTGC	GACACCTCCTGCACCTCG

5. Discussion

Ophthalmic manifestations are frequently observed in neurological disorders (London *et al.*, 2013), and therefore, retinal symptoms can aid in disease diagnosis (Wolf et al., 2023). RD3 is a retinal specific protein that is involved in photoreceptor physiology , and its dysfunction is related to LCA12 blindness (Azadi *et al.*, 2010; Dizhoor *et al.*, 2021; Friedman *et al.*, 2006; Peshenko *et al.*, 2021; Preising *et al.*, 2012; Wimberg *et al.*, 2018a). Patients with RD3 non-sense mutations displayed phenotypes such as nystagmus since birth, macular rearrangement, and thin retinal vessels (Perrault *et al.*, 2013). Although several studies addressed the physiological and pathological role of RD3 in photoreceptor cells and its relationship to retinal diseases, the molecular and cellular mechanisms of its actions remained unclear, both in retina and non-retina tissues (Dizhoor and Peshenko, 2021; Peshenko and Dizhoor, 2020; Sharma *et al.*, 2023). Recent studies showed that RD3 expression levels correlate with the progression of neuroblastoma, an early onset cancer derived from abnormal neurons (Khan *et al.*, 2015; Somasundaram *et al.*, 2019). In this thesis, I aimed to further unravel the physiological and pathological roles of RD3 that result in specific phenotypes and diseases. I found two new interaction partners for RD3 in physiological condition that complements our knowledge of RD3 in brain second messenger pathways. I analyzed and unraveled the correlation between RD3 and GBM and characterized a novel pathological role of RD3 in brain diseases. Further, I investigated the overexpression of RD3 in HEK293T inducing cell cycle arrest at G2/M phase and activating programmed cell death.

5.1 Unveiling the role of RD3 in the nucleotide cycle: an evolving discovery

The second messenger guanosine 3', 5'-cyclic monophosphate (cGMP) is one of the major cyclic nucleotide second messengers that regulates various physiological functions (Guo et al., 2007; Ibarra *et al.*, 2001; Koch and Dell'Orco, 2015; Kuhn, 2016; Olcese *et al.*, 2002; Peshenko *et al.*, 2011b). For example, it plays a crucial role in cellular responses to extracellular signals, including phototransduction,

neurotransmission, olfaction, thermosensation, and immune responses (Koch and Dell'Orco, 2015; Kuhn, 2016; Pandey, 2021; Sharma, 2010; Sharma et al., 2016; Sharma *et al.*, 2023). Despite its importance, the precise mechanisms underlying cGMP signaling have remained elusive. However, recent advances in research have shed light on a more recently discovered protein called RD3, which has emerged as a key player in the cGMP pathway (Azadi *et al.*, 2010; Chen *et al.*, 2022; Dizhoor *et al.*, 2021; Peshenko *et al.*, 2011a; Wimberg *et al.*, 2018a).

The prime cause of LCA blindness has been attributed to abnormality in retinal cGMP content (Dizhoor and Peshenko, 2021; Koch and Dell'orco, 2013; Kuhn, 2016; Sharma *et al.*, 2016; Sharon *et al.*, 2018; Wimberg et al., 2018b; Zagel *et al.*, 2013). Several studies have revealed that mutations in GC-E, GCAPs, or RD3 directly affect cGMP concentration in the retina, leading to the degeneration of photoreceptor cells (see Figure 22) (Ames, 2022; Preising *et al.*, 2012; Sharon *et al.*, 2018). However, only RD3 has been found to be associated with LCA 12, a rare and severe form of early-onset retinal degeneration disease (Preising *et al.*, 2012). This raises the question of why LCA12 manifests in such severe degeneration. Wimberg et al. (2018a) found that purified RD3 increases the activity of GUK1 and hypothesized that co-expression of RD3 and GUK1 in photoreceptor inner segments leads to an enhanced synthesis of GDP from 5'-GMP. However, Dizhoor et al. (2021) have disputed this proposal (see Figure 23). The research findings indicate that RD3 promotes survival of photoreceptors through inhibition of guanylate cyclase activation, instead of facilitating GMP recycling (Dizhoor *et al.*, 2021). We here focus on GC-A and GC-B (coded by gene *Npr1* and *Npr2*, respectively), the two natriuretic peptides-stimulated GCs that possess similar protein regions and homologous amino acid sequence to photoreceptor GCs (see Figure 10). Therefore, they are putative candidates of functional binding partners of RD3 in both retina and non-retina tissues.

In the line to unravel the potential role of RD3 in controlling GC-A and GC-B function, we initially examined the expression patterns of *rd3, Npr1,* and *Npr2* in the

developmental stages of brain and retina tissues and aligned those with previous functional studies (Kuhn, 2016; Peshenko *et al.*, 2016; Sharma *et al.*, 2023). These findings may also facilitate further analysis as gene expression patterns can be linked to specific developmental processes at distinct stages. We then showed their gene expression profiling in neurons, astrocyte, and microglia to dictate potential target functional cell (see Figure 15 A). Further functional tests were conducted using a well-established cyclase activity assay to demonstrate RD3 preparation capability in inhibiting the enzyme activity of GC-E at similar range described previously (Wimberg *et al.*, 2018a). Additional tests were performed by using ANP and CNP to assess the peptides in activating GC-A and GC-B, respectively, and allowing comparison with previously described biochemical properties (Kuhn, 2016). By utilizing the aforementioned molecules, the performed assay unraveled a new regulatory feature of RD3 in inhibiting GC-A and GC-B. Moreover, these RD3-Natriuretic peptide GCs complexes were also analyzed in astrocytes (see Figure 15 B). This study presented two functional partners GC-A and GC-B, that provided a novel perspective to the physiological role of RD3 other than in photoreceptors.

In our study, it was discovered that in the retina the expression level of *Npr2* is significantly higher, approximately ten times more than *Npr1* but almost ten times lower than *rd3* (see Figure 11). This discrepancy in expression levels may be linked to the proportion of cells expressing these molecules in retina since the photoreceptor cells density was significantly higher than the other major cell classes (Jeon et al., 1998). The presence of natriuretic peptides and their receptors in retinal bipolar, Müller, amacrine, and ganglion cells across various vertebrate species has been demonstrated in previous studies (Abdelalim *et al.*, 2008; Blute et al., 2000; Cao and Yang, 2007; Duda et al., 1993; Fernandez-Durango et al., 1989; Kutty et al., 1992; Spreca et al., 1999; Xu et al., 2010; Yu *et al.*, 2006). Nonetheless, the relationship between expression levels and protein levels as well as the role of these molecules in retinal physiology remains unclear.

One of the major functions of RD3 in retina is its requirement in enzyme trafficking of photoreceptor GCs (Azadi *et al.*, 2010). Interestingly, the ligand-bound GC-A colocalized with Rab11, a protein from the small GTPase superfamily that shares subcellular localization with RD3, suggesting a potential pathway of RD3 in trafficking of GC-A (Azadi *et al.*, 2010; Mani et al., 2016; Mani et al., 2015). Nonetheless, current evidence indicates that natriuretic peptides and their receptors in retina are more likely involved in physiological processes other than those in photoreceptor cells (Abdelalim *et al.*, 2008; Blute *et al.*, 2000; Cao and Yang, 2007; Duda *et al.*, 1993; Fernandez-Durango *et al.*, 1989; Kutty *et al.*, 1992; Spreca *et al.*, 1999; Xu *et al.*, 2010; Yu *et al.*, 2006). For instance, natriuretic peptides aid in dopaminergic and cholinergic signaling in amacrine cells (Abdelalim *et al.*, 2008). Additionally, Yu et al. (2006) discovered that these peptides modulate GABA-receptor activity in bipolar cells. They also report immunolabelling of GC-A and GC-B in the outer plexiform layer (OPL). RD3 primarily localizes to the inner segments of photoreceptor cells, with weak expression in the OPL (Azadi *et al.*, 2010; Dizhoor *et al.*, 2019; Wimberg *et al.*, 2018a). Natriuretic peptide signaling via GC-A or GC-B increases cGMP levels, which targets cyclic nucleotide-gated ion channels or cGMP-dependent protein kinase (PKG). This pathway is thought to be responsible for inhibiting GABA-receptor currents by BNP (Yu *et al.*, 2006). As such, RD3 might be involved in the cGMP balances by inhibiting either GC-A or GC-B in the OPL, but further high-resolution immunohistochemistry of GC-A, GC-B, and RD3 are needed to elucidate their functional relationship.

The expression of RD3 has been detected in various organs and tissues, including the brain (Aravindan *et al.*, 2017; Khan *et al.*, 2015), where the expression level appears to be significantly lower than in the retina. We found that the expression of RD3 was more than 100-fold higher in the retina than in different parts of the brain (see Figure 12), which is in broad agreement with the report by Aravindan et al. (2017), who reported significant but modest or low expression in the human cerebellum and olfactory bulb compared to the retina. Upon analysis of *rd3*, *Npr1*, and *Npr2* expression levels during mice development, it became apparent that *Npr2* displayed a stronger

113

expression in all brain regions analyzed in comparison to both *rd3* and *Npr1*. These findings are consistent with previous reports identifying *Npr2* mRNA expression pattern in the neocortex, hippocampus, and olfactory bulb (Herman et al., 1996). GC-B has a critical function in the bifurcation of axons during development (Schmidt et al., 2018) extending previous observations that the natriuretic peptide systems play roles in regulating neural development (DiCicco-Bloom et al., 2004; Muller et al., 2009). Furthermore, it is noteworthy that our results show an age-related clustering, especially in *Npr1*, which aligns with observations of higher *Npr1* expression levels observed in Alzheimer's patients (Mahinrad et al., 2018). The evidence presented collectively suggests that natriuretic peptides and their receptors can be important diagnostic biomarkers for aging and age-related degenerative diseases in the nervous system (Kuhn, 2016; Mahinrad *et al.*, 2018; Regan et al., 2021).

Accordingly, inhibition of GC-A or GC-B by RD3 in the CNS appears to be a crucial regulatory mechanism. In our study, we observed higher expression of *rd3*, *Npr1* and *Npr2* in astrocyte compared to neurons and microglia (see Figure 15A), in consistent with previous findings of *Npr1* and *Npr2* localization in brain (Friedl et al., 1989; Goncalves et al., 1995; Hosli and Hosli, 1992). Moreover, Friedl et al., (1989) showed in the primary astrocyte culture with the ANP can elevate the intracellular cGMP product. Therefore, a test for endogenous GC activities was performed in astrocytes with ANP and CNP simulation (see Figure 15B). The results displayed comparable levels of cGMP accumulation by ANP and CNP, which is in agreement with previous findings (Deschepper and Picard, 1994). Further, our results demonstrate that RD3 inhibited both GCA and GC-B in astrocytes, indicating its potential effectiveness in the primary cell culture. But these *in situ* and *in vitro* studies can provide only circumstantial evidence for RD3 regulating GC-A and GC-B activities. Even so, this evidence suggested an impact on retinopathies. For example, the ANP/GC-A/cGMP signaling pathway counters neovascularization in proliferative retinopathies in astrocytes (Burtenshaw and Cahill, 2020; Špiranec Spes et al., 2020). Consequently, the inhibitory effect of RD3 might associate with angiogenesis in the progress of

retinopathies, which could also be mechanisms of thin retinal vessels in LCA12.

In summary, our study provides a view of RD3 in controlling the activities of GC-A and GC-B in retinal and non-retinal tissues. However, there are still many open questions and limitations from this study that need to be addressed and fulfilled by future research. For example, how can RD3 interfere with the cyclase activities of GC-A and GC-B, the intercellular trafficking or protein modification? To answer this question, a more direct protein-protein interaction of RD3 and GC-A, GC-B should first be determined in both in vivo and in vitro, and the pull-down assays from native tissues or methods like yeast two hybrid screen could be applied. Further questions would be, are GC-A and GC-B also involved in RD3 induced retinal degeneration, if yes, then how? To these purposes, the RD3 transgenic mouse can be used for detecting the gene expression changes and revealing the potential cell targets. This ongoing work will presumably shed light on some of these questions.
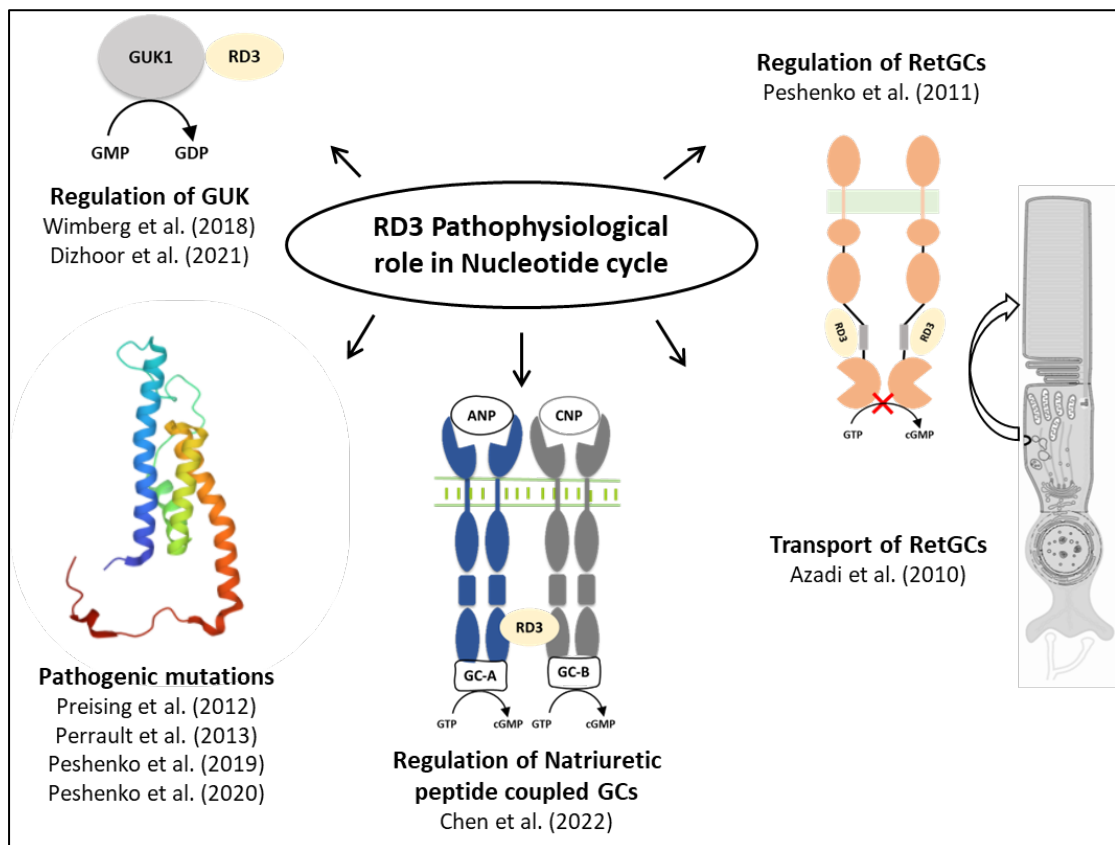

Figure 23: Overview of the RD3 progress in nucleotide cycle. In 2010, Azadi et al. reported the

discovery of RD3's role in the trafficking of photoreceptor GCs from the inner to the outer segments, providing the first insight into RD3's involvement in the nucleotide cycle. Subsequently, it was discovered that RD3 inhibits the catalytic function of guanylate cyclase in photoreceptor GCs in the presence of GCAPs (Peshenko *et al.*, 2011a). Additionally, another regulator of the cGMP pathway was found to interact with RD3 to catalyze the conversion of GMP to GDP (Wimberg *et al.*, 2018a). Furthermore, pathogenetic mutations of RD3 to LCA12 have been proposed to affect the binding sensitivities of RD3 to photoreceptor GCs (Perrault *et al.*, 2013; Peshenko and Dizhoor, 2020; Peshenko *et al.*, 2019; Preising *et al.*, 2012). A recent study revealed that RD3 also controls two natriuretic peptide-coupled GCs, GC-A and GC-B (Chen *et al.*, 2022).

5.2 The role of RD3 in programmed cell death: a novel perspective

Programmed cell death, also known as apoptosis, is a crucial biological process that plays a dominance role in maintaining tissue homeostasis and eliminating damaged or unwanted cells (Vitale et al., 2023). Dysregulation of apoptosis has been implicated in various diseases, including cancer, neurodegenerative disorders, and autoimmune conditions (Bertheloot et al., 2021; Jan and Chaudhry, 2019; Johnson Olaleye et al., 2021; Krawczyk et al., 2020; Sharma et al., 2019). Understanding the molecular mechanisms underlying apoptosis is essential for developing targeted therapies to modulate this process.

Our previous research suggests a novel function of RD3 in inhibiting GC-A and GC-B in neuronal tissue, but any pathological role in the brain remains to be determined (Chen *et al.*, 2022). In order to expand our knowledge, we examined the *RD3* transcript level in human glioma samples and discovered a notable reduction in *RD3* transcript levels in GBM. In conjunction with clinical characteristics, we showed that low *RD3* expression is connected to unfavorable characterization (see Table 2). Further, we tested the diagnosis and prognosis value of *RD3* in glioma (see Figure 17). We found RD3 is sufficient to be a potential diagnostic biomarker and low RD3 expression involved in poor survival rate. These results suggested a new pathological role of RD3

116

in glioma, but additional research is necessary to delineate the molecular mechanisms involved.

Recent research has shed light on the role of RD3, a relatively unexplored protein, in regular ER stress mediating programmed cell death of photoreceptor cells (Dizhoor *et al.*, 2021; Plana-Bonamaiso *et al.*, 2020). This novel pathogenic role of RD3 was suggested to explain photoreceptor degeneration. However, the underlying mechanism and any extrapolation to non-retina tissues remained elusive. Here, the immunocytochemistry study was conducted to understand the cell morphology or process changes when RD3 overexpress, and we found the nuclei of RD3 positive cells (with RFP-tag) were in the interphase of M phase. Therefore, we suggested that RD3 might involve in cellular progress of HEK293T (see Figure 18). We then employed MTT assay to test the effect of RD3 overexpression in HEK293T cells and found less cell viability in cells expression the RD3 construct compared to an empty (RD3-free) RFP construct, indicating a potential functional role of RD3 in cell processes (see Figure 19). Cell cycle arrest is an important repair mechanism for cells in DNA damage, that is associated with apoptosis (Park et al., 2019). Interestingly, we detected the cell cycle of RD3 positive cells (RFP-tag) was arrested in G2/M phase prone to activate cell apoptosis. Hence, we inferred that RD3 induced cell damage. Entering mitosis with a G2/M deficient checkpoint would activate cell apoptosis to prevent malignancies. Further, we discussed RD3 mutations and their impact to its function, since the amino acid substitutions are known to cause a loss of RD3 function in functional assays , which in some cases are correlated with retinal dystrophy type LCA12 (Azadi et al., 2010; Peshenko and Dizhoor, 2020; Preising et al., 2012; Zulliger et al., 2015). Our results showed that the point mutants of RD3 can significantly mitigate the cell apoptosis induced by RD3 overexpression leading to cell cycle arrest.

RD3 is a retina specific protein, but recent publications indicate pathophysiological role in neuronal tissues (Aravindan *et al.*, 2017; Chen *et al.*, 2022; Khan *et al.*, 2015; Somasundaram *et al.*, 2019). For example, loss of RD3 expression correlates with the

progression of neuroblastoma pathogenesis and a poor survival prognosis (Aravindan *et al.*, 2017; Khan *et al.*, 2015; Somasundaram *et al.*, 2019). Moreover, RD3 inhibited GC-A and GC-B in astrocytes from neuronal tissues (Chen *et al.*, 2022). To extended our understanding of RD3 in the brain and its correlation to neurological diseases, we therefore focused on glioma, the cancer has been found to cause vision impairment as an early indication of tumor progression and affected by the elevation of cGMP (Liao et al., 2023; Lin and Huang, 2017; Lincoff *et al.*, 2012; Sanati et al., 2022; Xie *et al.*, 2015). Extending studies were performed by using a data mining approach, we screened and analyzed collected clinical evidence and multi-cohort data sets with respect to *RD3* expression. By this way, we assessed the prognostic and diagnostic value of *RD3* in glioma, particularly in GBM. We employed the ROC test to judge the diagnostic value of *RD3* expression in GBM, which is a true-false algorithm showing the performance of a classification model at all classification thresholds. The evaluation yielded an index (called AUC) lying normally between 0.5 to 1 (the value closer to 1 indicates good performance). The results showed a significant low expression of RD3 in GBM compared to non-tumor tissues, while a parallel ROC curve test yielded high AUC value in four out of five patient cohorts, and even an excellent index larger than 0.9. Therefore, we propose that *RD3* expression can act as a diagnostic parameter in the progression of glioblastoma. Furthermore, we discovered that lower *RD3* expression is linked to an adverse clinical prognosis for GBM patients with 5 years overall survival less than 25%. Our results resemble previous findings obtained from tissue of neuroblastoma patients, in which the loss of *RD3* is associated with tumor invasion, tumorosphere formation, and metastasis (Khan *et al.*, 2015; Somasundaram *et al.*, 2019). Khan et al. (2015) suggested that RD3 functions as a metastasis suppressor, which would be supported by our findings from GBM samples.

Studies have shown interesting findings about RD3 transcript alteration, the loss of RD3 can lead to pathogenic phenotypes, while its re-expression appears to be benign (Dizhoor *et al.*, 2019; Khan *et al.*, 2015; Plana-Bonamaiso *et al.*, 2020). For example, RD3 was found to be absent in aggressive neuroblastoma cells, and its re-gain can

significantly decrease the cell metastasis. Furthermore, in RD3 knockout mice, photoreceptor cell apoptosis was found to occur, and this process could be partially reversed by RD3 re-expression (Plana-Bonamaiso *et al.*, 2020). Although the mechanism underlying this effect is not yet clear, it suggests that the expression of RD3 must be maintained at a critical intracellular level. To investigate this hypothetical role of RD3 in cell progression, we overexpressed both RD3 wild type and selected RD3 mutants in HEK293 cells reason of its commonly low expression (Aravindan *et al.*, 2017; Chen *et al.*, 2022; Khan *et al.*, 2015). As a consequence, RD3 overexpression showed a clear effect on arresting the cell cycle in the G2/M phase and activating the programmed cell death (see Figure 21 and 22). These results seem to contradict the finding that of RD3 deficient can activate programmed cell death (Cheng and Molday, 2013; Plana-Bonamaiso *et al.*, 2020). However, this capacity indicates that RD3 might prevent tumor progression by facilitating cell death of neoplastic transformed cells or arresting the cell cycle.

In our study, we observed that RD3 point mutants located on the surface exposure region at critical helices had a weaker impact on cell cycle arrest and apoptosis in HEK293T cells, compared to the RD3 wild type, except for R68W (see Figure 18, 21 and 22). This implies that RD3 has a particular effect on cell cycle control in epithelial cells (HEK293T cells), and any disruption may weaken or reduce its impact. However, there is currently no definite evidence available on the RD3 target in the cell cycle process. RD3 likely participates in a signal transduction pathway that includes a membrane-bound guanylate cyclase with interaction profile is not limited to photoreceptor guanylate cyclases. For example, recent findings indicate that RD3 regulates the activity of natriuretic peptide receptor guanylate cyclases similar to photoreceptor cyclases (Chen *et al.*, 2022). Additionally, knockdown of GC-A has been linked to cell cycle arrest, activated cell apoptosis in HUVECs, and promotion of tumor malignancy through angiogenesis (Li *et al.*, 2021). These provide a more specifically RD3 upregulation model may broadly be applicable in inhibiting GC-A to trigger cell cycle arrest and activate cell apoptosis in diverse cells and diseases.

Vascular endothelial growth factor (VEGF) is a major angiogenic factor that has been identified as a therapeutic target for both retinal diseases and GBM (Adamis et al., 2020; Ahir et al., 2020). NPs and their receptors are involved in the VEGF pathway, the critical mediator of angiogenesis in the retinopathies and cancer progression (Adamis *et al.*, 2020; Khasraw *et al.*, 2014; Spiranec Spes *et al.*, 2020; Tamura et al., 2020). Studies indicate that VEGF may impede NPs secretion from endothelial cells. On the flip side, CNP (and other NPs) hinder the production of VEGF, which affects the GCs/cGMP signaling pathway (Bubb et al., 2019; Pedram et al., 2001). Additionally, research has shown that the VEGF/GC-A/cGMP cascade stimulates the angiogenesis of cancer (Li *et al.*, 2021). In this context, combining the role of RD3 in regulating GC-A and GC-B, one can hypothesized that RD3 inhibits the binding of NPs to their receptors, resulting in elevated NP content and consequent suppression of VEGF, contributing to reduced angiogenesis in glioma, while the mutants of RD3 may be benign to this process.

Along with the cGMP cascade in vision, the guanylate kinase, an enzyme catalyzing the 5'-GMP to GDP conversion (Fitzgibbon *et al.*, 1996) could be candidate functional partner for RD3 in cancer. Wimberg et al. (2018a) described a biochemical function of RD3 in regulating GUK that provides another possible role of RD3 in controlling cGMP homeostasis. GUK is an essential ubiquitous enzyme involved in the nucleotide metabolism of cells and is involved in diverse cellular mechanisms. As a crucial housekeeping gene, it has been found to control the process of cancer cellular viability, proliferation, and clonogenic potential (da Rocha et al., 2006; Khan *et al.*, 2019), and thus used as the pharmacological targeting therapies. For example, 5'-GMP analogues serve as potent GUK inhibitors or as antiviral and anticancer prodrugs (Elion, 1989). Furthermore, the NMR spectroscopy based structure analysis provided a view of potential protein sites of GUK for drug development and its knockdown can led to the apoptosis of lung tumor cells (Khan *et al.*, 2019). In glioma, GUK was found to be significantly down-regulated in low-grade diffuse astrocytoma, indicating a diagnostic

value of the RD3-GUK complex in glioma progression. (Huang et al., 2000).

In summary, this study demonstrates that reduced RD3 gene expression may serve as a reliable diagnostic and prognostic marker for glioblastoma. Moreover, RD3 overexpression affected the progression of the cell cycle and initiated apoptotic pathways. These findings expand the known functions of RD3 in photoreceptor cells to other cell types across various organs.

5.3 Future perspective

Recent studies provided an overview of protein structure mutants in RD3 and their impact on the function of photoreceptor guanylate cyclases (Dizhoor *et al.*, 2021; Peshenko and Dizhoor, 2020; Peshenko *et al.*, 2019). This offers valuable supplementation for explaining how RD3 mutations cause LCA12. Moreover, Wimberg et al. (2018a) suggests in their study that GUK serves as a biochemical function partner for RD3 and demonstrates that RD3 interacts at various stages within the nucleotide cycle of photoreceptor cells. However, the phenotypic effects on cells aside from photoreceptors remain largely unknown and molecular mechanisms need to be elucidated. We identified two natriuretic peptides coupled guanylate cyclases GC-A and GC-B that inhibited by RD3, provided a RD3-ANP/CNP-cGMP cascade in the astrocyte. As GC-A and GC-B execute their function mainly in vascular management (Kuhn, 2016; Pandey, 2021; Pedram *et al.*, 2001; Schmidt *et al.*, 2018; Shuhaibar *et al.*, 2016; Spiranec Spes *et al.*, 2020), we propose that the dysfunction of RD3 can disrupt the GCs-cGMP balance in retinal vasculature. Further studies in the angiogenic function of RD3 might be of great importance, as its functional partner GC-A has been shown to interact with retina neovascularization (Spiranec Spes *et al.*, 2020). Moreover, the direct or indirect interaction between RD3 and GC-A or GC-B remains to be established, pull-down assays or hybrid two yeast methods could be utilized. It would also be intriguing to investigate how RD3 mutants affect the cyclase activities of GC-A and GC-B in both retina and non-retina tissues, similar to the study conducted on GC-E.

Current evidence strongly supports the assertion that RD3 primarily fulfills its physiological role through active involvement in cGMP metabolism (Chen *et al.*, 2022; Dizhoor *et al.*, 2021; Wimberg *et al.*, 2018b). For example, RD3 has been implicated in facilitating the trafficking of GC-E from the inner to outer segments of photoreceptor cells (Azadi *et al.*, 2010), but whether these function can extends to other guanylate cyclases such as GC-A and GC-B remain to be elusive. Further, the RD3 was found to biochemically activate GUK (Wimberg *et al.*, 2018a), though this interaction show no impact to photoreceptor cells (Dizhoor *et al.*, 2021). These raise a question of what function does this particular RD3-GUK pathway serve. With this object, RD3 is involved in the process of GTP to cGMP and GMP to GDP, but any correlated cellular or molecular mechanisms still need to be investigated. Addressing these queries will not only deepen the comprehension of RD3's cellular processes but also establish more focused therapeutic interventions for RD3-related disorders in both retina and brain. Continued research is necessary to understand the complex molecular mechanisms by which RD3 operates within the cGMP pathway. A more detailed comprehension of its regulatory functions can be achieved by understanding the precise interactions of RD3 with guanylate cyclases and other cellular components.

Another major open question regarding RD3 is its pathological role in both retina and non-retina tissues. The mutation of RD3 is associated with LCA12 blindness (Perrault *et al.*, 2013; Peshenko *et al.*, 2016; Preising *et al.*, 2012), but the alteration of RD3's transcript seems to be more crucial for its function. In retina, the loss of RD3 is involved in the ER stress induced apoptosis of photoreceptor cells, and eventually result the retina degeneration (Dizhoor *et al.*, 2019; 2021; Plana-Bonamaiso *et al.*, 2020). In non-retina tissue, RD3 expression changes were found to impact neuroblastoma cell progression like metastasis, that is associated with the aggressive development of cancer (Khan *et al.*, 2015; Somasundaram *et al.*, 2019). In our study, we extended pathology research into glioma and indicated that lower expression of RD3 could be the potential diagnosis and prognosis factor to identify the severeness of cancer. To

confirm this finding, the multi-omics method based on clinical characteristics and analytics could be applied. Any potential ophthalmological manifestations should also be considered. Furthermore, we revealed that overexpression of RD3 can induce cell cycle arrest in G2/M phase to activate the cell apoptosis in epithelial cells, though it is controversial to its function in photoreceptor cells (Plana-Bonamaiso *et al.*, 2020), but may explain why the RD3 overexpressed in cancer cells can impact its metastasis (Khan *et al.*, 2015). Although our study has not yet demonstrated a direct interaction between RD3 and glioma, our hypothesis that RD3 functions through the VEGF/GC-A/cGMP cascade to control cell cycle arrest, apoptosis, and angiogenesis is reasonable. As we determined the RD3 regulatory features of GC-A (Chen *et al.*, 2022), the molecular that affects the VEGF and results in tumor angiogenesis, growth, and metastasis interference (Li *et al.*, 2021). These need to be verified by *in vitro* and *in vivo* methods. Additionally, our results of RD3 mutants in mitigating cell apoptosis indicate its potential pathogenic to tumor. However, any evidence regarding RD3 gene expression interact to variants still needs to be determined by quantitative RT-PCR.

Future research may focus on translating the knowledge gained from basic RD3 studies into clinical applications. Investigating its potential as a diagnostic marker for various disorders, including retinal degeneration and brain diseases, could open avenues for early detection and intervention. Furthermore, the development of targeted therapeutic strategies to modulate RD3 function may hold promise for treating related diseases.

References

Abdelalim, E.M., Masuda, C., and Tooyama, I. (2008). Expression of natriuretic peptide-activated guanylate cyclases by cholinergic and dopaminergic amacrine cells of the rat retina. Peptides *29*, 622-628. 10.1016/j.peptides.2007.11.021.

Adamis, A.P., Brittain, C.J., Dandekar, A., and Hopkins, J.J. (2020). Building on the success of anti-vascular endothelial growth factor therapy: a vision for the next decade. Eye (Lond) *34*, 1966-1972. 10.1038/s41433-020-0895-z.

Ahir, B.K., Engelhard, H.H., and Lakka, S.S. (2020). Tumor Development and Angiogenesis in Adult Brain Tumor: Glioblastoma. Mol Neurobiol *57*, 2461-2478. 10.1007/s12035-020-01892-8.

Ames, J.B. (2022). Structural basis of retinal membrane guanylate cyclase regulation by GCAP1 and RD3. Front Mol Neurosci *15*, 988142. 10.3389/fnmol.2022.988142.

Aravindan, S., Somasundaram, D.B., Kam, K.L., Subramanian, K., Yu, Z., Herman, T.S., Fung, K.M., and Aravindan, N. (2017). Retinal Degeneration Protein 3 (RD3) in normal human tissues: Novel insights. Sci Rep *7*, 13154. 10.1038/s41598-017-13337-9.

Azadi, S., Molday, L.L., and Molday, R.S. (2010). RD3, the protein associated with Leber congenital amaurosis type 12, is required for guanylate cyclase trafficking in photoreceptor cells. Proc Natl Acad Sci U S A *107*, 21158-21163. 10.1073/pnas.1010460107.

Baba AI, C.C. (2007). Comparative Oncology. (Bucharest (RO): The Publishing House of the Romanian Academy).

Bale, T.A., and Rosenblum, M.K. (2022). The 2021 WHO Classification of Tumors of the Central Nervous System: An update on pediatric low-grade gliomas and glioneuronal tumors. Brain Pathol *32*, e13060. 10.1111/bpa.13060.

Barmashenko, G., Buttgereit, J., Herring, N., Bader, M., Ozcelik, C., Manahan-Vaughan, D., and Braunewell, K.H. (2014). Regulation of hippocampal synaptic plasticity thresholds and changes in exploratory and learning behavior in dominant negative NPR-B mutant rats. Front Mol Neurosci *7*, 95. 10.3389/fnmol.2014.00095.

Barthel, F.P., Johnson, K.C., Varn, F.S., Moskalik, A.D., Tanner, G., Kocakavuk, E., Anderson, K.J., Abiola, O., Aldape, K., Alfaro, K.D., et al. (2019). Longitudinal molecular trajectories of diffuse glioma in adults. Nature *576*, 112-120. 10.1038/s41586-019-1775-1.

Bennett, B.D., Bennett, G.L., Vitangcol, R.V., Jewett, J.R., Burnier, J., Henzel, W., and Lowe, D.G. (1991). Extracellular domain-IgG fusion proteins for three human natriuretic peptide

receptors. Hormone pharmacology and application to solid phase screening of synthetic peptide antisera. J Biol Chem *266*, 23060-23067.

Bertheloot, D., Latz, E., and Franklin, B.S. (2021). Necroptosis, pyroptosis and apoptosis: an intricate game of cell death. Cell Mol Immunol *18*, 1106-1121. 10.1038/s41423-020-00630-3.

Bi, J., Chowdhry, S., Wu, S., Zhang, W., Masui, K., and Mischel, P.S. (2020). Altered cellular metabolism in gliomas - an emerging landscape of actionable co-dependency targets. Nat Rev Cancer *20*, 57-70. 10.1038/s41568-019-0226-5.

Blute, T.A., Lee, H.K., Huffmaster, T., Haverkamp, S., and Eldred, W.D. (2000). Localization of natriuretic peptides and their activation of particulate guanylate cyclase and nitric oxide synthase in the retina. J Comp Neurol *424*, 689-700.

Brat, D.J., Aldape, K., Colman, H., Figrarella-Branger, D., Fuller, G.N., Giannini, C., Holland, E.C., Jenkins, R.B., Kleinschmidt-DeMasters, B., Komori, T., et al. (2020). cIMPACT-NOW update 5: recommended grading criteria and terminologies for IDH-mutant astrocytomas. Acta Neuropathol *139*, 603-608. 10.1007/s00401-020-02127-9.

Brat, D.J., Aldape, K., Colman, H., Holland, E.C., Louis, D.N., Jenkins, R.B., Kleinschmidt-DeMasters, B.K., Perry, A., Reifenberger, G., Stupp, R., et al. (2018). cIMPACT-NOW update 3: recommended diagnostic criteria for "Diffuse astrocytic glioma, IDH-wildtype, with molecular features of glioblastoma, WHO grade IV". Acta Neuropathol *136*, 805-810. 10.1007/s00401-018-1913-0.

Bubb, K.J., Aubdool, A.A., Moyes, A.J., Lewis, S., Drayton, J.P., Tang, O., Mehta, V., Zachary, I.C., Abraham, D.J., Tsui, J., and Hobbs, A.J. (2019). Endothelial C-Type Natriuretic Peptide Is a Critical Regulator of Angiogenesis and Vascular Remodeling. Circulation *139*, 1612-1628. 10.1161/CIRCULATIONAHA.118.036344.

Campbell, M., and Humphries, P. (2013). The Blood-Retina Barrier. In Biology and Regulation of Blood-Tissue Barriers, C.Y. Cheng, ed. (Springer New York), pp. 70-84. 10.1007/978-1-4614-4711-5_3.

Cao, L.H., and Yang, X.L. (2007). Natriuretic peptide receptor-A is functionally expressed on bullfrog retinal Muller cells. Brain Res Bull *71*, 410-415. 10.1016/j.brainresbull.2006.10.010.

Cao, L.H., and Yang, X.L. (2008). Natriuretic peptides and their receptors in the central nervous system. Prog Neurobiol *84*, 234-248. 10.1016/j.pneurobio.2007.12.003.

Chang, B., Heckenlively, J.R., Hawes, N.L., and Roderick, T.H. (1993). New Mouse Primary Retinal Degeneration (rd-3). Genomics *16*, 45-49. https://doi.org/10.1006/geno.1993.1138.

Chen, Y., Brauer, A.U., and Koch, K.W. (2022). Retinal degeneration protein 3 controls membrane guanylate cyclase activities in brain tissue. Front Mol Neurosci *15*, 1076430. 10.3389/fnmol.2022.1076430.

Cheng, C.L., and Molday, R.S. (2013). Changes in gene expression associated with retinal degeneration in the rd3 mouse. Mol Vis *19*, 955-969.

Chinkers, M., and Wilson, E.M. (1992). Ligand-independent oligomerization of natriuretic peptide receptors. Identification of heteromeric receptors and a dominant negative mutant. J Biol Chem *267*, 18589-18597.

Cideciyan, A.V. (2010). Leber congenital amaurosis due to RPE65 mutations and its treatment with gene therapy. Prog Retin Eye Res *29*, 398-427. 10.1016/j.preteyeres.2010.04.002.

Correia, S.S., Iyengar, R.R., Germano, P., Tang, K., Bernier, S.G., Schwartzkopf, C.D., Tobin, J., Lee, T.W., Liu, G., Jacobson, S., et al. (2021). The CNS-Penetrant Soluble Guanylate Cyclase Stimulator CY6463 Reveals its Therapeutic Potential in Neurodegenerative Diseases. Front Pharmacol *12*, 656561. 10.3389/fphar.2021.656561.

Cosnarovici, M.M., Cosnarovici, R.V., and Piciu, D. (2021). Updates on the 2016 World Health Organization Classification of Pediatric Tumors of the Central Nervous System - a systematic review. Med Pharm Rep *94*, 282-288. 10.15386/mpr-1811.

da Rocha, A.A., Giorgi, R.R., de Sa, S.V., Correa-Giannella, M.L., Fortes, M.A., Cavaleiro, A.M., Machado, M.C., Cescato, V.A., Bronstein, M.D., and Giannella-Neto, D. (2006). Hepatocyte growth factor-regulated tyrosine kinase substrate (HGS) and guanylate kinase 1 (GUK1) are differentially expressed in GH-secreting adenomas. Pituitary *9*, 83-92. 10.1007/s11102-006-9277-1.

Dale Purves, G.A., David Fitzpatrick, William Hall, Anthony-Samuel Lamantia, Leonard White (2012). Neuroscience. 5th Edition (Yale J Biol Med. 2013 Mar 12;86(1):113-4. eCollection 2013 Mar.).

de Hond, A.A.H., Steyerberg, E.W., and van Calster, B. (2022). Interpreting area under the receiver operating characteristic curve. Lancet Digit Health *4*, e853-e855. 10.1016/S2589-7500(22)00188-1.

Decker, J.M., Wojtowicz, A.M., Bartsch, J.C., Liotta, A., Braunewell, K.H., Heinemann, U., and Behrens, C.J. (2010). C-type natriuretic peptide modulates bidirectional plasticity in hippocampal area CA1 in vitro. Neuroscience *169*, 8-22. 10.1016/j.neuroscience.2010.04.064.

Derbyshire, E.R., and Marletta, M.A. (2012). Structure and regulation of soluble guanylate cyclase. Annu Rev Biochem *81*, 533-559. 10.1146/annurev-biochem-050410-100030.

DiCicco-Bloom, E., Lelievre, V., Zhou, X., Rodriguez, W., Tam, J., and Waschek, J.A. (2004). Embryonic expression and multifunctional actions of the natriuretic peptides and receptors in the developing nervous system. Dev Biol *271*, 161-175. 10.1016/j.ydbio.2004.03.028.

Dizhoor, A.M., Olshevskaya, E.V., and Peshenko, I.V. (2019). Retinal guanylyl cyclase activation by calcium sensor proteins mediates photoreceptor degeneration in an rd3 mouse model of congenital human blindness. J Biol Chem *294*, 13729-13739. 10.1074/jbc.RA119.009948.

Dizhoor, A.M., Olshevskaya, E.V., and Peshenko, I.V. (2021). Retinal degeneration-3 protein promotes photoreceptor survival by suppressing activation of guanylyl cyclase rather than accelerating GMP recycling. J Biol Chem *296*, 100362. 10.1016/j.jbc.2021.100362.

Dizhoor, A.M., and Peshenko, I.V. (2021). Regulation of retinal membrane guanylyl cyclase (RetGC) by negative calcium feedback and RD3 protein. Pflugers Arch *473*, 1393-1410. 10.1007/s00424-021-02523-4.

Duda, T., Goraczniak, R.M., Sitaramayya, A., and Sharma, R.K. (1993). Cloning and expression of an ATP-regulated human retina C-type natriuretic factor receptor guanylate cyclase. Biochemistry *32*, 1391-1395. 10.1021/bi00057a001.

Duda, T., and Koch, K.W. (2002). Retinal diseases linked with photoreceptor guanylate cyclase. Mol Cell Biochem *230*, 129-138.

Elion, G.B. (1989). The purine path to chemotherapy. Science *244*, 41-47. 10.1126/science.2649979.

Ellison, D.W., Aldape, K.D., Capper, D., Fouladi, M., Gilbert, M.R., Gilbertson, R.J., Hawkins, C., Merchant, T.E., Pajtler, K., Venneti, S., and Louis, D.N. (2020). cIMPACT-NOW update 7: advancing the molecular classification of ependymal tumors. Brain Pathol *30*, 863-866. 10.1111/bpa.12866.

Ellison, D.W., Hawkins, C., Jones, D.T.W., Onar-Thomas, A., Pfister, S.M., Reifenberger, G., and Louis, D.N. (2019). cIMPACT-NOW update 4: diffuse gliomas characterized by MYB, MYBL1, or FGFR1 alterations or BRAF(V600E) mutation. Acta Neuropathol *137*, 683-687. 10.1007/s00401-019-01987-0.

Fernandez-Durango, R., Sanchez, D., Gutkowska, J., Carrier, F., and Fernandez-Cruz, A. (1989). Identification and characterization of atrial natriuretic factor receptors in the rat retina. Life Sci *44*, 1837-1846. 10.1016/0024-3205(89)90301-9.

Fitzgibbon, J., Katsanis, N., Wells, D., Delhanty, J., Vallins, W., and Hunt, D.M. (1996). Human guanylate kinase (GUK1): cDNA sequence, expression and chromosomal localisation. FEBS Lett *385*, 185-188. 10.1016/0014-5793(96)00365-1.

Friedl, A., Harmening, C., Schmalz, F., Schuricht, B., Schiller, M., and Hamprecht, B. (1989). Elevation by atrial natriuretic factors of cyclic GMP levels in astroglia-rich cultures from murine brain. J Neurochem *52*, 589-597. 10.1111/j.1471-4159.1989.tb09160.x.

Friedman, J.S., Chang, B., Kannabiran, C., Chakarova, C., Singh, H.P., Jalali, S., Hawes, N.L., Branham, K., Othman, M., Filippova, E., et al. (2006). Premature truncation of a novel protein, RD3, exhibiting subnuclear localization is associated with retinal degeneration. Am J Hum Genet *79*, 1059-1070. 10.1086/510021.

Ghanta, M., Panchanathan, E., Lakkakula, B., and Narayanaswamy, A. (2017). Retrospection on the Role of Soluble Guanylate Cyclase in Parkinson's Disease. J Pharmacol Pharmacother *8*, 87-91. 10.4103/jpp.JPP_45_17.

Giovannini, D., Andreola, F., Spitalieri, P., Krasnowska, E.K., Colini Baldeschi, A., Rossi, S., Sangiuolo, F., Cozzolino, M., and Serafino, A. (2021). Natriuretic peptides are neuroprotective on in vitro models of PD and promote dopaminergic differentiation of hiPSCs-derived neurons via the Wnt/beta-catenin signaling. Cell Death Discov *7*, 330. 10.1038/s41420-021-00723-6.

Goncalves, J., Grove, K.L., and Deschepper, C.F. (1995). Generation of cyclic guanosine monophosphate in brain slices incubated with atrial or C-type natriuretic peptides: comparison of the amplitudes and cellular distribution of the responses. Regul Pept *57*, 55-63. 10.1016/0167-0115(95)00018-7.

Goodenberger, M.L., and Jenkins, R.B. (2012). Genetics of adult glioma. Cancer Genet *205*, 613-621. 10.1016/j.cancergen.2012.10.009.

Gritsch, S., Batchelor, T.T., and Gonzalez Castro, L.N. (2022). Diagnostic, therapeutic, and prognostic implications of the 2021 World Health Organization classification of tumors of the central nervous system. Cancer *128*, 47-58. 10.1002/cncr.33918.

Guo, D., Tan, Y.C., Wang, D., Madhusoodanan, K.S., Zheng, Y., Maack, T., Zhang, J.J., and Huang, X.Y. (2007). A Rac-cGMP signaling pathway. Cell *128*, 341-355. 10.1016/j.cell.2006.11.048.

Haines, D.E., and Mihailoff, G.A. (2018). Chapter 10 - An Overview of the Brainstem. In Fundamental Neuroscience for Basic and Clinical Applications (Fifth Edition), D.E. Haines, and G.A. Mihailoff, eds. (Elsevier), pp. 152-159. https://doi.org/10.1016/B978-0-323-39632-5.00010-4.

Herman, J.P., Dolgas, C.M., Rucker, D., and Langub, M.C., Jr. (1996). Localization of natriuretic peptide-activated guanylate cyclase mRNAs in the rat brain. J Comp Neurol *369*, 165-187. 10.1002/(SICI)1096-9861(19960527)369:2<165::AID-CNE1>3.0.CO;2-1.

Hoon, M., Okawa, H., Della Santina, L., and Wong, R.O. (2014). Functional architecture of the retina: development and disease. Prog Retin Eye Res *42*, 44-84. 10.1016/j.preteyeres.2014.06.003.

Hosli, E., and Hosli, L. (1992). Autoradiographic localization of binding sites for arginine vasopressin and atrial natriuretic peptide on astrocytes and neurons of cultured rat central nervous system. Neuroscience *51*, 159-166. 10.1016/0306-4522(92)90480-p.

Huang, H., Colella, S., Kurrer, M., Yonekawa, Y., Kleihues, P., and Ohgaki, H. (2000). Gene expression profiling of low-grade diffuse astrocytomas by cDNA arrays. Cancer Res *60*, 6868-6874.

Ibarra, C., Nedvetsky, P.I., Gerlach, M., Riederer, P., and Schmidt, H.H. (2001). Regional and age-dependent expression of the nitric oxide receptor, soluble guanylyl cyclase, in the human brain. Brain Res *907*, 54-60. 10.1016/s0006-8993(01)02588-4.

Iwata, T., Uchida-Mizuno, K., Katafuchi, T., Ito, T., Hagiwara, H., and Hirose, S. (1991). Bifunctional atrial natriuretic peptide receptor (type A) exists as a disulfide-linked tetramer in plasma membranes of bovine adrenal cortex. J Biochem *110*, 35-39. 10.1093/oxfordjournals.jbchem.a123539.

Jacobson, S.G., Cideciyan, A.V., Ho, A.C., Roman, A.J., Wu, V., Garafalo, A.V., Sumaroka, A., Krishnan, A.K., Swider, M., Mascio, A.A., et al. (2022). Night vision restored in days after decades of congenital blindness. iScience *25*, 105274. 10.1016/j.isci.2022.105274.

Jäkel, S., and Dimou, L. (2017). Glial Cells and Their Function in the Adult Brain: A Journey through the History of Their Ablation. Frontiers in Cellular Neuroscience *11*. 10.3389/fncel.2017.00024.

Jamshidi, P., and Brat, D.J. (2022). The 2021 WHO classification of central nervous system tumors: what neurologists need to know. Curr Opin Neurol *35*, 764-771. 10.1097/WCO.0000000000001109.

Jan, R., and Chaudhry, G.E. (2019). Understanding Apoptosis and Apoptotic Pathways Targeted Cancer Therapeutics. Adv Pharm Bull *9*, 205-218. 10.15171/apb.2019.024.

Jeon, C.J., Strettoi, E., and Masland, R.H. (1998). The major cell populations of the mouse retina. J Neurosci *18*, 8936-8946. 10.1523/JNEUROSCI.18-21-08936.1998.

Johnson Olaleye, O., Adenike, T.O., Oluwaseun Titilope, O., and Oyedotun, M.O. (2021). Reactive Oxygen Species in Neurodegenerative Diseases: Implications in Pathogenesis and Treatment Strategies. In Reactive Oxygen Species, A. Rizwan, ed. (IntechOpen), pp. Ch. 9. 10.5772/intechopen.99976.

Kettenmann, H., Hanisch, U.K., Noda, M., and Verkhratsky, A. (2011). Physiology of microglia. Physiol Rev *91*, 461-553. 10.1152/physrev.00011.2010.

Khan, F.H., Pandian, V., Ramraj, S.K., Aravindan, S., Natarajan, M., Azadi, S., Herman, T.S., and Aravindan, N. (2015). RD3 loss dictates high-risk aggressive neuroblastoma and poor clinical outcomes. Oncotarget *6*, 36522-36534. 10.18632/oncotarget.5204.

Khan, N., Shah, P.P., Ban, D., Trigo-Mourino, P., Carneiro, M.G., DeLeeuw, L., Dean, W.L., Trent, J.O., Beverly, L.J., Konrad, M., et al. (2019). Solution structure and functional investigation of human guanylate kinase reveals allosteric networking and a crucial role for the enzyme in cancer. J Biol Chem *294*, 11920-11933. 10.1074/jbc.RA119.009251.

Khasraw, M., Ameratunga, M.S., Grant, R., Wheeler, H., and Pavlakis, N. (2014). Antiangiogenic therapy for high-grade glioma. Cochrane Database Syst Rev, CD008218. 10.1002/14651858.CD008218.pub3.

Khasraw, M., and Lassman, A.B. (2010). Advances in the treatment of malignant gliomas. Curr Oncol Rep *12*, 26-33. 10.1007/s11912-009-0077-4.

Kishi, Y., Okudaira, S., Tanaka, M., Hama, K., Shida, D., Kitayama, J., Yamori, T., Aoki, J., Fujimaki, T., and Arai, H. (2006). Autotaxin is overexpressed in glioblastoma multiforme and contributes to cell motility of glioblastoma by converting lysophosphatidylcholine to lysophosphatidic acid. J Biol Chem *281*, 17492-17500. 10.1074/jbc.M601803200.

Koch, K.W., and Dell'orco, D. (2013). A calcium-relay mechanism in vertebrate phototransduction. ACS Chem Neurosci *4*, 909-917. 10.1021/cn400027z.

Koch, K.W., and Dell'Orco, D. (2015). Protein and Signaling Networks in Vertebrate Photoreceptor Cells. Front Mol Neurosci *8*, 67. 10.3389/fnmol.2015.00067.

Koch, K.W., Duda, T., and Sharma, R.K. (2002). Photoreceptor specific guanylate cyclases in vertebrate phototransduction. Mol Cell Biochem *230*, 97-106.

Koller, K.J., Lowe, D.G., Bennett, G.L., Minamino, N., Kangawa, K., Matsuo, H., and Goeddel, D.V. (1991). Selective activation of the B natriuretic peptide receptor by C-type natriuretic peptide (CNP). Science *252*, 120-123. 10.1126/science.1672777.

Krawczyk, A., Miskiewicz, J., Strzelec, K., Wcislo-Dziadecka, D., and Strzalka-Mrozik, B. (2020). Apoptosis in Autoimmunological Diseases, with Particular Consideration of Molecular Aspects of Psoriasis. Med Sci Monit *26*, e922035. 10.12659/MSM.922035.

Kuhn, M. (2016). Molecular Physiology of Membrane Guanylyl Cyclase Receptors. Physiol Rev *96*, 751-804. 10.1152/physrev.00022.2015.

Kutty, R.K., Fletcher, R.T., Chader, G.J., and Krishna, G. (1992). Expression of guanylate cyclase-A mRNA in the rat retina: detection using polymerase chain reaction. Biochem Biophys Res Commun *182*, 851-857. 10.1016/0006-291x(92)91810-d.

Labrecque, J., Deschenes, J., McNicoll, N., and De Lean, A. (2001). Agonistic induction of a covalent dimer in a mutant of natriuretic peptide receptor-A documents a juxtamembrane interaction that accompanies receptor activation. J Biol Chem *276*, 8064-8072. 10.1074/jbc.M005550200.

Langenickel, T., Buttgereit, J., Pagel, I., Dietz, R., Willenbrock, R., and Bader, M. (2004). Forced homodimerization by site-directed mutagenesis alters guanylyl cyclase activity of natriuretic peptide receptor B. Hypertension *43*, 460-465. 10.1161/01.HYP.0000110907.33263.0b.

Lavorgna, G., Lestingi, M., Ziviello, C., Testa, F., Simonelli, F., Manitto, M.P., Brancato, R., Ferrari, M., Rinaldi, E., Ciccodicola, A., and Banfi, S. (2003). Identification and characterization of C1orf36, a transcript highly expressed in photoreceptor cells, and mutation analysis in retinitis pigmentosa. Biochem Biophys Res Commun *308*, 414-421. 10.1016/s0006-291x(03)01410-4.

Levin, E.R., Gardner, D.G., and Samson, W.K. (1998). Natriuretic peptides. N Engl J Med *339*, 321-328. 10.1056/NEJM199807303390507.

Li, Z., Fan, H., Cao, J., Sun, G., Sen, W., Lv, J., Xuan, Z., Xia, Y., Wang, L., Zhang, D., et al. (2021). Natriuretic peptide receptor a promotes gastric malignancy through angiogenesis process. Cell Death Dis *12*, 968. 10.1038/s41419-021-04266-7.

Liao, H., Zhu, Z., and Peng, Y. (2018). Potential Utility of Retinal Imaging for Alzheimer's Disease: A Review. Front Aging Neurosci *10*, 188. 10.3389/fnagi.2018.00188.

Liao, Y.F., Pan, H.J., Abudurezeke, N., Yuan, C.L., Yuan, Y.L., Zhao, S.D., Zhang, D.D., and Huang, S. (2023). Functional Axis of PDE5/cGMP Mediates Timosaponin-AIII-Elicited Growth Suppression of Glioblastoma U87MG Cells. Molecules *28*. 10.3390/molecules28093795.

Lin, C.Y., and Huang, H.M. (2017). Unilateral malignant optic glioma following glioblastoma multiforme in the young: a case report and literature review. BMC Ophthalmol *17*, 21. 10.1186/s12886-017-0415-5.

Lincoff, N.S., Chung, C., Balos, L., Corbo, J.C., and Sharma, A. (2012). Combing the globe for terrorism. J Neuroophthalmol *32*, 82-85. 10.1097/WNO.0b013e31824095d1.

London, A., Benhar, I., and Schwartz, M. (2013). The retina as a window to the brain-from eye research to CNS disorders. Nat Rev Neurol *9*, 44-53. 10.1038/nrneurol.2012.227.

Louis, D.N. (2016). WHO classification of tumours of the central nervous system. (No Title).

Louis, D.N., Giannini, C., Capper, D., Paulus, W., Figarella-Branger, D., Lopes, M.B., Batchelor, T.T., Cairncross, J.G., van den Bent, M., Wick, W., and Wesseling, P. (2018a). cIMPACT-NOW update 2: diagnostic clarifications for diffuse midline glioma, H3 K27M-mutant and diffuse astrocytoma/anaplastic astrocytoma, IDH-mutant. Acta Neuropathol *135*, 639-642. 10.1007/s00401-018-1826-y.

Louis, D.N., Perry, A., Wesseling, P., Brat, D.J., Cree, I.A., Figarella-Branger, D., Hawkins, C., Ng, H.K., Pfister, S.M., Reifenberger, G., et al. (2021). The 2021 WHO Classification of Tumors of the Central Nervous System: a summary. Neuro Oncol *23*, 1231-1251. 10.1093/neuonc/noab106.

Louis, D.N., Wesseling, P., Aldape, K., Brat, D.J., Capper, D., Cree, I.A., Eberhart, C., Figarella-Branger, D., Fouladi, M., Fuller, G.N., et al. (2020). cIMPACT-NOW update 6: new entity and diagnostic principle recommendations of the cIMPACT-Utrecht meeting on future CNS tumor classification and grading. Brain Pathol *30*, 844-856. 10.1111/bpa.12832.

Louis, D.N., Wesseling, P., Paulus, W., Giannini, C., Batchelor, T.T., Cairncross, J.G., Capper, D., Figarella-Branger, D., Lopes, M.B., Wick, W., and van den Bent, M. (2018b). cIMPACT-NOW update 1: Not Otherwise Specified (NOS) and Not Elsewhere Classified (NEC). Acta Neuropathol *135*, 481-484. 10.1007/s00401-018-1808-0.

Mahinrad, S., Bulk, M., van der Velpen, I., Mahfouz, A., van Roon-Mom, W., Fedarko, N., Yasar, S., Sabayan, B., van Heemst, D., and van der Weerd, L. (2018). Natriuretic Peptides in Post-mortem Brain Tissue and Cerebrospinal Fluid of Non-demented Humans and Alzheimer's Disease Patients. Front Neurosci *12*, 864. 10.3389/fnins.2018.00864.

Malan, L., van Wyk, R., von Kanel, R., Ziemssen, T., Vilser, W., Nilsson, P.M., Magnusson, M., Jujic, A., Mak, D.W., Steyn, F., and Malan, N.T. (2023). The chronic stress risk phenotype mirrored in the human retina as a neurodegenerative condition. Stress *26*, 2210687. 10.1080/10253890.2023.2210687.

Mani, I., Garg, R., and Pandey, K.N. (2016). Role of FQQI motif in the internalization, trafficking, and signaling of guanylyl-cyclase/natriuretic peptide receptor-A in cultured murine mesangial cells. Am J Physiol Renal Physiol *310*, F68-84. 10.1152/ajprenal.00205.2015.

Mani, I., Garg, R., Tripathi, S., and Pandey, K.N. (2015). Subcellular trafficking of guanylyl cyclase/natriuretic peptide receptor-A with concurrent generation of intracellular cGMP. Biosci Rep *35*. 10.1042/BSR20150136.

Mills, G.B., and Moolenaar, W.H. (2003). The emerging role of lysophosphatidic acid in cancer. Nat Rev Cancer *3*, 582-591. 10.1038/nrc1143.

Molday, L.L., Djajadi, H., Yan, P., Szczygiel, L., Boye, S.L., Chiodo, V.A., Gregory-Evans, K., Sarunic, M.V., Hauswirth, W.W., and Molday, R.S. (2013). RD3 gene delivery restores guanylate cyclase localization and rescues photoreceptors in the Rd3 mouse model of Leber congenital amaurosis 12. Hum Mol Genet *22*, 3894-3905. 10.1093/hmg/ddt244.

Molday, L.L., Jefferies, T., and Molday, R.S. (2014). Insights into the role of RD3 in guanylate cyclase trafficking, photoreceptor degeneration, and Leber congenital amaurosis. Front Mol Neurosci *7*, 44. 10.3389/fnmol.2014.00044.

Muller, D., Hida, B., Guidone, G., Speth, R.C., Michurina, T.V., Enikolopov, G., and Middendorff, R. (2009). Expression of guanylyl cyclase (GC)-A and GC-B during brain development: evidence for a role of GC-B in perinatal neurogenesis. Endocrinology *150*, 5520-5529. 10.1210/en.2009-0490.

Norris, G.T., and Kipnis, J. (2019). Immune cells and CNS physiology: Microglia and beyond. J Exp Med *216*, 60-70. 10.1084/jem.20180199.

Olcese, J., Majora, C., Stephan, A., and Muller, D. (2002). Nocturnal accumulation of cyclic 3',5'-guanosine monophosphate (cGMP) in the chick pineal organ is dependent on activation of guanylyl cyclase-B. J Neuroendocrinol *14*, 14-18. 10.1046/j.0007-1331.2001.00732.x.

Ortuno-Lizaran, I., Sanchez-Saez, X., Lax, P., Serrano, G.E., Beach, T.G., Adler, C.H., and Cuenca, N. (2020). Dopaminergic Retinal Cell Loss and Visual Dysfunction in Parkinson Disease. Ann Neurol *88*, 893-906. 10.1002/ana.25897.

Ostrom, Q.T., Bauchet, L., Davis, F.G., Deltour, I., Fisher, J.L., Langer, C.E., Pekmezci, M., Schwartzbaum, J.A., Turner, M.C., Walsh, K.M., et al. (2014). The epidemiology of glioma in adults: a "state of the science" review. Neuro Oncol *16*, 896-913. 10.1093/neuonc/nou087.

Pandey, K.N. (2021). Molecular Signaling Mechanisms and Function of Natriuretic Peptide Receptor-A in the Pathophysiology of Cardiovascular Homeostasis. Front Physiol *12*, 693099. 10.3389/fphys.2021.693099.

Park, C., Cha, H.J., Lee, H., Hwang-Bo, H., Ji, S.Y., Kim, M.Y., Hong, S.H., Jeong, J.W., Han, M.H., Choi, S.H., et al. (2019). Induction of G2/M Cell Cycle Arrest and Apoptosis by Genistein in Human Bladder Cancer T24 Cells through Inhibition of the ROS-Dependent PI3k/Akt Signal Transduction Pathway. Antioxidants (Basel) *8*. 10.3390/antiox8090327.

Park, H.J., and Friston, K. (2013). Structural and functional brain networks: from connections to cognition. Science *342*, 1238411. 10.1126/science.1238411.

Pedram, A., Razandi, M., and Levin, E.R. (2001). Natriuretic peptides suppress vascular

endothelial cell growth factor signaling to angiogenesis. Endocrinology *142*, 1578-1586. 10.1210/endo.142.4.8099.

Perrault, I., Estrada-Cuzcano, A., Lopez, I., Kohl, S., Li, S., Testa, F., Zekveld-Vroon, R., Wang, X., Pomares, E., Andorf, J., et al. (2013). Union makes strength: a worldwide collaborative genetic and clinical study to provide a comprehensive survey of RD3 mutations and delineate the associated phenotype. PLoS One *8*, e51622. 10.1371/journal.pone.0051622.

Peshenko, I.V., and Dizhoor, A.M. (2020). Two clusters of surface-exposed amino acid residues enable high-affinity binding of retinal degeneration-3 (RD3) protein to retinal guanylyl cyclase. J Biol Chem *295*, 10781-10793. 10.1074/jbc.RA120.013789.

Peshenko, I.V., Olshevskaya, E.V., Azadi, S., Molday, L.L., Molday, R.S., and Dizhoor, A.M. (2011a). Retinal degeneration 3 (RD3) protein inhibits catalytic activity of retinal membrane guanylyl cyclase (RetGC) and its stimulation by activating proteins. Biochemistry *50*, 9511-9519. 10.1021/bi201342b.

Peshenko, I.V., Olshevskaya, E.V., and Dizhoor, A.M. (2016). Functional Study and Mapping Sites for Interaction with the Target Enzyme in Retinal Degeneration 3 (RD3) Protein. J Biol Chem *291*, 19713-19723. 10.1074/jbc.M116.742288.

Peshenko, I.V., Olshevskaya, E.V., and Dizhoor, A.M. (2021). Retinal degeneration-3 protein attenuates photoreceptor degeneration in transgenic mice expressing dominant mutation of human retinal guanylyl cyclase. J Biol Chem *297*, 101201. 10.1016/j.jbc.2021.101201.

Peshenko, I.V., Olshevskaya, E.V., Savchenko, A.B., Karan, S., Palczewski, K., Baehr, W., and Dizhoor, A.M. (2011b). Enzymatic properties and regulation of the native isozymes of retinal membrane guanylyl cyclase (RetGC) from mouse photoreceptors. Biochemistry *50*, 5590-5600. 10.1021/bi200491b.

Peshenko, I.V., Yu, Q., Lim, S., Cudia, D., Dizhoor, A.M., and Ames, J.B. (2019). Retinal degeneration 3 (RD3) protein, a retinal guanylyl cyclase regulator, forms a monomeric and elongated four-helix bundle. J Biol Chem *294*, 2318-2328. 10.1074/jbc.RA118.006106.

Plana-Bonamaiso, A., Lopez-Begines, S., Andilla, J., Fidalgo, M.J., Loza-Alvarez, P., Estanyol, J.M., Villa, P., and Mendez, A. (2020). GCAP neuronal calcium sensor proteins mediate photoreceptor cell death in the rd3 mouse model of LCA12 congenital blindness by involving endoplasmic reticulum stress. Cell Death Dis *11*, 62. 10.1038/s41419-020-2255-0.

Potter, L.R., and Hunter, T. (1998). Phosphorylation of the kinase homology domain is essential for activation of the A-type natriuretic peptide receptor. Mol Cell Biol *18*, 2164-2172. 10.1128/MCB.18.4.2164.

Potter, L.R., Yoder, A.R., Flora, D.R., Antos, L.K., and Dickey, D.M. (2009). Natriuretic peptides: their structures, receptors, physiologic functions and therapeutic applications. Handb Exp Pharmacol, 341-366. 10.1007/978-3-540-68964-5_15.

Preising, M.N., Hausotter-Will, N., Solbach, M.C., Friedburg, C., Ruschendorf, F., and Lorenz, B. (2012). Mutations in RD3 are associated with an extremely rare and severe form of early onset retinal dystrophy. Invest Ophthalmol Vis Sci *53*, 3463-3472. 10.1167/iovs.12-9519.

Regan, J.T., Mirczuk, S.M., Scudder, C.J., Stacey, E., Khan, S., Worwood, M., Powles, T., Dennis-Beron, J.S., Ginley-Hidinger, M., McGonnell, I.M., et al. (2021). Sensitivity of the Natriuretic Peptide/cGMP System to Hyperammonaemia in Rat C6 Glioma Cells and GPNT Brain Endothelial Cells. Cells *10*. 10.3390/cells10020398.

Reithmeier, T., Graf, E., Piroth, T., Trippel, M., Pinsker, M.O., and Nikkhah, G. (2010). BCNU for recurrent glioblastoma multiforme: efficacy, toxicity and prognostic factors. BMC Cancer *10*, 30. 10.1186/1471-2407-10-30.

Rollin, R., Mediero, A., Roldan-Pallares, M., Fernandez-Cruz, A., and Fernandez-Durango, R. (2004). Natriuretic peptide system in the human retina. Mol Vis *10*, 15-22.

Sanati, M., Aminyavari, S., Mollazadeh, H., Bibak, B., Mohtashami, E., and Afshari, A.R. (2022). How do phosphodiesterase-5 inhibitors affect cancer? A focus on glioblastoma multiforme. Pharmacol Rep *74*, 323-339. 10.1007/s43440-021-00349-6.

Schmidt, H., Dickey, D.M., Dumoulin, A., Octave, M., Robinson, J.W., Kuhn, R., Feil, R., Potter, L.R., and Rathjen, F.G. (2018). Regulation of the Natriuretic Peptide Receptor 2 (Npr2) by Phosphorylation of Juxtamembrane Serine and Threonine Residues Is Essential for Bifurcation of Sensory Axons. J Neurosci *38*, 9768-9780. 10.1523/JNEUROSCI.0495-18.2018.

Schroter, J., Zahedi, R.P., Hartmann, M., Gassner, B., Gazinski, A., Waschke, J., Sickmann, A., and Kuhn, M. (2010). Homologous desensitization of guanylyl cyclase A, the receptor for atrial natriuretic peptide, is associated with a complex phosphorylation pattern. FEBS J *277*, 2440-2453. 10.1111/j.1742-4658.2010.07658.x.

Sharma, A., Boise, L.H., and Shanmugam, M. (2019). Cancer Metabolism and the Evasion of Apoptotic Cell Death. Cancers (Basel) *11*. 10.3390/cancers11081144.

Sharma, R.K. (2010). Membrane guanylate cyclase is a beautiful signal transduction machine: overview. Mol Cell Biochem *334*, 3-36. 10.1007/s11010-009-0336-6.

Sharma, R.K., Duda, T., and Makino, C.L. (2016). Integrative Signaling Networks of Membrane Guanylate Cyclases: Biochemistry and Physiology. Front Mol Neurosci *9*, 83. 10.3389/fnmol.2016.00083.

Sharma, R.K., Pandey, K.N., Duda, T., and Makino, C.L. (2023). Editorial: Multi-limbed membrane guanylate cyclase cellular signaling pathways. Front Mol Neurosci *16*, 1185637. 10.3389/fnmol.2023.1185637.

Sharon, D., Wimberg, H., Kinarty, Y., and Koch, K.W. (2018). Genotype-functional-phenotype correlations in photoreceptor guanylate cyclase (GC-E) encoded by GUCY2D. Prog Retin Eye Res *63*, 69-91. 10.1016/j.preteyeres.2017.10.003.

Shuhaibar, L.C., Egbert, J.R., Edmund, A.B., Uliasz, T.F., Dickey, D.M., Yee, S.P., Potter, L.R., and Jaffe, L.A. (2016). Dephosphorylation of juxtamembrane serines and threonines of the NPR2 guanylyl cyclase is required for rapid resumption of oocyte meiosis in response to luteinizing hormone. Dev Biol *409*, 194-201. 10.1016/j.ydbio.2015.10.025.

Somasundaram, D.B., Subramanian, K., Aravindan, S., Yu, Z., Natarajan, M., Herman, T., and Aravindan, N. (2019). De novo regulation of RD3 synthesis in residual neuroblastoma cells after intensive multi-modal clinical therapy harmonizes disease evolution. Sci Rep *9*, 11766. 10.1038/s41598-019-48034-2.

Spiranec Spes, K., Hupp, S., Werner, F., Koch, F., Volker, K., Krebes, L., Kammerer, U., Heinze, K.G., Braunger, B.M., and Kuhn, M. (2020). Natriuretic Peptides Attenuate Retinal Pathological Neovascularization Via Cyclic Guanosine Monophosphate Signaling in Pericytes and Astrocytes. Arterioscler Thromb Vasc Biol *40*, 159-174. 10.1161/ATVBAHA.119.313400.

Spreca, A., Giambanco, I., and Rambotti, M.G. (1999). Ultracytochemical study of guanylate cyclases A and B in light- and dark-adapted retinas. Histochem J *31*, 477-483. 10.1023/a:1003712110751.

Suga, S., Nakao, K., Hosoda, K., Mukoyama, M., Ogawa, Y., Shirakami, G., Arai, H., Saito, Y., Kambayashi, Y., Inouye, K., and et al. (1992). Receptor selectivity of natriuretic peptide family, atrial natriuretic peptide, brain natriuretic peptide, and C-type natriuretic peptide. Endocrinology *130*, 229-239. 10.1210/endo.130.1.1309330.

Sulmann, S., Kussrow, A., Bornhop, D.J., and Koch, K.W. (2017). Label-free quantification of calcium-sensor targeting to photoreceptor guanylate cyclase and rhodopsin kinase by backscattering interferometry. Sci Rep *7*, 45515. 10.1038/srep45515.

Tamura, R., Morimoto, Y., Kosugi, K., Sato, M., Oishi, Y., Ueda, R., Kikuchi, R., Nagashima, H., Hikichi, T., Noji, S., et al. (2020). Clinical and histopathological analyses of VEGF receptors peptide vaccine in patients with primary glioblastoma - a case series. BMC Cancer *20*, 196. 10.1186/s12885-020-6589-x.

Tan, A.C., Ashley, D.M., Lopez, G.Y., Malinzak, M., Friedman, H.S., and Khasraw, M. (2020). Management of glioblastoma: State of the art and future directions. CA Cancer J Clin *70*,

299-312. 10.3322/caac.21613.

Vitale, I., Pietrocola, F., Guilbaud, E., Aaronson, S.A., Abrams, J.M., Adam, D., Agostini, M., Agostinis, P., Alnemri, E.S., Altucci, L., et al. (2023). Apoptotic cell death in disease-Current understanding of the NCCD 2023. Cell Death Differ *30*, 1097-1154. 10.1038/s41418-023-01153-w.

Wimberg, H., Janssen-Bienhold, U., and Koch, K.W. (2018a). Control of the Nucleotide Cycle in Photoreceptor Cell Extracts by Retinal Degeneration Protein 3. Front Mol Neurosci *11*, 52. 10.3389/fnmol.2018.00052.

Wimberg, H., Lev, D., Yosovich, K., Namburi, P., Banin, E., Sharon, D., and Koch, K.W. (2018b). Photoreceptor Guanylate Cyclase (GUCY2D) Mutations Cause Retinal Dystrophies by Severe Malfunction of Ca(2+)-Dependent Cyclic GMP Synthesis. Front Mol Neurosci *11*, 348. 10.3389/fnmol.2018.00348.

Wolf, J., Rasmussen, D.K., Sun, Y.J., Vu, J.T., Wang, E., Espinosa, C., Bigini, F., Chang, R.T., Montague, A.A., Tang, P.H., et al. (2023). Liquid-biopsy proteomics combined with AI identifies cellular drivers of eye aging and disease in vivo. Cell *186*, 4868-4884 e4812. 10.1016/j.cell.2023.09.012.

Wood, I.K. (1996). Neuroscience: Exploring the brain. Journal of Child and Family Studies *5*, 377-379. 10.1007/BF02234670.

Xie, K., Liu, C.Y., Hasso, A.N., and Crow, R.W. (2015). Visual field changes as an early indicator of glioblastoma multiforme progression: two cases of functional vision changes before MRI detection. Clin Ophthalmol *9*, 1041-1047. 10.2147/OPTH.S79723.

Xu, G.Z., Tian, J., Zhong, Y.M., and Yang, X.L. (2010). Natriuretic peptide receptors are expressed in rat retinal ganglion cells. Brain Res Bull *82*, 188-192. 10.1016/j.brainresbull.2010.03.004.

Yoder, A.R., Robinson, J.W., Dickey, D.M., Andersland, J., Rose, B.A., Stone, M.D., Griffin, T.J., and Potter, L.R. (2012). A functional screen provides evidence for a conserved, regulatory, juxtamembrane phosphorylation site in guanylyl cyclase a and B. PLoS One *7*, e36747. 10.1371/journal.pone.0036747.

Yoder, A.R., Stone, M.D., Griffin, T.J., and Potter, L.R. (2010). Mass spectrometric identification of phosphorylation sites in guanylyl cyclase A and B. Biochemistry *49*, 10137-10145. 10.1021/bi101700e.

Yu, Y.C., Cao, L.H., and Yang, X.L. (2006). Modulation by brain natriuretic peptide of GABA receptors on rat retinal ON-type bipolar cells. J Neurosci *26*, 696-707. 10.1523/JNEUROSCI.3653-05.2006.

Zagel, P., Dell'Orco, D., and Koch, K.W. (2013). The dimerization domain in outer segment guanylate cyclase is a Ca(2)(+)-sensitive control switch module. Biochemistry *52*, 5065-5074. 10.1021/bi400288p.

Zulliger, R., Naash, M.I., Rajala, R.V., Molday, R.S., and Azadi, S. (2015). Impaired association of retinal degeneration-3 with guanylate cyclase-1 and guanylate cyclase-activating protein-1 leads to leber congenital amaurosis-1. J Biol Chem *290*, 3488-3499. 10.1074/jbc.M114.616656.

Curriculum vitae

Yaoyu Chen

Tel: (+49) 15256414698, (+86) 18077341556

Email: yaoyu.chen@uni.oldenburg.de, 1991chenyu@gmail.com

Address: Artillerieweg 44, 26129, Oldenburg

Education

2018-present	**PhD student:** Carl von Ossietzky Universität Oldenburg (European Medical School), Oldenburg, Germany
2014-2017	**Master of Medicine** (Biomedical engineering)**:** Jilin University School of Pharmaceutical Sciences, Changchun, China
2010-2014	**Bachelor of Engineering** (Biopharmaceuticals)**:** Zhuhai College of Jilin University, Zhuhai, China

Research Experience

2018-present

PhD student at Carl Von Ossietzky University of Oldenburg

Supervisor: Prof. Karl-Wilhelm Koch, Prof. Anja U. Bräuer (Vice Dean)

Graduate Dissertation:

The physiological and pathological role of Retinal Degeneration Protein 3 (RD3) in the brain

Research direction and results:

1. The research on Retinal degeneration protein 3 (RD3) has primarily and largely focused on the retina, but its molecular mechanisms in diseases remain unclear. In our study, we unveiled the expression pattern of RD3 during brain development in mice. Furthermore, we generated in vitro RD3 protein to investigate its regulatory role in guanylate cyclase A or B joint cGMP synthesis. Simultaneously, we observed that these regulatory interactions were also present in astrocytes. These findings provide evidence for the involvement of RD3 in neuronal signaling and suggest that RD3 may have functions beyond the retina, indicating a broader role in the brain[1].

2. Recent evidence suggests a correlation between abnormal RD3 expression and nervous system cancers, including neuroblastoma. Based on our previous finding of higher RD3 levels in astrocytes, we

have initiated investigations into its correlation with glioma. Through a multicohort analysis, we have observed that the downregulation of RD3 is indicative of an advanced stage of glioma. In addition, we found that RD3 can induce G2/M phase arrest and activating cell apoptosis in HEK 293T. While the RD3 mutants can alleviate the cell death. These ongoing studies aim to unravel the functional implications of RD3 and evaluate its potential in prognostic and diagnostic value to cancer research.

2015-2017 Cooperation research program at Guangzhou Institutes of Biomedicine and Health, Chinese Academy of Sciences.

Supervisor: Prof. DuanQing Pei, Dr. JingLei Cai

Graduate Dissertation:

Generation of Larger Teeth from Human iPS Cells with Pig Dental Mesenchyme.

Research direction and results:

1. In this study, we successfully generated larger teeth by fusing human induced pluripotent stem (iPS) cells with pig dental mesenchyme through in vivo kidney transplantation. This achievement demonstrates the remarkable multipotential of iPS cells in the field of medical regenerative therapies. Moreover, the results indicate that dental mesenchyme plays a crucial role as an epigenetic niche in determining tooth morphology and development. In summary, this work sheds light on the potential applications of iPS cells in dental regenerative medicine and provides valuable insights into the complex mechanisms underlying tooth formation.

2. In an experiment, we implanted Collagen/Matrigel-coated iPS cell-derived neuronal cells into rats in vivo, demonstrating the efficacy and capabilities of our novel neural generation protocol. The use of Collagen/Matrigel coating method provided a supportive microenvironment for the iPS cell-derived neurons and showed a potential translational value. These findings highlight the potential of our protocol for generating functional neural cells and pave the way for future advancements in neural regenerative medicine and therapies for neurological disorders[2].

2014-2015 Course studies at Jilin University.

Supervisor: Prof. YuLai Zhou

Publications

1. **<u>Chen Y,</u>** Bräuer AU, and Koch K-W (2022) Retinal degeneration protein 3 controls membrane guanylate cyclase activities in brain tissue. Front. Mol. Neurosci. 15:1076430.doi: 10.3389

2. Liu P, Chen S, Wang Y, Chen X, Guo Y, Liu C, Wang H, Zhao Y, Wu D, Shan Y, Zhang J, Wu C, Li D, Zhang Y, Zhou T, **<u>Chen Y,</u>** Liu X, Li C, Wang L, Jia B, Liu J, Feng B, Cai J, Pei D. Efficient induction of neural progenitor cells from human ESC/iPSCs on Type I Collagen. Sci China Life Sci. 2021 Dec;64(12):2100-2113. doi: 10.1007/s11427-020-1897-0. Epub 2021 Mar 16. PMID: 33740188.

3. Jia B, Huang L, **<u>Chen Y</u>**, Liu S, Chen C, Xiong K, Song L, Zhou Y, Yang X, Zhong M. A novel contiguous deletion involving NDP, MAOB and EFHC2 gene in a patient with familial Norrie disease: bilateral blindness and leukocoria without other deficits. J Genet. 2017 Dec;96(6):1015-1020.

4. Yang Y, Zhao Y, Liu X, **<u>Chen Y</u>**, Liu P*, Zhao L. Effect of SOX2 on odontoblast differentiation of dental pulp stem cells. Mol Med Rep. 2017 Oct 17; 10.3892

Skills and expertise

- Recombinant protein expression and purification.
- Molecular cloning (PCR, RNAi, Point Mutation, CRISPR/Cas9, etc)
- Cell culture and transfection (primary cell linages, Immortalized cell line, iPS cell, etc)
- Animal experiment (Tissue separation, transplantation, implantation)
- Western Blot, Immunoprecipitation (Co-IP), IF, IHC, Confocal, and Live cell imaging
- R programming and Python.

Danksagung

I would like first to extend my sincere gratitude to Prof. Karl-Wilhelm Koch and Prof. Anja Bräuer for providing me with the invaluable opportunity to conduct my work in Oldenburg. Your great patience, guidance, support, and encouragement have been instrumental in shaping my research experience and contributing to the success of this endeavor. I am truly thankful for your mentorship and the enriching environment you created for academic and professional growth. To Prof. Karl-Wilhelm Koch, your broad knowledge and solid background really gave me a deep impression, thanks for your constructive, efficient, timely, and kindly help to all processes of my research work in particularly the dissertation, really hope that we can have cooperate in the future. To Prof. Anja Bräuer, your excellent characteristics and creative thinking really infected me and improved my confidence, especially after corona quarantine, thanks for providing me these good research environments.

I would also like to thank all the members of the Biochemie and Anatomie research group. Your unwavering support and advice have been instrumental in making my life and work in our lab both enjoyable and seamless. A special thank you goes to Dr. Alexander Scholten and Dr. Haijia Wu for your professional guidance in molecular cloning and guanylate cyclase assay. Your expertise and mentorship have been invaluable in shaping my research journey. I also extend my appreciation to Dr. Isabel Groß and Anne Gläser for your selfless assistance, which played a crucial role in ensuring a swift start to my lab work. Your willingness to share your knowledge and provide support has been truly impactful. A heartfelt thanks goes to Jennifer Sevecke-Rave and Beate Bous for your kind assistance in the lab. Your contributions have not gone unnoticed, and your collaborative spirit has greatly enriched the work environment.

Next, I want to express my heartfelt appreciation to all my friends in Oldenburg. Your companionship and our shared sports activities have truly added vibrant colors to my

life here. I am particularly grateful to Dr. Haijia Wu for the warm welcome to me when I first arrived in Oldenburg, and the memories of our basketball games and cooking sessions are etched fondly in my mind. I want to extend my thanks to Shumian Zhao for enduring challenging times together online. Our shared enjoyment of playing games and engaging in conversations has created lasting memories. To Michiel von Bulck, with whom I've shared both work and life experiences over the years, it's truly heartening to witness your happiness in finding a girlfriend. I wish you all the best in your future endeavors. A special note of appreciation goes to my small badminton group, comprised of Michiel, Sang, Kumarah, and Daryl. It feels like destiny brought us together, and our bond has grown to resemble that of a close-knit family. Together, we've navigated through various experiences, and I cherish the moments we've enjoyed together.

Then I'd like to express my heartfelt gratitude to my family. Without your unwavering support, I would never have been able to persist in my studies abroad. Your tolerance and understanding have been a source of strength for me, especially during challenging times. I deeply regret not being able to join the funeral of grandpa, and it saddens me that I couldn't be there with the family during such a significant moment. Despite the physical distance, please know that your support has been a constant presence in my journey, and I am grateful for the sacrifices you've made to enable my pursuit of education and personal growth.

Lastly, I want to express my deep gratitude to my girlfriend, Dr. Huanhuan Li. Although we crossed paths before, little did we imagine that fate would bring us together. Fortunately, life granted us a second chance in Europe, and I am genuinely thrilled to have experienced many new things by your side. Your support has played a significant role in my personal growth and overall development. With your assistance, I've experienced remarkable improvements in various aspects of my life. I want to thank you for your unwavering support and patience. I sincerely hope that we can continue to be life companions in the future.

Erklärung

Hiermit erkläre ich, dass ich die vorliegende Arbeit selbstständig verfasst habe und keine als die angegebenen Quellen und Hilfsmittel verwendet habe. Ich versichere, dass diese Arbeit weder in ihrer Gesamtheit noch in Teilen einer anderen Hochschule zur Begutachtung in einem Promotionsverfahren vorliegt oder vorgelegen hat und dass ich die Leitlinien guter wissenschaftlicher Praxis der Carl von Ossietzky Universität Oldenburg befolgt habe. Weiterhin versichere ich, dass im Zusammenhang mit dem Promotionsvorhaben keine kommerziellen Vermittlungs- oder Beratungsdienste (Promotionsberatung) in Anspruch genommen worden sind.

_____ (Ort, Datum) _____ (Yaoyu Chen)